AD NUMBER

ADB805969

LIMITATION CHANGES

TO:

Approved for public release; distribution is unlimited.

FROM:

Distribution authorized to DoD only; Administrative/Operational Use; MAR 1947. Other requests shall be referred to National Aeronautics and Space Administration, Washington, DC. Pre-dates formal DoD distribution statements. Treat as DoD only.

AUTHORITY

NASA TR Server website

NATIONAL ADVISORY COMMITTEE FOR AERONAUTICS

TECHNICAL NOTE

No. 1100

ELASTIC PROPERTIES IN TENSION AND SHEAR OF HIGH STRENGTH NONFERROUS METALS AND STAINLESS STEEL - EFFECT OF PREVIOUS DEFORMATION AND HEAT TREATMENT

By R. W. Mebs and D. J. McAdam, Jr.
National Bureau of Standards

Washington
March 1947

NATIONAL ADVISORY COMMITTEE FOR AERONAUTICS

TECHNICAL NOTE NO. 1100

ELASTIC PROPERTIES IN TENSION AND SHEAR OF HIGH STRENGTH NONFERROUS METALS AND STAINLESS STEEL -- EFFECT OF PREVIOUS DEFORMATION AND HEAT TREATMENT

By R. W. Mebs and D. J. McAdam, Jr.

SUMMARY

A résumé is given of an investigation of the influence of plastic deformation and of annealing temperature on the tensile and shear elastic properties of high strength nonferrous metals and stainless steels in the form of rods and tubes. The data were obtained from earlier technical reports and notes, and from unpublished work in this investigation. There are also included data obtained from published and unpublished work performed on an independent investigation.

The rod materials, namely, nickel, monel, Inconel, copper, 13:2 Cr-Ni steel, and 18:8 Cr-Ni steel, were tested in tension; 18:8 Cr-Ni steel tubes were tested in shear, and nickel, monel, aluminum-monel, and Inconel tubes were tested in both tension and shear.

There are first described experiments on the relationship between hysteresis and creep, as obtained with repeated cyclic stressing of annealed stainless steel specimens over a constant load range. These tests, which preceded the measurements of elastic properties, assisted in devising the loading time schedule used in such measurements.

From corrected stress-set curves are derived the five proof stresses used as indices of elastic or yield strength. From corrected stress-strain curves are derived the secant modulus and its variation with stress. The relationship between the forms of the stress-set and stress-strain curves and the values of the properties derived is discussed.

Curves of variation of proof stress and modulus with prior extension, as obtained with single rod specimens, consist in wavelike basic curves with superposed oscillations due to differences of rest interval and extension spacing; the effects of these differences are studied. Oscillations of proof stress and modulus are generally opposite in manner. The

use of a series of tubular specimens corresponding to different amounts of prior extension of cold reduction gave curves almost devoid of oscillation since the effects of variation of rest interval and extension spacing were removed. Comparison is also obtained between the variation of the several properties, as measured in tension and in shear. The rise of proof stress with extension is studied, and the work-hardening rates of the various metals evaluated. The ratio between the tensile and shear proof stresses for the various annealed and cold-worked tubular metals is likewise calculated.

The influence of annealing or tempering temperature on the proof stresses and moduli for the cold-worked metals and for air-hardened 13:2 Cr-Ni steel is investigated. An improvement of elastic strength generally is obtained, without important loss of yield strength, by annealing at suitable temperature.

The variation of the proof stress and modulus of elasticity with plastic deformation or annealing temperature is explained in terms of the relative dominance of three important factors: namely, (a) internal stress, (b) lattice-expansion or work-hardening, and (c) crystal reorientation.

Effective values of Poisson's ratio were computed from tensile and shear moduli obtained on tubular specimens. The variation of Poisson's ratio with plastic deformation and annealing temperature is explained in terms of the degree of anisotropy produced by changes of (a) internal stress and (b) crystal orientation.

INTRODUCTION

An investigation of the elastic properties of high strength aircraft metals has been conducted at the National Bureau of Standards for several years under the sponsorship of the National Advisory Committee for Aeronautics. A series of papers (references 1 to 6) have been presented. The first two (references 1 and 2) were comprehensive technical reports upon the tensile elastic properties of stainless steels and nonferrous metals. The remaining reports comprise a series of technical notes (references 3 to 6) upon the low temperature properties of 18:8 Cr-Ni steel, upon the shear elastic properties of stainless steel and nonferrous metal tubing, and upon Poisson's ratio for stainless steel.

The present paper is a summary of the preceding reports, and also contains considerable additional information consisting of (a) the results of tension tests on nonferrous tubing not previously reported, (b) some useful information obtained on nickel rod in another investigation in this laboratory (reference 7), and (c) some unpublished results

obtained in another project upon the influence of annealing temperature on the tensile elastic properties of nonferrous rod materials. These additional data are believed to add substantially to the value of this summarizing paper.

The elastic properties of a metal, as considered in this report, comprise the elastic strength, the elastic modulus, and associated indices. These properties may be derived in both tension and shear.

By elastic strength is usually meant the stress necessary to deform the metal to a boundary between elastic and inelastic strain. As shown in several of the preceding papers (references 1, 2, 3, 4, and 7), this boundary is not definite but depends upon the sensitivity of the method of measurement. For practical purposes, therefore, the elastic strength and yield strength of a metal are expressed in terms of five indices termed "proof stresses." These are the stresses necessary to cause permanent strains of 0.001, 0.003, 0.01, 0.03, and 0.1 percent. The values so obtained are found to vary with the amount and direction of previous stressing beyond the elastic strength.

As the stress-strain line for many metals is curved, the modulus of elasticity must be defined in terms of two or more indices. These indices may be taken as the modulus of elasticity at zero stress, and at one or more elevated stresses, and the linear stress coefficient of the modulus at zero stress, C_0. In previous papers (references 1, 2, 4, and 7), the quadratic stress coefficient of the modulus C' was used. This index is not evaluated in the present summary. When the five proof stresses and the variation of the modulus with stress are known, a fairly good picture of the elastic properties of a metal is obtained.

Additional indices were derived for some of these metals: namely, the tensile-shear proof stress ratio, the work-hardening rate, and Poisson's ratio. Poisson's ratio was derived from measured values of the tension and shear moduli, by use of an appropriate formula. Values of Poisson's ratio for 18:8 Cr-Ni steel were derived from tension and torsion measurements on cold-drawn rod and tubing, respectively. (See reference 5.) From values of the shear modulus derived previously (reference 6) and of the tension modulus presented here for the first time, the values of Poisson's ratio were derived for nonferrous metal tubing. The tensile-shear proof stress ratios and the work-hardening rates of these nonferrous metals are likewise presented as new data. There are also presented the elastic properties of 18:8 Cr-Ni steel rod at low temperatures.

In this paper, considerable data contained in the earlier reports were necessarily eliminated, for the sake of conciseness and clarity. The data presented are believed to be representative of each material

tested. Where feasible, summarizing statements give the results of work for which data are not presented.

A study is made of the variation of the several elastic properties of metals, in tension and in shear, with cold deformation and heat treatment. This variation is shown to be influenced by the relative dominance of three factors.

The metals studied and apparatus used are described in part I. In the development of the method of testing used, a preliminary investigation was made of the relationship between hysteresis and creep for annealed 18:8 Cr-Ni steel. These tests are discussed in part II. Part III gives the methods of measurement, and of plotting stress-set and stress-deviation curves. The effect of prior plastic deformation on the tensile and shear elastic strengths of the various metals studied is discussed in part IV. The influence of annealing temperature on the elastic strength is presented in part V. This section also includes a discussion of the low temperature tests of 18:8 Cr-Ni steel. Part VI contains a study of the influence of prior plastic deformation on the tensile and shear moduli and their linear stress coefficients for the metals investigated. The influence of annealing temperature on these moduli and their stress coefficients is discussed in part VII. The effect of lowering the test temperature on the tensile modulus is also studied. The variation of the calculated values of Poisson's ratio with plastic deformation and annealing temperature also is presented in parts VI and VII, respectively. The conclusions reached in this report are based on a comparison of the diagrams obtained with the several metals.

I. MATERIALS AND APPARATUS

1. Materials and Specimens

The materials used in this investigation consist of several nonferrous metals, namely, nickel, monel, aluminum-monel, Inconel, copper, and two stainless steels, namely, 13:2 Cr-Ni steel and 18:8 Cr-Ni steel. Nickel, monel, aluminum-monel, and Inconel were supplied in both the rod and the tubular form by the International Nickel Company. Results obtained with aluminum-monel rod were fragmentary, and are given only in an earlier report (reference 2). The oxygen-free copper rod was furnished by the Scomet Engineering Company. The 13:2 Cr-Ni steel rod was furnished by the Carpenter Steel Company. The cold-drawn 18:8 Cr-Ni steel rod was furnished by the Allegheny-Ludlum Steel Corporation. The annealed 18:8 Cr-Ni steel rod was obtained from the stock room in this laboratory. The 18:8 Cr-Ni steel tubing was purchased on the open market.

The 13:2 Cr-Ni steel rod was supplied in the annealed condition

(heated to 1240° F and slowly cooled in the furnace). The 18:8 Cr-Ni steel rod upon which hysteresis measurements were made had been soft-annealed. The copper rod was cold-rolled. All the other rod material was furnished in the cold-drawn condition. The 18:8 Cr-Ni steel tubing was cold-drawn during manufacture. Nickel, monel, aluminum-monel, and Inconel tubing were each supplied in several hardness grades as obtained by cold reduction without intermediate anneal; aluminum-monel and Inconel tubing were also supplied in a soft-annealed condition. There also was supplied nickel, monel, aluminum-monel, and Inconel tubing which had been severely cold-reduced and then normalized or stress-relief-annealed at 500° F.

Cold reduction in the manufacture of the nonferrous tubing was obtained by "cold-drawing" or by the "tube reducer" method. The cold-drawing method consists in drawing the tubing between a standard drawing die and a mandrel. The tube reducer method consists in kneading the tubing over a mandrel by the use of rolls. The latter method was used only in producing severely cold-reduced tubing. Both methods will be frequently referred to as cold reduction, in order to differentiate from cold deformation obtained by tensile extension of specimens soft-annealed in the laboratory.

Chemical compositions of all the materials are listed in table 1. Mechanical and thermal treatments of individual rod specimens are listed in table 2, and of individual tubular specimens in table 3. The methods and amounts of cold reduction imparted to the materials during manufacture are also listed in tables 2 and 3. In each serial designation, the first letter or series of letters identifies the material as to composition, form, and degree of cold work during manufacture. Any annealing or tempering treatment is indicated by a number following these letters, denoting the number of degrees Fahrenheit in hundreds. If the specimen was extended following the annealing treatment, and before test, these numbers are followed by the letter R and an additional number indicating the nominal extension in percent. For 13:2 Cr-Ni steel (table 2) the letter E is followed by a second letter which indicates the method of cooling from 1750° F, namely, A for air cooling and F for furnace cooling; the final number indicates the tempering temperature in hundreds.

The original rod diameters and the diameters of the rod test specimens are given in table 1. The gage diameters of these specimens were made as large as possible in order to decrease the error of estimating the stress; the error (in pounds) in estimating the load is practically independent of the load, for any scale range of the testing machine. In other respects, the rod specimens were according to the standard of the American Society for Testing Materials for threaded specimens with 2-inch gage length. The ratio of gage length to diameter for the rod specimens was unimportant in this investigation, because the tests did not require extension beyond the point of beginning local contraction.

All tubes were of 1-inch outside diameter, nominal size. The nickel, monel, aluminum-monel, and Inconel tubes were of 0.085-inch wall thickness and the stainless steel tubes of 0.1-inch wall thickness, nominal size. The specimens were thoroughly cleaned, after which the length, average outside diameter, and weight of each were accurately measured. The average wall thickness of each specimen was computed from these data, and from a density value carefully determined by the hydrostatic weighing method on a small sample of the same material.

Single rod specimens were prepared corresponding to each treatment indicated in table 2. Duplicate specimens of nickel, monel, aluminum-monel, and Inconel tubes were prepared corresponding to each treatment indicated in table 3; identical tubular specimens were tested in tension and in torsion. Only single specimens of 18:8 Cr-Ni steel tubes were prepared corresponding to each treatment listed in table 3. Before test, each tubular specimen had its ends fitted with tight plugs in order to prevent distortion during test.

2. Apparatus

A pendulum-hydraulic testing machine of 50,000-pound capacity was used for tension testing. The threaded rod specimens were held in grips with spherical seats. Wedge type grips held the tubular tension test specimens. Torsion tests were made in a manually operated pendulum-type testing machine of 13,000 inch-pound capacity.

Most of the room temperature tension tests were made with a pair of Tuckerman optical extensometers; these gages were attached to opposite sides of the specimens. The smallest gage division of this extensometer corresponds to a charge of length of 0.00004 inch. By means of a vernier on this instrument, it is possible to estimate changes of length to within about 0.000002 inch; this sensitivity corresponds to a strain sensitivity of 1×10^{-4} percent for the 2-inch gage length used. A limited number of measurements were also made with an Ewing extensometer of somewhat poorer sensitivity.

Room temperature torsion tests were made with an optical torsion meter (fig. 1) of high sensitivity, especially designed and constructed for measuring shear strain in this investigation. A description of this torsion meter was given in earlier report (reference 4). The smallest gage division on the scale of the collimator used in conjunction with the torsion meter represents a relative angular motion of 0.0002 radian of tube cross section a gage length ($2\frac{1}{2}$ in.) apart. This corresponds to a change of strain of less than 4.0×10^{-3} percent for the size tubular specimens used. By means of a vernier on the collimator scale, changes of strain of less than 2.0×10^{-4} percent can be detected.

For the low temperature tests described in this report, the specimen was immersed in a bath consisting of equal parts of carbon tetrachloride and chloroform, to which had been added an excess of solid carbon dioxide. The modified Tuckerman extensometer and chamber used (fig. 2) were described earlier (reference 3).

II. HYSTERESIS AND CREEP OF ANNEALED 18:8 Cr-Ni STEEL

As previously mentioned, the boundary between elastic and plastic strain is considerably affected by the amount and direction of any previous stressing beyond this boundary. One manifestation of this effect is known as mechanical hysteresis. By plotting strain measurements obtained at various stress increments, while raising and lowering the load in a single stress cycle, there would be obtained a curve the ascending and descending portions of which generally do not coincide. This would hold true even if the maximum stress were well below the technical elastic limit. The cycle of stress thus causes a hysteresis loop, which may or may not be closed at the bottom. The width of the loop and the degree of separation of the ascending and descending curves at the bottom depend on the stress range, the rate of loading and the number and character of the previous cycles.

1. General Description of Experiments on Hysteresis and Creep

In order to study in detail the interrelationship between stress, strain, and permanent set, it is important to understand the influence of hysteresis on the stress-strain characteristic and its relationship to positive and negative creep. In figure 3 are shown selected hysteresis loops of series obtained upon each of three similar 18:8 Cr-Ni steel rod specimens, DA-5, DA-3, and DA-4.[1] This rod material, DA, which was received in the soft-annealed condition, is the same as used in a previous investigation in this laboratory (reference 8). In each of the series, the specimen was loaded between constant values of upper and lower load; the lower load was just sufficient to preserve alinement of the grips, the adapter, and the specimen. With the stress range used for each specimen, considerable permanent set was obtained with the initial cycles. The stresses indicated were calculated by dividing the load by the cross sectional area at the beginning of each cycle. Such stresses are termed true stresses.

In figure 3 the origin of each loop has been shifted forward by a constant abscissa interval from the origin of the preceding loop plotted.

[1]In the designation of these three specimens, the final number is used for identification only; it bears no relation to any annealing temperature.

The number of each cycle in the series is given at the top. The cycle time, in minutes, is given at the top of each loop in the upper row and inside each loop in the lower row. The total plastic extension prior to each cycle is also given inside each loop. The time interval between cycles is indicated by the symbol at the beginning of each cycle.

Because of the greater stress range in the cycles of the upper row, the plastic extension of specimen DA-5 in the first few cycles was greater than obtained on specimen DA-3 in the lower row. (These specimens are designated 1A-5 and 1A-3, respectively, in reference 1.) Nevertheless, the permanent set per cycle decreased more rapidly in the upper row than in the lower row, owing probably to the greater work-hardening at the greater stress range in these cycles. Because of accidental overstressing, only 29 cycles could be obtained upon specimen DA-3; only the first 5 cycles are shown. A new specimen of this material, DA-4 (designated 1A-4 in reference 1) was given 30 rapid cycles over the same stress range, without measuring strain, and the experiment then was continued. Some few cycles obtained on specimen DA-4 are given in the right-hand portion of the lower row of figure 3. A comprehensive discussion and additional data, relative to these tests, are found in an earlier report (reference 1).

2. Hysteresis Experiments on Specimen DA-5

The first 4 cycles in the upper row of figure 3 are represented by ordinary stress-strain curves. The first cycle, because of the relatively high stress applied to this annealed material, caused an extension of 15 percent. The solid line represents the variation (with strain) of the nominal stress, that is, stress based on the original sectional area; the broken line represents the variation of stress based on the actual cross section corresponding to the strain. Each of the other loops of the upper row is a plot of the true stress as previously defined.

Comparison of loops 1 to 4, with allowance for the fact that the abscissa scale is much more sensitive for loops, 2, 3, and 4 than for loop 1, shows that each of these loops (both at the middle and at the bottom opening) is considerably narrower than the preceding loop. With continued cyclic repetition, the difference in form between any two adjacent loops gradually becomes smaller. In order to study these later variations, therefore, it is necessary to use a still more sensitive abscissa scale. For loops 5 to 161, consequently, abscissas represent deviations from a tensile modulus of 31×10^6 psi, plotted on a more open scale. (A more detailed discussion of the deviation method of plotting is given later in the description of fig. 4.)

Consideration is given now to the variation with cyclic repetition of the loop width at the middle, the width of the opening at the bottom, and the negative creep at the bottom. These values are listed in table 4;

values for cycles not shown in this figure may be found in an earlier report (reference 1, table III). For some cycles, strain measurements were not made, but the stress range was the same as for the measured cycles. The time for the unmeasured cycle was much less than for a measured cycle. The net plastic extension per cycle, consequently, was much less for the unmeasured than for the measured cycle.

With cyclic repetition, as shown in figure 3 and table 4, the width of the loop at the middle, and the width of the opening at the bottom tend to decrease. This general trend for each of these values, however, is sometimes interrupted or masked by any marked variation of the cycle time, or of the time interval between cycles. Each cycle represented in the upper row of figure 3 generally started immediately after the end of the cycle preceding it in the test. (The measured negative creep at the end of a cycle was viewed as part of that cycle.) After 11 short cycles 144 to 154, however, there was a rest interval of 1 day. Loop 155, which followed this rest interval, is much wider than loop 140. This widening effect is only temporary; during several subsequent loops the width rapidly decreases and the general trend is resumed.

The net permanent extension per cycle (width of the opening at the bottom of the loop) is the difference between the total positive creep and the total negative creep during the cycle. Most of the positive creep occurs at and near the top of the loop, and most of the negative creep occurs at and near the bottom. The bulging of the loop in the first part of the descent from the top gives qualitative evidence of positive creep; but the actual creep is less than indicated, owing to the use of the deviation method of plotting. It was not possible to make direct measurements of either the total positive or total negative creep occurring during a cycle. Values of the positive creep based on the bulging of the loop below the top, however, are listed in table 4; these values have only qualitative significance. They would be less had more time been allowed for positive creep at the top of the loop.

Positive creep during the first part of the descent from the top may have its counterpart in negative creep during the first part of the ascent from the bottom of the loop. That is, if time is not given for negative creep at the bottom of a loop, negative creep generally becomes evident during the first part of the ascent of the next loop in increasing the steepness of the curve. In an investigation of the stress-strain or stress-set relationship, therefore, care is necessary to eliminate or minimize the disturbing effect of negative creep near the end of a cycle, on the form of the following stress-strain or stress-set curve. In the cycles represented in figure 3 and in most of the experiments represented in the figures of this report, the disturbing effect of negative creep was minimized by allowing a rest interval before beginning the next cycle. Time was thus given for completion of important thermal creep and the most rapid part of the inelastic creep. Much longer time is necessary,

however, to eliminate entirely the influence of inelastic negative creep (reference 9). In table 4, the amounts of negative creep during 1 and 3 minutes are listed for specimen DA-5. That the rate of negative creep decreases rapidly is indicated by the greater creep occurring during the first minute than in the succeeding 2 minutes. The negative creep during the first minute for these cycles is not plotted in figure 3.

3. Hysteresis Experiments on Specimens DA-3 and DA-4

In the lower row of figure 3 the loops represent series of cycles obtained on two specimens DA-3 and DA-4. The stress range used was somewhat smaller than used with specimen DA-5. As noted before, overstress on specimen DA-3 after 29 cycles necessitated the continuation of these tests upon specimen DA-4, which was first given 30 rapid unmeasured cycles. The total extension during these first 30 cycles was not measured, but as explained earlier (reference 1), could be assumed to be about 3.5 percent.

The first five stress-strain loops for specimen DA-3 are plotted; the remaining selected loops shown were obtained with specimen DA-4, and are plotted as deviation from a modulus of 31×10^6 psi on a more open scale. Data on the cycles shown are listed in table 4. Data not shown for measured and unmeasured cycles on these specimens may be found in an an earlier report (reference 1, tables IV and V).

For cycles 83 through 388 upon specimen DA-4, the extensometer used was reset after each measured cycle, permitting some small unmeasured negative creep during this interim. This interval was therefore not considered a part of a cycle; as indicated by the first symbol of the succeeding cycle, this resetting generally required 2 minutes. The negative creep measured after the first minute rest interval, however, is considered a portion of the previous cycle.

Cycle 31 is somewhat wider than any of the loops immediately following (see reference 1) owing probably to an unstable condition induced during the preceding 30 rapid cycles. With slow cyclic repetition, the maximum loop width and the width of the opening at the bottom of the loop gradually decrease. The positive creep likewise gradually decreases. The 3-day interval preceding loop 116 causes it to be somewhat wider than loop 83. However, loop 118, which has a short prior rest interval, has considerably less loop width than loop 83. Loops 376 and 377 are not appreciably different from loop 118. Rapid cyclic stressing preceding loop 376 evidently did not cause it to differ appreciably from loop 377. Hence, loop 388 is effectively wider than loop 377 owing to the greatly increased cycle time, rather than because of the rapid cycles preceding it.

4. Variation of Creep with Cyclic Repetition

Negative creep at the bottom of the loop evidently decreases rapidly during the first few cycles, and changes more slowly with further cyclic stressing. With cyclic repetition, both the net positive and negative creep probably approach zero. The width of the loop at the middle, however, probably approaches a limiting value greater than zero. With a completely closed loop, the form and size would be independent of cycle time, producing "elastic," or better, "statical" hysteresis.

Statical hysteresis evidently had not been attained in specimens DA-5 or DA-4, since the loops are far from closure. Thousands, possibly millions, of cycles probably would be necessary to cause such closure (reference 10). With much shorter cycle time (higher cycle frequency), the number of cycles necessary to reach a condition of statical hysteresis would be still greater.

Negative creep frequently is called "elastic aftereffect." This term is erroneous, however, because negative creep is often caused by plastic deformation of parts of the microstructure of a metal. One kind of negative creep which is truly elastic is thermal creep, as caused by temperature equalization of a metal following a rapid change of stress. In a comprehensive discussion of thermal creep given in the earlier report (reference 1, p. 8) it is shown that the measurable thermal creep caused by loading or unloading, within the yield stress range, a specimen of the form and size used, probably would be complete within a minute. Calculation of the amount of total thermal negative creep for the loops illustrated in figure 3 gives a value of less than 0.001 percent. The negative creep observed at the end of each loop measured was therefore almost entirely inelastic creep. Although there may be a real difference between the so-called "drift" and other types of slow creep referred to in the literature, the authors are unable to make such a distinction in the discussion of the data to be presented.

III. MEASUREMENT OF STRESS, STRAIN, AND PERMANENT SET

1. Method of Test and Plotting of Results

In each series of hysteresis experiments previously described, the stress range was held constant. To investigate the elastic strength and modulus of elasticity, however, it has been found desirable to subject the metal to repeated stress cycles of increasing range, so as to obtain correlated stress-strain and stress-set curves. For this purpose specimens have been loaded and unloaded cyclically to progressively greater loads, until the total plastic extension reached at least 0.1 percent. The specimen was not completely unloaded during each cycle, but only to

a fixed lower value, in order to avoid disturbing the alinement of grips, adapters, and specimen.

By plotting for each cycle of stress, the strain as measured by difference in strain meter readings at each upper load and at the beginning of the first cycle of stress, against the stress corresponding to each upper load,[1] a stress-strain curve may be obtained from the series of stress cycles. Such a stress-strain curve is generally almost identical with a curve obtained with uninterrupted increase of stress. An actual stress-strain curve obtained by cyclic loading and unloading in tension is shown in figure 4A (designated uncorrected). Stress is plotted as ordinates and strain (extension) as abscissa. The experimental values are indicated as points on the curve, which has been extrapolated to zero stress.

For a more sensitive picture of the variation of strain with stress, it is desirable to plot a stress-deviation curve, as shown by the broken curve (designated uncorrected) in figure 4B. The strains represented in this figure are not the total strains, but are the calculated differences between the total strains and the strains corresponding to an assumed constant value of the modulus of elasticity (for this curve 32×10^6 psi). Figure 4B is plotted upon a more open abscissa scale than is figure 4A. By suitable choice of the assumed modulus value, the stress-deviation curve gives a very sensitive representation of the variation of strain with stress. Abscissa values on the broken curve in figure 4B correspond in figure 4A to the horizontal distances between the straight line representing a modulus of 32 million psi and the plotted stress-strain curve, measured at corresponding stress ordinates.

By plotting the stress for the upper load in each cycle against the permanent set, as measured by the difference in strain meter readings at the lower load, at the end of that cycle, and at the beginning of the first cycle, a stress-set curve is obtained. The stress-set curve corresponding to the stress-strain relationship in figures 4A and 4B is plotted in figure 4C. Experimental values are indicated on the curve. The extreme upper portion is not shown, owing to the sensitivity of the abscissa scale used.

The values of strain and permanent set measured for each cycle of stress will depend on the time schedule of loading and unloading. In addition to the change of elastic strain with change of load, positive creep will occur at and near the upper load; whereas negative creep will occur while at and near the lower load. In this investigation, therefore, the load was held for a period of 2 minutes at the upper and lower limit

---

[1]Each stress value is based upon the load and upon the dimensions of the specimen at the beginning of the series of cycles.

in each cycle before strain meter readings were obtained. After this holding time, as indicated in part II, the creep rate will have reached a small value. The use of such holding times made it unnecessary to maintain an ultrasensitive control of the rates of loading and unloading or to obtain readings at exactly prescribed times. The actual rates were maintained well within the required limits.

In order to investigate the influence of prior plastic extension on the stress-deviation and stress-set curves, some rod specimens were extended plastically by numerous increments to about the point of beginning local contraction. Correlated stress-strain and stress-set curves were obtained with the unextended specimen and after each increment of extension. Some of these increments were large, but others were equivalent only to the extension obtained in determining the previous stress-set curve. The distribution of these increments of extension over the range of prior deformation is termed "extension spacing." After each increment of extension, the specimen was permitted to rest before determining the stress-strain and stress-set curves;[1] the form of such curves will depend somewhat upon the duration of such a "rest interval." That certain changes occur in a test specimen during a rest interval is evidenced by negative creep during this period. As shown in earlier reports (references 1, 2, and 7), these changes are greatly accelerated by a slight elevation of the temperature during the rest interval.

In later tests, in a study of the influence of plastic deformation upon the elastic properties of nonferrous metal tubing and 18:8 Cr-Ni steel tubing, different laboratory-annealed specimens were extended varying amounts, following which single correlated stress-strain and stress-set curves were measured on each specimen. Thus the influence of varying extension spacing and rest interval were not factors in these later tests.

2. Accuracy of Determination of Set and Strain Values

Because of the change in elastic strain with load, any deviation in the actual load at which a strain meter reading is taken, from the recorded value, will introduce an error in the determination of strain or set. This deviation will depend upon the sensibility of reading the scale of the testing machine and the ability of the testing machine operator to maintain the load during strain meter readings.

---

[1]Since stress values are based upon the specimen cross section at the beginning of measurement of each stress-strain curve, they will be referred to in this report as "true" stresses, as distinguished from "nominal" stresses based upon the original cross section of the specimen.

A discussion of the relative influence of these factors is given in earlier reports (references 1, 2, and 7). It is there shown that these errors are negligible, or may be minimized by careful test procedures, so as not to mask the influence of important factors on the elastic properties of metals.

IV. THE INFLUENCE OF PRIOR PLASTIC DEFORMATION ON THE ELASTIC STRENGTH OF METALS

In studying the elastic strength of metals, as affected by plastic deformation, attention will be given first to annealed nickel. The influence of various factors upon the elastic strength of this metal will be studied in detail. A comparative study will then be made of the other metals.

1. Influence of Plastic Extension on the Stress-Set Curve and the Tensile Elastic Strength of Annealed Nickel Rod

In order to investigate the tensile elastic properties of fully annealed nickel rod, a specimen of cold-drawn rod (R) was annealed at 1400° F (reference 7). Correlated stress-deviation and stress-set curves obtained with this specimen (R-14) are shown in figure 5. The stress-set curves, similar to the curve found in figure 4C, are in the lower row of the figure. Directly above the origin of each stress-set curve is the origin of the corresponding stress-deviation curve, similar to that found in figure 4B.

The origin of each stress-set curve in figure 5 is shifted to the right a constant interval from the origin of the preceding curve, and has its own scale of abscissas. Distances between the origins have no relation to this scale. The curves were obtained consecutively from left to right, in pairs, by methods described in part III, and with intervening (varying) amounts of prior plastic extension. Curve 9 of this group is identical with the stress-set curve in figure 4C.

The prior extensions for individual curves are not indicated in figure 5. The curves are numbered consecutively, however, and the percentages of prior extension may be found by referring to the correspondingly numbered experimentally determined points in figure 7, which is derived from the stress-set curves in figure 5.

The rest intervals between two series of cycles from which a pair of stress-set curves were determined, range from 31 to 37 minutes;

between separate pairs of curves the rest interval was somewhat longer. The rest interval preceding each series of cycles from which a stress-set curve is obtained is indicated in figure 5 by the symbol placed at one or more experimentally determined points on the curve.

From each stress-set curve are derived five proof stress values corresponding to total sets of 0.001, 0.003, 0.01, 0.03, and 0.1 percent. In figure 7, these proof stresses are plotted against the corresponding percentages of total prior plastic extension. Stress is plotted on an offset scale in order to differentiate the curves for the several proof sets. As indices of elastic strength, the proof stresses based upon 0.001- and 0.003-percent set probably should receive more consideration than the proof stresses based on larger percentages of permanent set. The 0.1-percent proof stress should be viewed as an index of yield strength rather than as an index of elastic strength.

In each curve of figure 7, the points derived from experiment are distributed along the extension axis, in pairs, which are separated by relatively long intervening plastic extensions. Each pair of points is derived from a pair of stress-set curves determined with an intervening plastic extension equivalent only to that obtained in determining the first curve of the pair. The alternate long and short extensions were made in order to reveal the influence of the amount of intervening plastic extension on the form of the stress-set and stress-strain curves and on the derived tensile elastic properties.

The stress-set relationship, as affected by plastic extension, rest interval, and extension spacing may best be studied by considering the derived curves of variation of the proof stresses with prior plastic extension. In studying this relationship for annealed nickel, however, it also shall be of interest to consider the interrelationship of the forms of the derived curves (fig. 7) and the stress-set curves (fig. 5). The steeper the stress-set curves, the higher are the derived proof stresses. It should be noted that the oscillations in the curves for 0.001-percent proof stress are usually large and parallel to those for greater values of set. They are due principally, therefore, to variations in properties of the test specimen, not to any lack of sensitivity of the testing apparatus.

The first stress-set curve of each pair (fig. 5) generally is less steep than the second. This relationship is illustrated also by the relative height of the experimentally derived points in the diagram (fig. 7). The first point of each pair, with few exceptions, is lower than the second. Such differences are due partly to the differences in the duration of the rest interval; the longer the rest interval, the lower generally is the corresponding point on the derived diagram. This lowering is most prominent during the first portion of the rest interval and is slight after 1 day. The generally higher position of the second point

of a pair, however, is due partly to the influence of the extension spacing.

The oscillations due to the influence of the rest interval and of the extension spacing are superposed on curves of variation of the proof stresses due to prior plastic extension alone. The latter curves, hereafter termed "basic curves," would be smooth in form, but cannot be determined independently on a single specimen. The basic curves would be nearly parallel, however, to curves drawn through the mean position of the oscillations. If the basic curves were drawn in figure 7, all but the lowest curves would rise continuously, at a gradually decreasing rate. The basic curve for the 0.001-percent proof stress would not rise continuously, but would have several minima and maxima; it probably has a slight initial descent, as illustrated by the fact that point 3 is lower than point 1. In later measurements of the tension stress-set curves of nonferrous metal tubing, individual annealed specimens were extended varying amounts before test; such derived proof stress extension curves hence are basic curves devoid of the influence of the rest interval and of the extension spacing.

2. Internal Stresses and Their Effects on the Tensile Proof Stresses

The oscillations in proof stress-extension curves may be attributed to variations of one or more kinds of internal stress due to changes of extension spacing or rest interval. As shown by Heyn and Bauer (reference 11) and Masing (reference 12), the internal stresses induced are of three kinds. The first, termed macroscopic internal stress, is caused by nonuniformity of plastic deformation in different parts of a cross section. Heyn has devised a method for measuring approximately internal stresses of this kind. Such internal stress tends to lower the observed elastic strength. The second kind of internal stress, termed hereafter "microstructural stress," is due to initial differences in the resistance to plastic deformation of variously oriented grains of a polycrystalline aggregate, and to differences in the strength of different microconstituents; when the stress is removed following plastic deformation of the metal, some of the grains will be under tensile stress and others under compressive stress. According to Masing (reference 13) and others, microstructural stress is the cause of the Bauschinger Effect (reference 14) and of the "elastic aftereffect," better designated as negative creep. There is some evidence, however, that the influence of microstructural stress is very similar to that of macroscopic internal stress. The Bauschinger effect probably is due largely to the third kind of internal stress.

The third kind of internal stress described by Heyn and by Masing is associated with space-lattice changes involved in work-hardening. It has been shown by Smith and Wood (reference 15) that the plastic extension

of iron causes a three-dimensional expansion which remains after removal of the stress. This type of internal stress, termed "lattice expansion," cannot be wholly removed except by recrystallization. The authors of the present summary are of the opinion, however, that the lattice expansion diminished somewhat with rest at room temperature. The lattice expansion, therefore, probably is associated essentially with work-hardening. As it probably differs in direction parallel and normal to the direction of extension, this directional variation would account for the Bauschinger effect.

In future discussion, the unqualified term "internal stress" will signify only the combined effect of macroscopic internal stress and microstructural stress. The production of such internal stress tends to lower the proof stress. According to figure 7, and from results of interrupted tests on other metals to be described later, moderate to large extensions tend to induce internal stress; whereas slight extensions following such large reductions tend to remove it. During initial extension of nickel, the effect of induced internal stress also is evident in an actual slight lowering of the 0.001-percent basic proof stress curve.

Lattice expansion tends to cause a rise of proof stress, as evidenced by the general rise of all proof stresses with extension of annealed nickel (fig. 7). The oscillations superposed on the basic curves are due to fluctuations of the relative dominant influences of induced internal stress and lattice expansion. They are most evident in the lower proof stress curves.

Templin and Sturm (reference 16) show that uninterrupted plastic deformation by tensile extension tends to raise the subsequently measured tensile yield stresses (0.2-percent offset) far above the compressive yield stresses, an evidence of the Bauschinger effect. In cold-drawing, however, tensile and compressive yield stresses remained equal. Extending from the right boundary of figure 7 are short lines indicating the proof stresses obtained upon a specimen of the nickel rod (R) in the cold-drawn condition (cold-drawn to 60-percent reduction, that is, 150-percent equivalent extension, during manufacture). Extrapolation of the five proof stress curves to the right from 35-percent to 150-percent extension would give proof stress values somewhat higher than those obtained for the cold-drawn nickel rod, an evidence of the Bauschinger effect.

3. Influence of Plastic Deformation on the Tensile Elastic Strength of Nickel Tubing

Nickel tubing (TRF) which had been cold-reduced 75 to 80 percent in area of cross section, and normalized at 500° F during manufacture, was

soft-annealed at 1450° F. Individual specimens then were extended varying amounts ranging from 0.5 to 10.0 percent. (See table 3.) Tensile proof stresses, derived from tensile stress-set curves obtained with these specimens, and with an unextended annealed specimen are plotted in figure 8A. The amount of extension, given as equivalent reduction of area, is plotted as abscissa. The experimentally derived points are connected by straight lines. Smooth curves drawn through these points, however, would not deviate greatly from those lines. With increasing plastic extension (fig. 8A), all the proof stresses exhibit an initial decrease followed by a rise. The rise is more rapid for the higher proof sets.

In figure 8B are plotted tensile proof stresses measured upon nickel tubing cold-reduced 10, 20, 30, 40, and 75 to 80 percent, respectively, during manufacture. The amount of cold-reduction is plotted as abscissa. Symbols denoting the various cold-reduced grades are marked on the diagram along corresponding abscissa. (See table 3.) Proof stress values for the laboratory annealed specimen (TRF) are plotted at zero equivalent reduction in both figures 8A and 8B.

With increasing cold reduction (fig. 8B) the proof stresses show a general rise, which is greatest between zero and 10-percent reduction. Values of proof stress for the annealed tubing and for nickel tubing cold-reduced 10 percent are connected by broken straight lines because the course of these curves is least accurately defined in this range.

The intial decrease in proof stress with extension is probably due to the dominant influence of increase of internal stress; the subsequent rise of proof stress with extension (fig. 8A) and the rise with cold reduction (fig. 8B) may be attributed chiefly to the influence of the second factor, lattice expansion or work-hardening.

Extrapolation of the almost linear 0.03- and 0.10-percent proof stress curves in figure 8A to 10-percent reduction would give values approximately equal to that obtained with nickel tubing, TRA, cold-reduced 10 percent. Extrapolation of the lower proof stress curves for the extended tubing would give values lower than those obtained with the tubing cold-reduced 10 percent.

4. Influence of Plastic Deformation on the Shear Elastic Strength of Nickel Tubing

The procedure of measuring shear strain and shear permanent set, using the optical torsion meter and the pendulum type torsion testing machine was generally the same as the procedure followed in the tension measurements.

The tubing was as thin-walled as was deemed possible without danger of buckling during measurement of strain. The shear stress and strain increased from the inner to the outer portions of the wall. Assuming that both stress and strain increase linearly with distance from the axis of the tube, the shear stress τ at the mean fiber would be given by (reference 17)

$$\tau = \frac{2M}{\pi D^2 t}\left[\frac{1}{\left(1 - 2\frac{t}{D} + 2\left(\frac{t}{D}\right)^2\right)}\right] \tag{1}$$

and the shear strain γ would be given by

$$\gamma = \frac{\bar{r}\theta}{L} = \frac{\theta D}{2L}\left(1 - \frac{t}{D}\right) \tag{2}$$

where

M applied torque in inch-pounds

D outer diameter of tube

t thickness of tube

$\bar{r}$ mean radius $\left(\frac{D - t}{2}\right)$

θ angle of twist in gage length L

Shear stresses and strains computed by formulas (1) and (2) will not deviate significantly from the true average values, even at large plastic strains.

Nickel tubing TRF, which had been cold-reduced 75 to 80 percent in area and normalized at 500° F during manufacture, was soft-annealed at 1450° F. (See reference 6.) Individual specimens then were extended various amounts ranging nominally from 0.5 to 10.0 percent, respectively. These specimens are described in table 3. Shear proof stress values derived from shear stress-set curves measured upon these specimens are plotted in figure 17A. The amount of extension expressed as equivalent reduction of area is plotted as abscissa. The experimentally derived points are connected by straight lines. A smooth curve drawn through the experimentally derived points would not deviate greatly from these lines. With increasing extension the 0.1- and 0.03-percent shear proof stresses show a slight initial rise; the lower proof stresses exhibit an initial decrease. At greater extensions all proof stresses rise; this rise is most rapid at the greater values of set. Figure 17B shows

shear proof stresses obtained with nickel tubing cold-reduced 10, 20, 30, 40, and 75 to 80 percent during manufacture. The amount of cold reduction in cross section is plotted as abscissa. The symbols denoting the various cold-reduced grades are marked in the diagram along corresponding abscissa. Proof stresses for the fully annealed nickel specimens are plotted at zero equivalent reduction of area in both figures 17A and 17B. Solid lines connecting the points representing the various cold reductions would correspond closely to the actual variation of these proof stresses.

The initial decrease of the lower proof stresses with extension of the annealed metal (fig. 17A) probably is due to an increase of internal stress. The subsequent rise of proof stress with extension (fig. 17A) and the rise with cold reduction (fig. 17B) may be attributed to the lattice-expansion factor.

5. Influence of Plastic Deformation on the Elastic Strength of Monel, Aluminum-Monel, Inconel, and Copper

The variation of tensile proof stress with prior plastic extension as determined upon a specimen of cold-drawn monel rod, soft-annealed at 1400° F (G-14) is shown in figure 9. (See reference 2.) The methods of testing, with intervening (varying) extensions, were similar to those employed upon nickel specimen R-14. These tests are described at length in an earlier report. (See reference 2.) The heat treatment is described in table 2.

A series of cold-reduced monel tubular specimens TGE was soft-annealed at 1400° F and was then extended a chosen amount, which ranged from 0.5 to 10 percent. Figure 10A shows the variation of the proof stress with equivalent reduction, as obtained from single tests on each of the extended annealed specimens.

Figure 10B shows the tensile proof stresses for the various cold-reduced grades of monel tubing, plotted against the amount of cold reduction. Values for annealed monel TGE are plotted at zero reduction in each diagram. The specimens used in deriving figure 10 are described in table 3.

With tensile extension (figs. 9 and 10A), the proof stresses generally exhibit an initial small decrease, followed by a rise; this rise is most rapid for the higher proof stresses. With cold reduction (fig. 10B) all proof stresses rise continuously. The initial decrease may be attributed to the influence of induced internal stress. The subsequent rise with tensile extension and the rise with cold reduction probably are due to lattice expansion, that is, work-hardening.

Figure 18A shows the variation of shear proof stress with equivalent reduction as measured by single tests upon each of a series of cold-reduced monel tubular specimens TGE, which were soft-annealed at 1400° F and then each extended a different amount before test. Figure 18B shows the variation of shear proof stress with cold reduction for the several grades of cold-reduced monel tubing. These tests were described in an earlier report. (See reference 6.) The specimens tested are described in table 3. With extension (fig. 18A), there occurs an initial drop in all shear proof stresses owing to dominance of induced internal stress. This is followed by a rise, due to dominance of lattice expansion. The rise with increasing cold reduction in figure 18B is likewise ascribed to lattice expansion.

With extension of annealed aluminum-monel tubing, THD (fig. 11A), the tensile proof stresses exhibit an initial decrease followed by an increase. The variation is similar to that obtained with extension of annealed monel rod (fig. 9) and tubing (fig. 10A). With increasing cold reduction (fig. 11B), all proof stresses for this metal rise. Values for the laboratory- and factory-annealed tubing are plotted at zero reduction of area; broken lines connect these points with points representing the smallest cold reduction. This diagram is similar to that obtained with monel tubing (fig. 10B).

The shear proof stresses first decrease and later increase, with increase of extension of annealed aluminum-monel tubing THD as shown in figure 19A. (See also reference 6.) With cold reduction of aluminum-monel (fig. 19B), all shear proof stresses rise. Values for the laboratory- and factory-annealed specimens are plotted at zero reduction; broken lines connect these points with points representing the smallest cold reductions. These diagrams are in many respects similar to those obtained upon nickel tubing (fig. 17).

The variation with extension of the tensile proof stresses of a single Inconel rod specimen (L), cold-drawn and annealed at 1750° F, is shown in figure 12. (See also reference 2.) Figure 13 shows the variation of tensile proof stress with extension of Inconel tubing TLD, annealed at 1750° F, and with cold-reduction of Inconel tubing TL as measured upon a series of single specimens prepared in a manner similar to that employed in the tests on nickel, monel, and aluminum-monel tubing. The rod specimen L-17.5 is described in table 2, the tubular specimens in table 3.

With tensile extension of annealed Inconel (figs. 12 and 13A), there is exhibited an initial decrease in all tensile proof stresses, followed by a rise similar to that found for monel and aluminum-monel. With cold reduction (fig. 13B), all proof stresses rise. Values for the laboratory-annealed specimens lie somewhat above those for the factory-annealed product. This difference possibly is due to a

straightening operation given this metal following factory annealing, thereby inducing some internal stress. The initial decrease of proof stress with extension can be attributed to induced internal stress; the subsequent rise with tensile extension and the rise with cold reduction may be attributed to lattice expansion.

With increase of tensile extension of soft-annealed Inconel tubing TLD (fig. 20A), the shear proof stress exhibits an initial decrease followed by a rise, similar to that obtained with other metals. With increase of cold reduction of Inconel (fig. 20B), the shear proof stresses rise in a manner similar to that obtained with aluminum-monel metal (fig. 19B). Values for both the laboratory- and factory-annealed specimens are plotted at zero reduction of area, and broken lines connect these points with points representing the smallest cold reductions. The actual variation of the shear proof stresses over this range may deviate appreciably from such an indicated linear relationship. The solid lines connecting the points representing the various cold reductions would correspond more nearly to the actual variation of these proof stresses.

A specimen of cold-rolled copper rod N was annealed at 600° F (references 2 and 7), according to the treatment given in table 2. Correlated tensile stress-strain and stress-set curves were obtained upon this specimen at intervals between extension increments, similar to the method employed with annealed nickel, monel, and Inconel rod.

In figure 14A is shown a plot of tensile proof stress versus the amount of prior extension of the annealed copper rod N-6. All proof stresses exhibit a rise with extension. The proof stress values for 0.001- and 0.003-percent set, however, oscillate somewhat about their mean positions, in a manner similar to that obtained with extension of other annealed rod materials. Lattice expansion or work-hardening evidently dominates throughout this rise.

In figure 14B is shown the variation of proof stress with extension for cold-rolled copper rod N (references 2 and 7). This material had been reduced 75 percent in area of cross section (300-percent equivalent extension) during manufacture, without intermediate anneal. This diagram is typical of that obtained with extension of severely cold-worked metals. An initial small extension produces a large rise of proof stress, especially for the lower values of set, due to relief of internal stress induced during the cold-rolling. With succeeding small extensions, the lower proof stresses oscillate over wide ranges. As the extension at maximum load is small, about 1 percent, negligible work-hardening would occur up to this point. Extended discussion of the influence of extension upon the proof stresses of many cold-worked metals is found in the earlier reports (references 1, 2, and 7).

6. The Effect of Plastic Deformation on the Elastic Strength of Two Stainless Steels

Two types of chromium-nickel stainless steels were studied in this investigation. One steel, composed principally of 13-percent chromium and about 2-percent nickel, is a heat treatable stainless steel possessing deep hardening characteristics. (See reference 2.) The tensile-elastic properties were obtained of this steel in its softest condition, and also after air-cooling from 1750° F and tempering at various temperatures, followed by furnace cooling. The softest condition is obtained by holding at a temperature of about 1260° F, followed by furnace cooling. This material was obtained from the manufacturer in the softest condition.

The other steel studied was 18:8 chromium-nickel steel. This alloy usually is austenitic at room temperature although structural changes may occur at low temperatures or from long exposure to elevated temperatures. Commercial hardening is generally produced by cold-work. It may be softened by water quenching from above 1800° F. This high temperature is used in order to prevent intergranular precipitation of carbides. An extended investigation has been carried on with this alloy in both the annealed and cold-worked conditions, and for several different compositions (references 1 and 2). A specimen of the soft "as-received" 13:2 Cr-Ni steel rod was extended by small stages to the beginning of local contraction; after each of the stages, correlated stress-strain and stress-set curves were determined. (See reference 2.)

Figure 15 shows the variation with extension of the tensile proof stresses of this material. With extension, all proof stresses show an initial sharp rise. At greater extensions, the proof stresses for the smaller values of permanent set oscillate between high and low values; the low points generally correspond to the larger prior rest intervals. At various stages of the test, the specimen was loaded cyclically between 1000 and 80,000 psi, nominal[1] stress, immediately preceding a stress-set curve. The proof stress values obtained from such curves are indicated by diamond-shaped symbols in the diagram. These generally are at high points in figure 15; whereas low values generally are found following long rest intervals. The basic proof stress-extension curves would tend to rise continuously with extension.

The general rise of proof stress may be attributed to work-hardening. Part of the oscillation is due to variation of induced internal stress. However, high values of proof stress generally follow short rest intervals

[1]The nominal stress, as differentiated from the true stress, is calculated by dividing the load by the original cross sectional gage area of the specimen.

because appreciable negative creep was not permitted to occur after the preceding stress cycle; this, in turn, tends to diminish the amount of positive creep during measurement, especially at the lower values of set.

A specimen of 18:8 Cr-Ni steel rod DM, which had been cold-drawn to a moderate degree (designated half-hard) was water-quenched from 1830° F in order to place it in its softest condition. (See reference 2.) Details of heat treatment are given in table 2. Stress-strain and stress-set curves were then obtained with this specimen (DM-18.3) as annealed, and at intervals between successive stages of extension, in a manner similar to the tests on other rod specimens.

With prior extension, the 0.1-, 0.03- and 0.01-percent proof stress curves (fig. 16) show a continuous rise. The 0.003-percent proof stress curve also exhibits a slight rise, although this rise is nearly masked by the wide fluctuation of values. The 0.001-percent proof stress curve rises during early extension but exhibits no rise at greater extensions; it likewise fluctuates appreciably. Otherwise, the curves are similar to those obtained upon other metals. Apparently lattice expansion predominates during early extension, as evidenced by a steady rise of proof stress. The wide fluctuations of proof stress give evidence of large variations of internal stress superimposed upon the normal effect of difference in rest interval.

In earlier tests, not described here (references 1, 2, and 7), upon cold-drawn 18:8 Cr-Ni steel, as well as on other cold-drawn metals, it was found that extension of these specimens gave fluctuations of proof stress appreciably greater than those obtained during extension of annealed metal. This indicates a wider variation of internal stress in the cold-worked metal.

Slight prestretching of cold-worked specimens of both nonferrous metals and stainless steel generally gave some elevation of the several proof stresses, owing to relief of internal stress.

In an investigation not connected with this project, the authors studied the effect of prior plastic deformation on the tensile proof stresses of annealed 0.04-percent carbon steel. (See reference 7.) The forms of the basic curves, and the fluctuations due to rest interval and extension spacing were similar to those obtained with the nonferrous metals and chromium-nickel steels studied here. It was found, however, that the intermittent method of measuring series of stress-strain and stress-set curves on those steels produced appreciable age-hardening additional to that obtained in ordinary tension tests to fracture.

Next to be considered is the effect of plastic deformation on the shear elastic strength of the 18:8 alloy. A number of specimens of cold-drawn 18:8 Cr-Ni steel tubing TC were water-quenched from 1900° F

and each then extended a different amount, ranging from 0.5 to 20 percent, respectively. A description of these specimens is given in table 3. Shear stress-strain and stress-set curves were measured upon each specimen and upon an unextended annealed specimen.

Figure 21 shows the variation of shear proof stress with prior plastic extension of annealed 18:8 Cr-Ni steel tubing TC-19. The 0.1-, 0.03-, and 0.01-percent shear proof stresses rise continuously with extension. The curve for 0.001-percent set, however, decreases to a minimum for small values of extension and rises only slightly with subsequent extension. These variations are qualitatively similar to those obtained in the curves of tensile proof stress for some metals.

The increase of internal stress with extension probably predominates in causing the initial decrease of the 0.001-percent proof stress. The rise with extension of the remaining proof stresses may be attributed to the dominant influence of the lattice-expansion factor. Since separate specimens were used, these curves are devoid of the fluctuation due to influence of extension spacing and rest interval.

A number of other tests were also made upon factory annealed, half-hard and hard grades of 18:8 Cr-Ni steel tubing, in order to determine the effect of prior torsion upon their shear elastic properties.

The influence of prior plastic torsion was found to be in many respects similar to the effects of prior extension; these results are given in an earlier report. (See reference 4.)

7. Various Strength Indices for Nonferrous Metals and Chromium-Nickel Steels

From the proof stress values enumerated above may be evaluated the "proof-stress ratio," and the tensile and shear "work-hardening rates."

The proof-stress ratio may be defined as the ratio of tensile to shear "yield stress." In figure 22, this ratio for 0.1-percent set is plotted against the amount of cold work received, expressed as reduction of area, for the various nonferrous tubular metals. This ratio may be considered only as an empirical value, because equivalent nominal (0.1 percent) sets in tension and shear are not directly comparable. On the left side of the diagram are found values obtained with annealed tubing, in the center values for cold-drawn tubing, and on the right for tubing work-hardened by the tube-reducer method. (See table 3.) Generally lower values of this ratio are obtained in the middle range of the reduction of area. The high values obtained with nickel and monel at 75-percent reduction of area (300-percent equivalent extension) might be

associated with directional effects due to preferred crystal orientation in these metals. (See pt. VI of this paper and references 2, 4, 6, and 7.) Factory annealing of aluminum-monel and Inconel tubing gave lower values for this ratio than did laboratory annealed tubing.

Another important index is the work-hardening rate, as represented by the ratio between the yield stress after slight plastic extension and the initial yield stress, for the soft-annealed metal. Such indices have been obtained from curves for the 0.1-percent proof stress by determining the ratio between the proof stress at 3-percent equivalent reduction (3.1-percent extension) and the initial proof stress. Values obtained from tensile and shear proof stress curves are given in table 5 for rod and tubular materials.

It will be noted that the highest work-hardening rate for nonferrous metals is obtained in tension with copper rod, followed in order by nickel, Inconel, monel, and aluminum-monel. In shear, the highest rate is obtained with nickel, followed in order by monel, Inconel, and aluminum-monel. For nickel, the tensile work-hardening rate is greater for the tubular than for the rod material; for Inconel the rod material has the larger rate. These differences, however, are too small to be significant. The work-hardening rate for nickel is somewhat greater in shear than in tension; for aluminum-monel and Inconel the tensile work-hardening rate is slightly larger. Monel gives work-hardening rates which are nearly equivalent for the various testing methods used; this is likewise true for 18:8 Cr-Ni steel.

V. INFLUENCE OF ANNEALING TEMPERATURE ON THE ELASTIC STRENGTH OF METALS

Annealing of cold-worked metals at temperatures below the recrystallization range will sometimes produce an improvement of elastic properties above those obtained on the unannealed metals. In order to determine the variation of proof stresses over the whole annealing temperature range, individual specimens of each of the several cold-worked metals were annealed at different temperatures distributed over this range, before measuring stress-strain and stress-set curves. First, a detailed study will be made of the effect of annealing temperature on the elastic strength of cold-worked nickel, followed by comparative studies of other metals.

1. Influence of Annealing Temperature on the Tensile Elastic Strength of Nickel Rod and Tubing

Figure 23A shows the variation of tensile proof stress with annealing temperature for nickel rod R, cold-drawn 60 percent in reduction

of area during manufacture. The heat treatments of the various rod specimens are described in table 2. Smooth curves have been drawn through the mean positions of the points.

With increase of annealing temperature, all proof stresses rise, reaching a maximum at about 400° F for the 0.10-percent proof stress, and at about 500° F for the remaining proof stresses; the rise of the 0.10-percent proof stress is the slowest. With further increase of annealing temperature, the tensile proof stresses decrease; the maximum rate of decrease is between 1100° and 1200° F, that is, in the recrystallization range. The position of the 0.001-percent proof stress curve is not well defined because the error of estimation of this value is evidently quite large. The initial rise may be attributed to relief of deleterious internal stress, the subsequent decrease to the removal of lattice expansion and to recrystallization.

In figure 24B is shown the variation of tensile proof stress with annealing temperature for nickel tubing TRE, cold-reduced 75 to 80 percent. Proof stress values obtained upon a soft-annealed specimen TRF are replotted from figure 8 at 1450° F. A description of the heat treatments of the various tubular specimens is given in table 3.

With increase of annealing temperature, all proof stresses rise, reaching a maximum at about 900° F, for the 0.001-percent proof stress and at 700° F for the remaining proof stresses; the rise of the 0.1-percent proof stress is very slight. With further increase of temperature, all proof stresses decrease and the decrease is at a maximum rate between 1100° F and 1200° F. This diagram is somewhat similar to that obtained for cold-drawn nickel rod (fig. 23A).

2. Influence of Annealing Temperature on the Shear Elastic Strength of Nickel Tubing

In figure 28B is shown the variation of the shear proof stress with annealing temperature for nickel tubing. (See reference 6.) These values were derived from tests on a series of specimens of cold-reduced nickel tubing TRF, which had been reduced 75 to 80 percent during manufacture and annealed in the laboratory at various temperatures. Values obtained upon an unannealed specimen are plotted at 100° F and those for a soft-annealed specimen TRF are replotted from figure 17 at 1450° F.

With increase of annealing temperature there is a continuous decrease of shear proof stress; this decrease is most rapid between 1100° and 1200° F. This decrease may be attributed to the dominant influence of relief of lattice expansion, and to recrystallization.

3. Influence of Annealing Temperature on the Elastic Strength of Monel, Aluminum-Monel, Inconel, and Copper

Figure 23B shows the variation of tensile proof stress with annealing temperature for cold-drawn monel rod G (reference 2); figure 24A gives a similar diagram for cold-reduced monel tubing TGD. With increase of annealing temperature, the proof stresses rise, reaching a maximum at 500° F for the 0.1-percent proof stress, and at higher temperatures for some of the lower proof stresses. The subsequent decrease in proof stress is most rapid above 1100° F for monel rod (fig. 23B), and above 1200° F for monel tubing (fig. 24A).

The initial rise in proof stress may be attributed to the predominant influence of relief of internal stress, the subsequent decrease to removal of lattice expension and to recrystallization. Although tubing TGD had received nominally the same cold work as had rod G, the latter shows a somewhat greater value of the 0.1-percent proof stress. Possibly equivalent reduction by different methods will not produce equivalent work-hardening. This apparent anamoly, however, may also be partly explained by differences in composition. A greater hardness of the rod material is also indicated by its lower recrystallization temperature range (above 1100° F). In many respects the tensile proof stress curves are similar to those for nickel.

Figure 28A shows the variation of shear proof stress with annealing temperature, for cold-reduced monel tubing TGD. (See reference 6.) The forms of these curves are in many respects similar to the curves for tensile proof stress for this metal (figs. 23B and 24A). The shear proof stresses, as would be expected, are nominally much lower than the tensile proof stresses.

With increase of annealing temperature for aluminum-monel metal tubing TH (fig. 25B), there are obtained maxima in the various tensile proof stresses, ranging from 1000° to 1075° F. There are also lower maxima in the temperature range 400° to 600° F. The upper maxima are due to precipitation-hardening, the lower maxima to relief of internal stress. All proof stresses drop rapidly for annealing temperatures above 1075° F, owing to the recrystallization.

With increase of the temperature of annealing aluminum-monel tubing (fig. 29B) there are obtained two maxima in the shear proof stress curves. (See reference 6.) The first and lower maximum due to internal stress relief, is obtained in the range 400° to 500° F. The second and higher maximum is obtained at 1075° F and is attributed to precipitation hardening of this alloy. At temperatures above 1075° F the shear proof stress drops rapidly, owing to recrystallization and to removal of lattice expansion.

Figure 26A shows the variation of the tensile proof stresses with annealing temperature for cold-drawn Inconel rod L. (See reference 2.) One unannealed cold-drawn specimen was tested shortly after manufacture of this material; a second was tested 40 months later. The time interval between receipt of the metal and the annealing of the specimens was from 26 to 39 months; between the receipt and the testing, the interval was 32 to 41 months. Results from tests on both specimens are plotted on the diagram. Smooth curves have been faired through the experimental points.

The 0.1-percent tensile proof stress value obtained in the early test on cold-drawn metal is somewhat greater than any other value on the diagram. The 0.001- and 0.003-percent proof stress values for this specimen, however, are somewhat lower than those obtained with the cold-drawn specimen tested 40 months later. Consideration of the values obtained in the early test will be deferred until after consideration of the remainder of the diagram. All proof stresses rise with increase of annealing temperature up to 800° F; at higher temperatures the proof stresses drop continuously. The most rapid drop is between 1100° and 1400° F. The initial rise of proof stress is attributed to relief of internal stress, the subsequent lowering to the removal of lattice-expansion effects and to recrystallization.

Apparently, the Inconel rod, as-received, had been severely cold-drawn, and probably contained considerable internal stress. The 40-month storage period probably caused a partial relief of internal stress and likewise a partial removal of lattice expansion. This relief of internal stress produced the increase of the 0.001- and 0.003-percent proof stresses; whereas the removal of lattice expansion produced the decrease of the 0.1- and 0.03-percent proof stresses.

With increase of temperature of annealing cold-reduced Inconel tubing TLC (fig. 25A), there are obtained maxima in the tensile proof stress curves between 700° and 1100° F. The rise to these maxima may be attributed to relief of internal stress; the subsequent lowering to removal of lattice expansion.

With increase of the temperature of annealing cold-reduced Inconel tubing TLC (fig. 29A), up to 600° or 700° F, there is a rise of shear proof stress; the subsequent decrease is most marked between 1100° and 1300° F. This diagram is similar to those obtained with nickel and monel tubing (fig. 28).

4. Influence of Annealing or Tempering Temperature on the Elastic Strength of Chromium-Nickel Stainless Steel

Figure 26B shows the variation of the tensile proof stress with tempering temperature for 13:2 Cr-Ni steel. (See reference 2.) Details of the heat treatments are given in table 2. Values obtained upon the specimen tested as-received are plotted at 1260° F. Curves are faired through the mean position of the points; because of the fluctuation of values, the positions of such curves must not be considered exact.

With increase of the tempering temperature, all proof stresses rise, reaching a maximum near 700° F. With further temperature increase, the proof stresses decrease to a minimum between 1300° and 1400° F, and then increase somewhat with rise in temperature up to 1750° F. It is therefore seen, that even with a controlled decelerated rate of furnace cooling from above 1400° F, some hardening of the material occurred. This material can be softened only by holding slightly below the transformation temperature.

The initial rise of proof stress with tempering temperature is due to relief of internal stress, the subsequent lowering is due to recrystallization. Internal stress evidently is produced even with air-hardening.

Some specimens of half-hard 18:8 Cr-Ni steel rod DM were annealed at various temperatures ranging from 500° to 1025° F for 1/2 hour. (See reference 2.) Another specimen was annealed for 44 hours at 482° F (250° C). Details of heat treatments are given in table 2. Correlated stress-strain and stress-set curves were measured on each specimen. The variation of proof stress with annealing temperature is shown in figure 27A. Values for the unextended, annealed specimen DM-18.3 are plotted at 1830° F and for an unannealed specimen at 100° F. Curves are faired through the mean positions of the points.

With increase of annealing temperature, there is a marked rise of proof stress, reaching a maximum between 800° and 900° F. No data were obtained for specimens annealed between 1025° and 1830° F; however, the curves have been drawn in this region according to the variation generally obtained with this alloy, so as to exhibit a rapid decrease between 1025° and 1300° F. The initial rise is due to relief of internal stress, the subsequent decrease to relief of lattice expansion and to recrystallization. Annealing at 482° F for an extended period gave little greater proof stress values than those obtained by the short-time anneal at 500° F. This result appears to indicate that greatly increasing the annealing time has not produced any gain in elastic strength.

Other tests discussed previously (reference 2) show that prestretching of stress-relief annealed 18:8 Cr-Ni steel specimens gave slight

improvement in proof stresses, additional to that obtained by the annealing treatment; this indicated that all internal stress was not relieved by such annealing treatment. Such an improvement of proof stress was not generally obtained with slight prestretching of stress-relief annealed nonferrous metals.

In studying the elastic properties of 18:8 Cr-Ni steel, some tests were made at sub-zero temperature, in order to determine the effect of variation of test temperature on the tensile elastic properties. For this purpose a series of half-hard 18:8 Cr-Ni steel rod specimens, DM, were annealed at 500°, 700°, 900°, and 1830° F for 1/2 hour, as indicated in table 2. These specimens and an unannealed specimen were tested at -110° F (-78.5° C) according to methods described in an earlier report. (See reference 3.) The extensometer and insulated chamber used are shown in figure 2.

Figure 27B shows the variation of the low temperature tensile proof stress with annealing temperature for this alloy. Comparison with figure 27A for room temperature tests indicates that the curves are similar in form, but generally give somewhat higher proof stresses. A similar rise of proof stress with decrease of test temperature was also obtained upon a severely cold-drawn 18:8 Cr-Ni steel rod. (See reference 3.)

Figure 30 shows the variation of the shear proof stress with the temperature of annealing cold-drawn 18:8 Cr-Ni steel tubing TC as measured at room temperature. There is a rise of shear proof stress with increase of annealing temperature up to 900° F, owing to induced internal stress. At higher temperatures, the shear proof stress decreases, the most rapid drop occurring near 1300° F. The approximate course of the curves in the range 1300° to 1900° F have been indicated by broken lines; no specimens were annealed in this interval. The subsequent drop of proof stress may be attributed to relief of lattice expansion and to recrystallization.

VI. INFLUENCE OF PRIOR PLASTIC DEFORMATION ON THE MODULUS OF ELASTICITY AND ITS LINEAR STRESS COEFFICIENT FOR VARIOUS METALS

1. Influence of Plastic Extension on the Stress-Deviation Curve and Derived Indices for Annealed Nickel Rod

An incomplete view of the elastic properties of a metal is obtained by considering only its stress-set relationship. Consideration should be given also to the influence of stress on the accompanying total strain and on the elastic strain. These relations are revealed by the stress-

deviation curves for nickel and by derived curves and indices. A comparative study later will be made upon other metals.

Stress-deviation curves for annealed nickel rod R-14 are shown in the upper row of figure 5. Curve 9 of this group is identical with the stress-deviation curve in figure 4B. On some of these curves, as well as on scattered stress-deviation curves for some other metals (not given in this report), are plotted strain values at stresses other than those corresponding to upper loads in the various stress cycles. The additional data were obtained following pauses of 2-minute duration at these stresses during the increase of load in the various cycles. They permitted considerable additional data to be secured, without greatly extending the test time. These additional strain values shown in figure 5 are not replotted in figure 4, although they were employed in drawing the uncorrected stress-strain and stress-deviation curves.

The solid line (corrected) curve in figure 4B is obtained by subtracting from the broken line curve, the amounts of permanent set at the same stress values in the curve in figure 4C. The solid line curves in the upper row in figure 5 are similarly obtained by using the adjacent broken-line stress-deviation curves and the stress-set curves immediately below.

Since the lines are plotted as deviation from a fixed modulus ($E_A = 32 \times 10^6$ psi) on an open scale, the strain scale is sensitive enough to reveal a curvature in most of these lines. The assumed modulus value selected causes some of the curves to show an initial backward tilt. There is a tendency for the first curve of a pair to be steeper than the second. From the shape of these curves, it is apparent that the modulus of elasticity decreases continuously with increase of stress. The secant modulus, given by the ratio of the stress to elastic strain, is used to study the variation of the modulus with stress, and with prior plastic extension.

Figure 4B illustrates the method of calculating the secant modulus from the corrected stress-deviation curve. In order to calculate the secant modulus at 25,000 psi, a straight line is drawn from the origin A through the intersection B. This line extended, intersects the 32,000-psi ordinate CD at E. The distance CE may be used to compute the modulus as follows: The strain corresponding to a modulus of 32×10^6 psi at a stress of 32,000 psi would be 0.1 percent. The distance CE has a value of 0.012 percent. The secant modulus at 25,000 psi would therefore be equal to 32,000 divided by 0.00112, that is, 28.53 million psi. By repeating this procedure of measuring the projection on line CD of lines intersecting the stress-deviation curve at various selected stresses, the variation of the secant modulus with stress can be evaluated.

Graphs of variation of the secant modulus of elasticity with stress, derived from the corrected stress-deviation curves in figure 5, are shown in figure 6. The lines are numbered consecutively in each figure to correspond to the stress-deviation curves from which they were derived. Each stress-modulus line has been shifted to the right from the preceding line, and has been given a separate abscissa scale; the scale of abscissa is indicated. Abscissas reading from left to right represent values of the secant modulus of elasticity (in million pounds per square inch). Ordinates represent stress. The points on the curves in figure 6 correspond to the selected points on the corrected stress-deviation curves at which the modulus was computed, not to stresses at which strains were observed. The prior plastic extension corresponding to each stress-modulus line is indicated in the derived diagram (fig. 35) at the correspondingly numbered point.

In the consecutive series of stress-modulus lines for fully annealed nickel rod (fig. 6) lines 1, 3, 4, 6, 7, and 8 are curved throughout their extent. Lines 2 and 3 are curved only at the higher values of stress. The other lines in the figure are approximately straight. The prior plastic extension beyond which all stress-modulus lines are straight is about 4 percent (fig. 35). It will be shown later that many annealed metals give straight stress-modulus lines only after being extended somewhat.

The modulus of elasticity at zero stress (E_0) may be determined directly from the stress-modulus line by extrapolating the line to zero stress. When the stress-modulus line is straight, the variation of the secant modulus (E) with stress (S) may be represented by

$$E = E_0 (1 - C_0 S) \tag{3}$$

where C_0 represents the linear stress coefficient of the secant modulus. When the stress-modulus line is curved from the origin, the equation would include terms containing higher powers of S. In earlier reports (references 1, 2, 4, and 7) a second coefficient C', of the square of S was evaluated. Since the curved stress-modulus lines generally do not represent true quadratic equations it has been considered desirable to evaluate the modulus at zero stress E_0, the linear stress coefficient of the modulus at zero stress, C_0, and the modulus at one or more elevated values of stress. It should be noted that some of the curved stress-modulus lines for nickel give a value of zero for C_0.

When a stress-modulus line is straight the corrected stress-strain curve would be represented by

$$\epsilon = S/E = \frac{S}{E_0(1 - C_0 S)} \tag{4}$$

where ϵ is the corrected strain. Since the correction term C_0S is generally small compared with 1, equation (2) may be written

$$\epsilon = (1/E_0)(S + C_0S^2) \tag{5}$$

the equation for a quadratic parabola. For annealed nickel extended more than 4 percent, therefore, the stress-strain line evidently would be a quadratic parabola; at smaller prior extensions the line would be a curve of higher order.

The diagram in figure 35 has been derived from values of E_0, C_0, and the modulus at 30,000 psi, E_{30}. Abscissas represent percentages of prior plastic extension. The ordinate scale for values of the modulus of elasticity is given on the left-hand border, and for the linear stress-coefficient, C_0, on the right-hand border.

The experimentally determined points in figure 35 are numbered to correspond to the consecutively numbered stress-modulus lines in figure 6, and to the consecutively numbered stress-deviation lines in figure 5. The points in figure 35 give a curve consisting of oscillations superposed on a smooth basic curve (not shown). The oscillations in the curve for C_0 is generally qualitatively similar to those in the curve of E_0, and is due to variations of extension spacing and rest interval. The more abrupt of the oscillations in figure 35 generally are associated with opposite oscillations in the proof stress-extension curves for this specimen (fig. 7). This is in accordance with the fact that the difference in steepness of the corrected stress-deviation curves of a pair generally is associated with an opposite difference in steepness of the corresponding stress-set curves. Increase of the rest interval apparently tends to decrease the slope of the stress-set curve and to increase the initial slope (E_0) and curvature (C_0) of the corrected stress-deviation curve. The basic curve for E_0 is indicated qualitatively in figure 35 by the dotted line. The basic C_0 and E_{30} curves are so clearly indicated by the sequence of experimentally determined points, that no dotted curves are needed.

The basic E_0 curve (fig. 35) first descends rapidly at a decreasing rate and reaches a minimum at slight plastic extension. With further extension, the curve rises rapidly above the value at zero plastic extension and continues to rise at a gradually decreasing rate. At the beginning of local contraction (35-percent extension), the E_0 curve is still rising slowly, and is considerably higher than at zero plastic extension. The value of E_0 at beginning local contraction is about the

same as that for the severely cold-drawn nickel, R (fig. 35).[1] Curve E_{30} rises steadily at a decreasing rate, over the indicated range for which it could be measured. Curve C_0 rises rapidly in a manner similar to the E_0 curve, between points 7 and 9. Beyond point 9, however, C_0 descends at a decreasing rate.

The variation of the modulus of elasticity and its linear stress coefficient, C_0, with plastic deformation or with heat treatment, is determined by the relative influence of certain fundamental factors: namely, (a) internal stress, and its distribution over the possible slip plane directions, (b) lattice expansion, and (c) preferred orientation. An extended discussion of the influence of these three factors is given in earlier reports. (See references 2, 4, and 7.) Induced internal stress tends to cause a rise in the tensile (E_0) or shear (G_0) moduli of metals. The magnitude of this effect, however, is determined by relative directions of the planes of maximum shear during prior deformation, and during subsequent modulus measurements; the effect will be greatest if the directions are parallel. The linear stress coefficient C_0 will likewise increase with increase of the induced internal stress.

Lattice expansion, or work-hardening, tends to cause lowering of the tension and shear moduli. It apparently is not directional in its effect, despite the earlier surmise that a possible difference in the amount of lattice expansion exists in directions normal to each other. Likewise, C_0 tends to decrease with increase of lattice expansion.

Cold deformation tends to orient the grains of a polycrystalline metal so as to aline certain crystalline planes along preferred directions. Owing to the large directional variation of the modulus within the crystals of many metals, such reorientation would tend to change the value of the modulus from that obtained when the grains are randomly oriented. Before studying the changes in relative dominance of the various factors upon the modulus, during extension of annealed nickel rod, a discussion will be given of the effect of crystal orientation on the elastic moduli of metals.

2. The Directional Variation of the Modulus of Single Crystals

As the metals considered in this report are either face-centered or body-centered cubic, only these two types of space lattice will be considered in the following discussion. The directional variation of the

[1]The short horizontal lines at the right-hand border of figure 35 indicate values obtained with unannealed cold-drawn nickel rod R. The horizontal arrows indicate values obtained with a cold-drawn nickel specimen that had been annealed for relief of internal stress at 500° F (R-5).

tensile and shear moduli in lattices of some metals of each of these types are illustrated by the diagrams in figures 31 to 34, which are adaptations of diagrams in reference 18. These diagrams are drawn with spherical coordinates having their origins at the intersection of the three mutually perpendicular axes of symmetry. The surface shown in each figure is the locus of all points representing (by distance and direction from the origin) values of the modulus of elasticity. The axes C represented in each figure are the cubic axes of symmetry.

In the discussion of crystal orientation, use will be made of the Miller indices of crystal planes and directions. A crystal plane is thereby denoted by a parentheses (---) with symbols, representing the reciprocals of the ratios of the intercepts of the three principal axes. A direction in a crystal is represented by a bracket [---] with the symbols of the crystal plane to which the direction is normal. A direction making equal angles with all three principal axes is denoted by [111] (octahedral), the direction of the cubic axes of symmetry by [100], and the dodecahedral by [110]. In figures 31 to 34 the principal crystal directions are denoted by letters, as explained in the key to these figures.

A typical diagram of variation of the tensile modulus of elasticity E of a face-centered cubic metal is the diagram for gold (fig. 31). The modulus for this metal is least in the direction of the cubic axes (C) and greatest in the direction of the octahedral axes (O). The ratio between the maximum and minimum values for gold, as given in reference 18, is 2.71. Diagrams for copper, silver, nickel, and several other face-centered cubic metals would be similar to figure 31. The diagram for another face-centered cubic metal, aluminum (fig. 32), however, is very different in form. As indicated by this nearly spherical diagram, the ratio of the modulus for octahedral and cubic directions is about 1.2. (See reference 18.) From strain measurements made in the present investigation, it is indicated that the space diagram for monel is probably more similar to that for aluminum (fig. 32) than to that for gold (fig. 31). The space diagrams for nickel, aluminum-monel, Inconel, and 18:8 Cr-Ni steel crystals, however, are probably similar to that for gold (fig. 31).

The diagram for a body-centered cubic metal, alpha iron, is shown in figure 33. This diagram is similar in form to figure 31, having a ratio of modulus values in the octahedral and cubic directions of 2.15. (See reference 18.) For tungsten, the corresponding ratio is about 1.0, so that its diagram would be nearly a sphere, like that for aluminum (fig. 32).

The directional variation of the shearing modulus (G), as illustrated by the diagram for alpha iron in figure 34, is opposite to that of the tensile modulus. The maximum value of the shearing modulus is

in the direction of the cubic axis (C), the minimum value in the direction of the octahedral axis (O). The ratios of values of the shear modulus in cubic and octahedral directions for the various metals are very nearly the same as the corresponding ratios of the tensile modulus in octahedral and cubic directions. When these ratios are considerably greater than 1, the production of preferred orientation would cause a marked variation of Poisson's ratio as obtained by the method described later in this report.

3. The Influence of Plastic Deformation on Crystal Orientation of Face-Centered Cubic Metals

An earlier report (reference 2) gave a comprehensive discussion of cylindrical and parallelopipedal deformation of both face-centered and body-centered cubic single crystals and polycrystalline aggregates. In this report, discussion will be limited to cylindrical deformation of polycrystalline aggregates, that is, deformation in which equal percentage changes occur in two dimensions and a necessarily opposite change in the third dimension. Such deformation is produced by extension or drawing.

Cylindrical deformation of a polycrystalline aggregate of a face-centered cubic metal causes some of the crystals to assume octahedral [111] orientation and others to assume cubic [100] orientation along the specimen axis. Ettisch, Polanyi, and Weissenberg (references 19 and 20) thus found that hard-drawn wires of such metals have double fiber texture. Sachs and Schiebold (reference 21), however, found that aluminum has almost entirely the octahedral [111] orientation. This conclusion was also verified by Schmid and Wasserman (referenence 22), who also found that the orientation textures of various face-centered cubic metals differ only in the proportions of the [111] and [100] orientations along the crystal axis. Copper was found to be predominantly octahedral [111], whereas silver was predominantly cubic [100]. Gold contained approximately equal proportions of the two orientations. Greenwood (reference 23) found cold-drawn nickel wires to have predominantly octahedral orientation. Cold-drawn monel has a similar orientation. (See reference 24.)

Although the orientation of cold-worked 18:8 Cr-Ni steel has not been determined by X-ray methods, the results of the present investigation suggest that it is predominantly cubic [100]. Such a conclusion is suggested by the appreciable rise of Poisson's ratio (as discussed later), as obtained by soft-annealing the cold-drawn alloy (fig. 68), a treatment that would change the crystal orientation from preferred to random distribution. As will be shown later, cold-drawn nickel, aluminum-monel, and Inconel tubing, however, exhibit a marked drop in Poisson's ratio, with soft-annealing, probably owing to the removal of preferred [111] orientation.

4. The Influence of Plastic Deformation on Crystal Orientation of Body-Centered Cubic Metals

As shown by Ettisch, Polanyi, and Weissenberg (reference 19) and others (reference 25), cold-drawn iron gives preferred dodecahedral [110] orientation in the axial direction. Such orientation was produced on iron, iron-silicon, and iron-vanadium alloys by drawing, or swaging plus drawing. (See reference 26.) Recrystallization would tend to reduce the amount of preferred orientation.

The only body-centered cubic metal included in this investigation is 13:2 Cr-Ni steel. With extension of the annealed alloy, the change of orientation from a random to a preferred [110] distribution would tend to produce only a small rise of the tensile modulus; such a tendency is not dominant over the range of extensions in figure 43. For annealed open-hearth iron, as studied earlier in another project at this laboratory (reference 7), the tendency to increase of the tensile modulus with extension was evidently small. Thus the effect upon the modulus of crystal reorientation is not so pronounced with body-centered cubic metals as with some face-centered cubic metals. A study of figure 33, together with the fact that the limiting extension of body-centered cubic metals is generally small, would account for the small influence of preferred orientation on the modulus of those metals.

5. Influence of Plastic Deformation on the Tensile Modulus of Elasticity and Its Linear Stress Coefficient for Nickel Rod and Tubing

The general rise of the tensile modulus E_0 with extension of annealed nickel R-14 (fig. 35) may be attributed to the dominant influence of the change of crystal orientation from random to preferred octahedral [111] orientation parallel to the specimen axis. Such orientation is obtained with cylindrical deformation of many face-centered cubic metals. The initial sharp drop of E_0 may be attributed to dominance of the work-hardening factor. The subsequent sharp rise of E_0 may be due in part to increasing internal stress, to which is attributed the initial rise of the C_0 curve. The subsequent descent of the C_0 curve is probably due to the dominant influence of lattice expansion.

Kawai (reference 27) found an initial sharp drop of the tensile modulus, followed by a slower rise, for nickel and copper. He erroneously attributed this initial drop to increasing internal stress and the subsequent rise correctly, at least in part, to preferred orientation. The effect of lattice expansion was not recognized in his work.

The variation of the tension modulus E, and its linear stress-coefficient C_0, with extension and cold reduction of tubing TR, is shown in figure 36. Proof stress curves for these specimens were given in figure 8. With extension of annealed nickel tubing TRF (fig. 36A), E_0 first decreases sharply, and then rises to a maximum, within the first 2-percent equivalent reduction. At greater extensions E_0 shows little variation; whereas E_{25} (the tension modulus at 25,000 psi) exhibits a continuous rise. With cold reduction of nickel tubing (fig. 36B), the tension modulus exhibits a general rise. With slight extension of annealed nickel tubing, TRF (fig. 36A), C_0 rises to a maximum at the same equivalent reduction at which E_0 reached a maximum. With cold reduction of nickel tubing (fig. 36B), C_0 rises to a maximum at moderate reduction, decreasing thereafter.

The initial sharp drop of E_0 with extension of annealed nickel tubing may be attributed to lattice expansion; whereas the subsequent sharp rise of E_0 and the rise of C_0 with initial extension may be attributed to dominance of induced internal stress. The rise of C_0 with cold reduction of nickel tubing probably is due to the same cause. The general rise of the modulus E with extension or cold reduction probably is due to the dominant influence of production of preferred octahedral [111] orientation parallel to the specimen axis. The drop in the C_0 curves after moderate deformation may be attributed to the effect of the lattice expansion.

In many respects the forms of the E and C_0 curves for extended annealed nickel tubing are qualitatively similar to those obtained for nickel rod. Such differences that appear to exist may be attributed to small differences in composition, to the form of the test specimens, to the use of a number of tubular specimens and a single rod specimen, and to experimental variations.

6. Influence of Plastic Deformation on the Shear Modulus of Elasticity and Its Linear Stress Coefficient for Nickel Tubing

The variation of the shear modulus of elasticity with extension of annealed nickel tubing and with cold reduction of nickel tubing is shown in figures 45A and 45B, respectively. Shear proof stress values for these specimens are given in figure 17. Values obtained for the fully annealed metal are plotted at zero equivalent reduction in both diagrams. The method of derivation of the shear modulus from the shear stress-strain and stress-set curves is similar to that employed in the derivation of tensile moduli.

The tensile modulus of nickel tubing (fig. 36) was derived for zero stress, and where possible, at 25,000 and at 50,000 psi. Nadai (reference 28) has suggested that the stress-strain curve for a metal in pure shear can be derived from its stress-strain curve in tension, by multiplying tension stresses by $1/\sqrt{3}$ and tension strains by 1.5. This relationship was derived for isotropic metals upon certain assumptions which are open to question. As a first approximation, however, it may be applied to many other metals. Therefore, shear modulus values were obtained at zero stress, and where possible, at 14,450 and 28,900 psi. These modulus values are to be utilized later in calculating Poisson's ratio for nickel tubing.

With extension of annealed nickel tubing TRF (fig. 45A), the shear modulus of elasticity, G_O, exhibits a sharp rise and decrease; at greater extensions little variation is noted. With increase of cold reduction of nickel tubing (fig. 45B), the shear modulus G exhibits an initial increase, followed by a decrease.

The fluctuations of the shear modulus with initial extension must not be considered significant, owing to the small stress range over which stress was measured. (See 0.1-percent proof stress, fig. 17A.) At greater extensions, however, where the stress range is greater, there appears to be a balance among the various factors affecting G. With increase of cold reduction (fig. 45A) up to 30 percent, the shear modulus rises, owing to the effect of induced internal stress. With subsequent cold reduction, the decrease of the shear modulus may be attributed to the combined dominant influence of lattice expansion and to the production of preferred [111] crystal orientation along the crystal axis; the reorientation factor would tend to cause a continuing decrease of the shear modulus, whereas it would tend to increase the tensile modulus.

With extension of annealed nickel tubing (fig. 45A), the linear stress coefficient of the shear modulus has a zero value over nearly the whole range; C_O reaches a maximum with 30-percent cold reduction of nickel tubing (fig. 45B) and then decreases. The initial rise of C_O with cold reduction may be attributed to the effect of induced internal stress, the subsequent decrease to the effect of lattice expansion.

7. Influence of Plastic Deformation on the Tensile and Shear Moduli of Elasticity for Monel, Aluminum-Monel, Inconel, and Copper

Figure 37 shows the variation of the tensile modulus E and its linear stress coefficient C_O with extension of annealed monel rod

G-14.[1] The tensile proof stress values for this specimen are shown in figure 9. E_0 shows little variation, whereas E_{25} and E_{50} exhibit a gradual rise. Evidently the various factors affecting E_0 are in near balance during such extension. The absolute values of the tensile modulus for monel, as would be expected, are less than those obtained with nickel. The modulus-extension curve for nickel rod had exhibited a general rise (fig. 35).

The linear stress coefficient of the tensile modulus, C_0, for annealed monel G-14 (fig. 37) exhibits a pronounced rise to a maximum during the first 10-percent extension, decreasing steadily thereafter. The rise is attributed to induced internal stress, the subsequent lowering to the dominant influence of lattice expansion. This C_0 curve is qualitatively similar to that obtained on annealed nickel (fig. 35).

With extension of annealed monel tubing TGE (fig. 38A) both E_0 and E_{25} first decrease and then increase; both changes are slight. With cold reduction of monel tubing (fig. 38B), the tension modulus increases slightly between 20- and 30-percent reduction; E_0 exhibits a small decrease at large reductions. Proof stress values for these specimens are given in figure 10. There evidently is a balance of influence of the various factors affecting the tensile modulus. The influence of preferred crystal orientation on the modulus of monel rod or tubing is evidently not so pronounced as upon nickel rod and tubing. This difference is probably not due to a lesser degree of preferred orientation obtained with monel, but rather to a smaller directional variation of the modulus of the monel crystal. The linear stress coefficient of the tensile modulus, C_0, for monel tubing remains zero during extension (fig. 38A), but rises to a maximum with 20-percent cold reduction (fig. 38B), decreasing thereafter. This rise is probably due to the dominant influence of induced internal stress.

With extension of annealed monel tubing TGE (fig. 46A) the shear moduli of elasticity, G_0 and $G_{14.45}$, both decrease. G_0, $G_{14.45}$, and $G_{28.8}$ all rise with increase of cold reduction of monel tubing (fig. 46B) from 10 to 20 percent and decrease continuously with further reduction to values below that obtained for the annealed metal. The initial rise with cold reduction of the shear modulus of monel tubing is ascribed to induced internal stress; the general decrease with extension and the subsequant decrease with reduction may be attributed to the dominant influence

[1]A correction of modulus values obtained from reference 2 was necessitated before plotting the corresponding diagrams in this report. Although diagrams showing the variation of the modulus were qualitatively correct in the earlier report, use of an important errata sheet attached to that report is required in order to obtain correct absolute values of the modulus.

of lattice expansion, and probably to a minor extent to the production of preferred octahedral [111] crystal orientation. With extension of annealed monel tubing, the linear stress coefficient of the shear modulus C_0 (fig. 46A) rises sharply and drops to zero within about $4\frac{1}{2}$-percent equivalent reduction. With cold reduction (fig. 46B) C_0 is zero for all grades except the monel cold-reduced 75 to 80 percent. The high values of C_0 give evidence of induced internal stress.

The tensile modulus of elasticity, E_0, for annealed aluminum-monel tubing THD (fig. 39A) exhibits an increase with small extension, whereas E_{25} decreases; these values become nearly constant with further extension. E_{50} exhibits a steady rise with extension of this tubing. Some rise of the tension modulus E is obtained for aluminum-monel tubing with increase of cold reduction from 40 to 60 percent (fig. 39B). No tubing was available having reductions less than 40 percent. For the annealed aluminum-monel tubing, the linear stress coefficient of the tension modulus, C_0 (fig. 39A), rises rapidly with extension. This rise, and the rise of E_0 with extension, may both be attributed to induced internal stress. The eventual rise of E with severe cold reduction of aluminum-monel tubing is probably due to the production of preferred octahedral [111] crystal orientation.

With increase in extension of annealed aluminum-monel tubing THD (fig. 47A), there is little variation of the shear modulus, G. With cold reduction of aluminum-monel tubing (fig. 47B), there is a continuous decrease of the shear modulus. Evidently there is a balance of influence of the various factors affecting G during extension. The lowering of the shear modulus with reduction may be attributed to lattice expansion, and probably in part to the production of preferred octahedral [111] crystal orientation.

The linear stress coefficient of the shear modulus, C_0, exhibits a rise during extension of annealed aluminum-monel tubing, THD (fig. 47A), owing to induced internal stress. With cold reduction (fig. 47B), the value of C_0 remains small.

With increase of extension of annealed Inconel rod, L-17.5 (fig. 40), there is a successive rapid rise and decrease of the tension modulus E_0, followed by a slower rise. E_{25} and E_{50} show a steady rise for prior extension greater than 4 percent. The initial rise of E_0 is probably due to relief of internal stress, the subsequent decrease to lattice expansion. The eventual rise may be attributed to dominance of the production of preferred octahedral [111] orientation along the specimen axis. A sharp rise of C_0 is obtained during early extension, owing to induced internal stress, followed by a steady decrease, due to lattice expansion.

With extension of annealed Inconel tubing TLD (fig. 41A), E_0 rises sharply to a maximum, and later approaches a constant value; E_{25} and E_{50} rise steadily from the low value measured at small extensions. With cold reduction of Inconel tubing (fig. 41B), the tension modulus exhibits a sharp rise between 50- and 75-percent reduction. Tubing cold-worked to smaller reduction was not available. The value of the tension modulus for the laboratory annealed Inconel is larger than that obtained for the corresponding factory-annealed product TLA. This same relationship was also observed for aluminum-monel tubing (fig. 39). The linear stress coefficient of the tensile modulus C_0 rises sharply with extension (fig. 41A), owing to induced internal stress.

With increase of extension of soft-annealed Inconel tubing TLD (fig. 48A), there is a continuous decrease of the shear modulus. A continuous decrease is likewise obtained with cold reduction of this metal (fig. 48B). This general decrease may be attributed to the combined dominant influence of lattice expansion and to the production of preferred octahedral [111] crystal orientation along the specimen axis. With early extension of annealed Inconel (fig. 48A), the linear stress coefficient of the shear modulus, C_0, rises owing to the predominance of internal stress, and later decreases owing to the dominant effect of lattice expansion. Factory annealed Inconel (TLA), (fig. 48B), gives a very high value for C_0 in shear. It has been surmised that this high value may be attributed to the internal stress probably induced by the straightening given this metal, following annealing. The value of C_0 decreases with cold work to zero at 75-percent reduction of area.

In figure 42A is shown a plot of the tensile modulus E and its linear stress coefficient C_0, with extension of annealed copper rod, N-6. The modulus at zero stress, E_0, exhibits an initial sharp decrease, followed by a slower rise at a decreasing rate. The dotted curve which is drawn through the mean positions of the experimental points would be parallel to a basic curve devoid of the influence of extension spacings and rest intervals. The initial sharp drop of the modulus E_0 may be attributed to the dominant influence of lattice expansion. The initial rate of lattice expansion is high. During subsequent extension, the rise of the tensile modulus may be attributed to the combined dominant influence of induced internal stress and the production of preferred octahedral [111] orientation. This diagram is somewhat similar to the diagram for nickel (figs. 35 and 36).

The linear stress coefficient of the tension modulus, C_0, exhibits a sharp rise, followed by a rapid drop at a decreasing rate, to a low value. The absolute values of C_0, for copper, are appreciably greater than those obtained with the higher strength metals. This is evident in the greater curvature of the stress-strain lines and the greater initial

slope of the stress modulus lines. (See references 2 and 7.) Apparently, induced internal stress is initially dominant in producing a rise of C_0; whereas lattice expansion shortly becomes dominant in causing the subsequent drop of C_0. This material is unique in giving curved stress-modulus lines (not shown, see reference 2) throughout the range of uniform extension. All the other metals tested gave curved stress-modulus characteristics (see figs. 6 and 35 for nickel) only over the early portion of the extension range.

In figure 42B is shown the variation of E_0 and C_0 with extension for cold-rolled copper N. The high value of E_0 may be attributed to the preferred [111] orientation produced by cold rolling. C_0 is small and shows no significant variation.

8. Influence of Plastic Deformation on the Modulus of Elasticity and Its Linear Stress Coefficient for Stainless Steels

Figure 43 shows the variation with extension of the tensile modulus of elasticity, and its linear stress coefficient, C_0, for the annealed 13:2 Cr-Ni steel rod specimen. The proof stress values for this specimen are shown in figure 15. An E_0 curve drawn through the mean position of the points would descend at a decreasing rate, approaching a nearly horizontal position at the maximum extension shown (14 percent). As the maximum load was reached at slightly less than 7 percent (extension), some stress-strain and stress-set curves evidently were obtained after extension beyond the beginning of local contraction. Since the reduced section did not have an abruptly curved contour and extended over an appreciable fraction of the gage length, determination of the beginning of local contraction was difficult. The E_{25} and E_{50} curves followed courses similar to the E_0 curve. The linear stress coefficient, C_0, exhibits an initial rise but varies little beyond this point. The E_0 and C_0 curves generally oscillate in directions opposite to those of the proof stress curves - that is, low values generally follow short rest intervals.

The work-hardening factor apparently dominates in causing the lowering of E_0 with extension. Any preferred orientation which might occur during extension of this specimen of body-centered cubic metal would likewise tend to raise the modulus; the orientation produced during such small extension, however, would be expected to be negligible. The initial rise of the C_0 curve is probably due to the dominant influence of increase of internal stress.

With increase of extension of annealed 18:8 Cr-Ni steel specimen

IM-18.3, the tension modulus E_0 (fig. 44) shows an initial slight rise during the first 5 percent of extension, followed by a steady and somewhat rapid decrease throughout the remainder of the extension range. The modulus E_{25} exhibits a steady drop; whereas E_{50} rises slowly during the first 20-percent extension, and then decreases. The linear stress coefficient, C_0, exhibits a rapid rise during the first 15-percent extension, followed by a gradual decrease.

The initial rise in the E_0 and C_0 curves may be attributed to a predominant influence of increasing internal stress, the subsequent decrease of the modulus may be attributed in part to lattice expansion. Some of this decrease, however, may be due to the production of preferred orientation. Unlike the other face-centered cubic metals, deformation of this ferrous alloy is believed to produce a predominantly cubic [100] orientation in the direction of the rod axis. Such orientation would tend to lower the tension modulus. Slight prestretching of cold-worked specimens, however, generally produces a lowering of the tensile modulus, owing to relief of internal stress.

In another investigation conducted in this laboratory (reference 7) a study was made of the effect of prior plastic extension on the tensile modulus of elasticity and its linear stress coefficient, C_0, for low and medium carbon steels. It was found that an initial rise of the modulus and C_0 is sometimes obtained with extension owing to induced internal stress. Subsequent deformation causes little variation or even a small decrease of the modulus (except for a slight rise for the 0.20-percent carbon steel); the lattice expansion factor thus becomes dominant. Evidently the change from random to preferred orientation produced at large deformations of these steels has a small, if any, elevating effect upon the modulus. The lowering effect of lattice expansion is generally dominant.

Figure 49 shows the variation of the shear modulus of elasticity G and its linear stress coefficient C_0, with prior extension of annealed 18:8 Cr-Ni steel tubing, TC-19. With increasing extension, G decreases almost continuously over the range shown. The linear stress coefficient, C_0, is zero except at an extension of 5 percent; no significance should be attached to this single small value. The continuous decrease of the shear modulus G, with extension, may be attributed to the dominant influence of lattice expansion.

9. Influence of Plastic Deformation on Poisson's Ratio for Metals

From measured tensile and shear modulus values for a metal an effective value of Poisson's ratio, μ, may be calculated according to the equation:

$$\mu = \frac{E}{2G} - 1 \qquad (6)$$

where E and G are the tension and shear moduli, respectively. (See reference 29.) If the metal is isotropic this value will be equal to Poisson's ratio, as commonly determined from the ratio of unit lateral contraction to extension, under tensile loading.

For the purpose of measuring the relative influence upon tensile and shear moduli of such variables as plastic deformation and annealing temperature - that is, to detect any changes in isotropy of the metal - the use of such a calculated effective value may have certain advantages over that obtained by simultaneous extension and contraction measurements.

Figure 59 shows the variation of the tensile modulus E, the shear modulus G, and Poisson's ratio μ, with extension and cold reduction of nickel tubing. The modulus curves have been drawn through the mean positions of the experimental points as obtained from figures 36 and 45; these curves are used in deriving Poisson's ratio. The abscissa scale is plotted as equivalent reduction of area. In figure 59A are plotted values obtained with extended annealed nickel tubing; in figure 59B are plotted values obtained with cold-reduced nickel tubing.

With extension up to 10 percent, annealed nickel tubing TRF shows little variation of Poisson's ratio. With cold reduction of nickel tubing (fig. 59B), a small decrease in μ is obtained at intermediate reductions and a marked rise is obtained at large reductions. During extension, the various factors apparently affect tensile and shear modulus values proportionally. The difference in effect of the reorientation on the tensile and shear moduli accounts for the eventual large rise of Poisson's ratio with cold reduction.

Figure 60 shows the variation of the tension modulus E, the shear modulus G, and Poisson's ratio μ, with extension and cold reduction of monel tubing TG. With increase of extension (fig. 60A), μ_o and μ_{s5} rise. This rise may be attributed partly to the directional influence of the internal stress and probably in part to the effect of the reorientation factor. However, owing to the less rapid initial rise of Poisson's ratio with cold reduction of monel tubing, as indicated in figure 60B, the reorientation factor is believed to influence the rise of μ with extension only to a minor degree.

With cold reduction of monel tubing (fig. 60B), Poisson's ratio reaches a minimum at intermediate reductions of area; this decrease is small and should not be considered significant. No single factor appears to dominate in this range. With further cold reduction μ_o and μ_{50}

rise rapidly, owing to the production of preferred octahedral [111] orientation along the specimen axis, which tends to increase the tensile modulus and decrease the shear modulus. The influence of this reorientation factor was not evident in the variation of the tension modulus E for monel tubing (fig. 38) and monel rod (fig. 37). Lattice expansion is believed to affect tensile and shear moduli similarly; it therefore is isotropic in its effect and would not influence μ.

With prior extension of annealed aluminum-monel THD (fig. 61A) and annealed Inconel TLD (fig. 62A) tubing, there is a rise in Poisson's ratio, μ_o, probably because of the directional influence of internal stress and possibly also because of reorientation. With increase in the cold reduction of aluminum-monel, TH (fig. 61B) and Inconel TL (fig. 62B) tubing, Poisson's ratio μ for these metals exhibits a steady rise. This rise may be attributed to the production of preferred [111] crystal orientation. Since tubing having intermediate cold reductions was not supplied in these two compositions, the variation of Poisson's ratio within this range of cold work could not be ascertained.

Attention will now be given to the range of numerical values of μ obtained with nonferrous metals. For the unextended laboratory-annealed metals, the derived value of Poisson's ratio ranges from 0.33 to 0.42. For annealed metals extended about 10 percent (9.1-percent equivalent reduction), the values range from 0.38 to 0.52. Factory-annealed aluminum-monel and Inconel gave values of 0.34 and 0.28, respectively. At intermediate cold reductions, values as low as 0.34 were obtained; whereas at greater cold reductions the values ranged from 0.40 for monel tubing to 0.51 for Inconel tubing. Minor fluctuations of this ratio might be attributed to the experimental error of measurements.

Poisson's ratio obtained by measuring the ratio of unit lateral contraction to unit longitudinal extension for an elastic isotropic metal will be found to be about 0.3. (See reference 30.) Such a metal, therefore, will expand in volume under tensile stress. A value of 0.5 obtained from such measurements would indicate that no volume change was obtained by extension. Lead, with a measured value for μ of 0.45, approaches this condition. In the present tests, however, where Poisson's ratio is calculated in terms of measured values of tension and shear elastic moduli of structural metals, an appreciable deviation of the effective value of Poisson's ratio from that obtained for the annealed metal would indicate a corresponding degree of anisotropy of the metal. (See reference 30.) Thus, with extension of annealed tubing, and with cold reduction, production of anisotropy is indicated by the rise of the values of Poisson's ratio obtained. It would be expected that the metals became anisotropic, owing to the production of preferred orientation, and to the production of internal stress having directional properties. Likewise, a removal of anisotropy is obtained with soft annealing.

From values of the shear modulus obtained upon 18:8 Cr-Ni steel tubing, TC, and the tension modulus obtained upon 18:8 Cr-Ni steel rod, DM, values of Poisson's ratio were calculated by use of equation (6). It was then possible to determine the variation of Poisson's ratio with extension of the soft-annealed alloy.

Figure 63 shows the variation of the tension modulus E, the shear modulus G, and Poisson's ratio μ with extension of annealed 18:8 Cr-Ni steel. The modulus curves are faired through the mean positions of the experimental values obtained from earlier tests (not shown, see figs. 44 and 49, respectively). With increase of plastic extension, μ rises from an initial value of 0.32 reaching a constant value of 0.40 after an extension of about 12 percent. The values of μ_{25} and μ_{50} are almost constant over the observed range of prior extension at about 0.32 and 0.24, respectively.

The initial rise of μ with extension coincides with the initial rise of E_0. This rise was attributed to the influence of residual internal stress. That such a rise is not evident in the curve of G_0 may be attributed to the difference in directions of the principal shear stress during prior extension and during torsion testing. This difference would not exist for tension testing. Thus, the internal stress induced is anisotropic in its influence upon subsequently measured elastic properties. With appreciable increase in stress during such testing, the residual internal stress would become negligible in comparison with the applied stress, or it may become relieved. The evidence of elastic anisotropy would then disappear, as indicated by the lower values obtained for μ_{25} and μ_{50}. Such wide variation of μ with stress, which indicates a directional influence of the internal stress, may also be noted in the diagrams for extended monel (fig. 60), aluminum-monel (fig. 61), and Inconel (fig. 62).

VII. INFLUENCE OF ANNEALING TEMPERATURE ON THE MODULUS OF ELASTICITY OF METALS

Attention will now be given to the variation of the tensile and shear moduli of elasticity and their linear stress coefficients with the temperature of annealing. From stress-strain and stress-set curves obtained on specimens annealed at various temperatures, values were obtained of the modulus of elasticity at zero and at elevated stresses, and of its linear stress coefficient, C_0.

1. Influence of Annealing Temperature on the Modulus of Elasticity and Its Linear Stress Coefficient for Cold-Worked Nonferrous Metal Rod and Tubing

Figure 50A shows the variation of the tensile modulus of elasticity and its linear stress coefficient, for cold-drawn nickel rod (R) specimens annealed at various temperatures, the proof stress values of which are given in figure 23A.

There is little variation of the modulus for annealing temperatures ranging between room temperature and 1100° F. At higher temperatures, there is a marked lowering of the modulus. The linear stress coefficient of the modulus, C_0, decreases with increase of annealing temperature, and the value is zero for temperatures of 700° F and greater; this means that the modulus does not vary appreciably with stress for annealing temperatures above 700° F.

The horizontal course of the modulus curve throughout the lower temperature range may be attributed to a balance of influence of the several factors affecting this property. The sudden drop of the modulus within the recrystallization range (above 1100° F) may be attributed to the combined dominant influences of relief of internal stress and the change of crystal orientation from preferred octahedral [111] along the specimen axis to a random distribution.

Figure 51A shows the variation of the tensile modulus of elasticity E and its linear stress coefficient, C_0, with annealing temperature for cold-reduced nickel tubing TRE. Proof stress curves for these specimens are given in figure 24B. With increase of annealing temperature up to about 1100° F, the tensile modulus shows little change. With increase above 1100° F a marked decrease of the modulus is found, probably due largely to removal of preferred orientation. A high value of C_0 is obtained at an annealing temperature of 1200° F, low values being obtained at all other temperatures. The reality of the high value of C_0 may be questioned, since the stress range over which strain is measured is small (see fig. 24B), thus lowering appreciably the accuracy of determining this index. The variation of the modulus with annealing temperature for cold-reduced nickel tubing is similar to that obtained for the cold-drawn rod. The modulus values obtained with the tubing are somewhat greater than with the rod, owing probably to the greater degree of cold work and hence a greater amount of preferred orientation, obtained with the tubing.

In figure 55A are plotted values of the shear modulus and its linear stress coefficient C_0, obtained upon the tubular nickel specimens annealed at various temperatures. Proof stress values for these specimens are plotted in figure 28B. With increase of annealing temperature, the

shear modulus G exhibits a small sharp rise between 1100° and 1200° F, followed by a larger drop with further increase in temperature. Possibly the sharp rise is due to removal of preferred orientation; the subsequent drop cannot be explained. However, for the 1400° F annealing temperature, the small range of stress over which strain is measured (see 0.1-percent proof stress, fig. 28B), does not permit an accurate determination of the shear modulus. The several factors affecting E are in apparent balance for annealing temperatures below 1100° F. There is no regular variation of the linear stress coefficient of the shear modulus, C_0, with increase of annealing temperature; the magnitude of C_0 is generally small.

With increase of the temperature of annealing cold-drawn monel rod-G (fig. 52A), up to 1100° F, there is little variation of the tensile modulus E_0; a small drop of the modulus occurs at higher temperatures. $E_{.5}$, E_{50}, and E_{100} rise rapidly with temperature from low values obtained with the cold-drawn metal (100° F), nearing the value of E_0 at 650° F. Proof stress values for these specimens are given in figure 23B. With increase of the temperature of annealing cold-reduced monel tubing TGD (fig. 53A), the modulus E shows little variation over the whole range. Proof stress values for these specimens are given in figure 24A. Evidently the several factors affecting the tensile modulus, E_0, are in approximate balance with elevation of the annealing temperature. The high value of C_0 for both cold-drawn rod (fig. 52A) and cold-reduced tubing (fig. 53A) is commensurate with the wide spread of modulus values for these metals. C_0 decreases rapidly with elevation of annealing temperature. This decrease may be attributed to relief of internal stress.

With increase of annealing temperature for cold-reduced monel tubing TGD (fig. 56), the shear modulus G shows little variation with annealing temperature, indicating that the various factors are in approximate balance. With increase of annealing temperature the linear stress coefficient of the shear modulus, C_0, oscillates about low values, reaching zero at 1400° F.

With increase of annealing temperature, the tension modulus E for cold-reduced aluminum-monel tubing THC (fig. 53B) rises gradually, reaching a maximum at 1075° F. At higher temperatures E_0 decreases. The initial rise of E is due to the dominant influence of relief of work-hardening effects; whereas reorientation occurring during recrystallization produces the subsequent lowering of the modulus. A high initial value of the linear stress coefficient of the tension modulus, C_0 for the cold-reduced metal (100° F) is commensurate with the large variation of the tension modulus with stress; both indicate the presence of internal stress. With increase in temperature C_0 decreases owing to internal stress relief.

With increase in the temperature of annealing aluminum-monel tubing (fig. 57), the shear modulus of elasticity, G, exhibits a gradual rise. This rise may be attributed to the combined dominant influence of the removal of lattice expansion effects, and to recrystallization. The linear stress coefficient of the shear modulus C_0 for aluminum-monel tubing exhibits a general decrease with increase of annealing temperature, owing to relief of internal stress; the absolute value is small.

Figure 50B shows the variation of the tensile modulus E and its linear stress coefficient, C_0, with the temperature of annealing cold-drawn Inconel rod L; the proof stress values for this specimen are given in figure 26A. Setting aside temporarily the values obtained in the early tests on cold-drawn rod, there is indicated a gradual rise of the tension modulus with increase of annealing temperature up to 1100° F, followed by a rapid decrease to values somewhat below that for the cold-drawn metal. The gradual rise may be attributed to the dominance of relief of lattice expansion, the subsequent lowering to recrystallization, that is, reorientation from a preferred to a random distribution.

The linear stress coefficient of the modulus, C_0 (fig. 50B), gives generally low values over the whole temperature range (ignoring results of early tests), except for a single high value at 1450° F. No great significance should be attached to this single high value, considering the small stress range over which strain was measured on this specimen (0.1-percent proof stress, fig. 26A).

The high value of E_0 and C_0 and the associated large variation of the modulus with stress, as obtained in the early tests on cold-drawn Inconel L (fig. 50B) indicate a dominant influence of the contained internal stress. As noted above, the specimens tested later, both cold-drawn and annealed, exhibited lower values of C_0, indicating a reduced amount of internal stress.

In review, when severely cold-drawn Inconel is permitted to rest a long period (in this case, over 3 years) both relief of internal stress and some softening occurs. Internal stress relief dominates in raising the lower proof stresses and in lowering E_0 and C_0. Softening, or relief of lattice expansion, dominates in decreasing the upper proof stresses. Subsequent annealing within the stress-relief annealing range causes further internal stress relief which dominates in raising all proof stresses and also causes further relief of lattice expansion, which dominates in raising the modulus.

With increase of the temperature of annealing cold-reduced Inconel tubing TLC up to 1100° F the tensile modulus E rises gradually owing to the dominant effect of removal of lattice expansion. With further increase of temperature, the modulus drops rapidly, owing to

recrystallization, or removal of preferred orientation. The linear stress coefficient of the tension modulus, C_0, is small, and shows no significant variation with temperature.

With increase of the temperature of annealing cold-reduced Inconel tubing TLC (fig. 55B), there is obtained a gradual elevation of the shear modulus owing to the combined dominant influence of relief of lattice expansion and recrystallization. The linear stress coefficient of the shear modulus, C_0, is small over the whole annealing temperature range for Inconel (fig. 55B) and shows no regular variation.

4 Influence of Annealing or Tempering Temperature on the Modulus of Elasticity of Stainless Steels

Figure 52B shows the variation of the tension modulus E and its linear stress coefficient C_0 with tempering temperature for air-hardened 13:2 Cr-Ni steel; the proof stress values for these specimens are shown in figure 26B. For air-cooled and furnace-cooled specimens, these variations are slight. Apparently, no single factor is dominant in this range. Single high values of E_0 and C_0 are obtained, however, for the as-received metal. Since this metal had been hot-rolled prior to the "annealing" treatment, evidently some of the deformation texture remained. It is believed such a texture would contain dodecahedral [110] orientation along the specimen axis. Heating up to 1750° F would cause complete recrystallization, and thus give a lower value of the tension modulus and its linear stress coefficient.

The tension modulus of elasticity of half-hard 18:8 Cr-Ni steel rod, DM, rises with increase of annealing temperature (fig. 54A) over the range indicated. Proof stress values for these specimens are shown in figure 27A. Evidently, relief of lattice expansion dominates over the entire range in causing this rise of E. Some of this rise, however, may be due to a change of crystal orientation from predominantly cubic to random distribution. The 44-hour annealing time at 482° F did not cause any significant change of E_0 or C_0 from the values obtained upon the specimen annealed 1/2 hour at 500° F.

Figure 54B shows the variation of the tensile modulus E, and its linear stress coefficient, C_0, with annealing temperature, as measured at -110° F (-78.5° C). There is a general increase of the tension modulus with annealing temperature, similar to that obtained in figure 54A at room temperature. The modulus values measured at low temperature, however, are somewhat higher than the room temperature values, over the entire range. Somewhat greater values of the linear stress coefficient of the modulus were obtained at low temperatures; the absolute values of

C_0 in figures 54A and 54B are small so that their apparent variations cannot be considered significant. A similar variation of the tension modulus with annealing temperature, and with lowering of test temperature, was also obtained with severely cold-drawn 18:8 Cr-Ni steel rod. (See reference 3.)

Figure 58 shows the variation of the shear modulus of elasticity, G, and its linear stress coefficient, C_0, with the temperature of annealing 18:8 Cr-Ni steel tubing, TC. There is an almost continuous increase of the modulus with temperature, over the range shown, owing to dominance of relief of lattice expansion. Considerable fluctuation of the value of C_0 is obtained; the magnitude of these values, however, is small, and thus cannot be considered significant.

5. Influence of Annealing Temperature on Poisson's Ratio for Various Metals

It will also be of interest to consider any changes in isotropy of a work-hardened metal caused by variation of annealing temperature. Such a study is obtained by calculating Poisson's ratio, from corresponding curves of variation of tensile and shear moduli with annealing temperature.

Figure 64 shows the variation of the tension and shear moduli and of the derived value of Poisson's ratio μ, with the temperature of annealing cold-reduced nickel tubing, TRE. Values obtained with fully annealed nickel tubing TRF are also used in plotting these curves. Experimental modulus values were replotted from figures 51A and 55A. Smooth curves are faired through the mean positions of the experimental points.

Poisson's ratio μ for nickel shows negligible variation with increase of annealing temperature up to 1100° F. Above this temperature, μ decreases rapidly. This decrease may be attributed principally to the change of crystal orientation from a preferred to a random distribution.

Figure 65 shows the variation of the tensile modulus E, the shear modulus G, and Poisson's ratio, μ, with annealing temperature for cold-reduced monel tubing TGD. The modulus curves are reproduced from figures 52A and 56, respectively. With increase of annealing temperature, Poisson's ratio first decreases, and then increases. The actual variation is small and may be within the limits of experimental error. There evidently is an approximate balance between the various factors that influence Poisson's ratio. The maximum cold work imparted to this unannealed tubing was not so great as that imparted to other metals.

Poisson's ratio for cold-reduced aluminum-monel (fig. 66) and Inconel (fig. 67) tubing varies with annealing temperature in a manner similar to that for nickel tubing (fig. 64). This property shows little change with increase of annealing temperature up to 1100° F. For higher annealing temperatures, μ for these metals drops rapidly owing to the removal of preferred orientation. Both of these metals had been severely cold-reduced (table 3) before annealing and testing.

Figure 68 shows the variation of the tension modulus E, the shear modulus G, and Poisson's ratio μ with the temperature of annealing cold-drawn 18:8 Cr-Ni steel. The modulus curves are faired through the mean positions of the points obtained in earlier tests. (See figs. 54 and 58, respectively.)

With increase of annealing temperature from room temperature to 1000° F, there is no significant variation of μ_o or μ_{50}; these two curves are nearly coincident. With further increase, μ_o rises from a value of 0.22 to about 0.31 at 1800° F. The relief of internal stress which occurs in the lower temperature range obviously does not affect Poisson's ratio. The internal stress induced by cold drawing apparently is isotropic in its effect; in cold-drawing tubing and rod, the directions of the planes of maximum shear will tend to be widely distributed.

The eventual rise of μ with annealing temperature is attributed to another cause. After severe cold deformation of 18:8 Cr-Ni steel rod, as obtained with the cold-drawn alloy, the low value of E_o (fig. 54A) can be attributed in part to the production of preferred cubic [100] orientation parallel to the specimen axis, such as occurs in some face-centered cubic metals. A low value of the shear modulus is not obtained with cold-drawn stainless steel tubing. (See fig. 58.) Hence, Poisson's ratio for cold-drawn alloy will be lower than the value obtained with annealed alloy. Therefore, recrystallization of the cold-drawn alloy should increase the value of Poisson's ratio. It was shown earlier that Poisson's ratio for cold-worked nickel, aluminum-monel, and Inconel tubing decreases within the recrystallization range; in these metals cold work produces preferred octahedral [111] orientation along the specimen axis.

CONCLUSIONS

The following conclusions apply to all the metals tested, except as indicated.

1. An incomplete view of the tensile elastic properties of a metal is obtained by considering either the stress-strain or stress-set relationship alone. Consideration should be given to both relationships.

2. In a study of elastic properties, consideration should be given to the time schedule followed during test. In the present investigation, measurements were made only after holding each load for a period of 2 minutes. This permitted the positive or negative creep to reach a very low rate, enabling both accurate, and sensitive strain and set measurements to be made.

3. Positive and negative creep occur during cyclic stressing of a specimen, even when well within the elastic limit of the metal, so as to give stress-strain characteristics of the form of hysteresis loops. The permanent set produced during each cycle, which prevents closure of the loop, diminished with continued cyclic stressing over a fixed load range; there is an accompanying decrease of loop width. Permanent set and loop width may be temporarily increased by increase of prior rest interval or cycle time. Complete closure of hysteresis loops would be expected only after many thousands of stress cycles.

4. The making of successive stress-strain and stress-set curves upon a single specimen, with intervening extension spacing and rest intervals, gave elastic property values much influenced by these two variables. A plot of any one of these elastic properties versus total extension often gave curves having many wide abrupt oscillations superposed upon more gradual wavelike curves. The wide oscillations are generally associated with variation of the rest intervals and the extension spacing, which greatly affect the positive and negative creep and the amounts of induced internal stress. The forms of the more gradual basic curves are determined by certain fundamental factors enumerated below.

5. With extension of soft-annealed metals, the basic tensile or shear proof stress-extension curves exhibited either an initial decrease or a slow rise, followed at greater extensions by a steeper rise. The most rapid initial decrease tends to occur in the curves corresponding to the smaller values of set; the subsequent rise is most rapid in the curves corresponding to the larger values of set. The general tendency of the basic proof stress-extension curves to rise because of the lattice expansion or work hardening is initially diminished, or overcome, by the lowering effect of the induced internal stress. The curves obtained with annealed tubing in both tension and shear, are devoid of much of the oscillation observed in the other curves, because these data were obtained by single tests upon a number of specimens which had each been extended a different amount after annealing.

6. Rest, following extension, tends to cause some slight lowering of the tensile proof stresses for the metals tested. This decrease is attributed to a dominant effect of a slight softening of the metal. This effect was quite evident after a 3-year rest period given some cold-drawn Inconel rod, after delivery.

7. The dominant effect of annealing of cold-worked metals at intermediate temperatures is an increase of tensile or shear proof stress due to relief of internal stress. This factor has the greatest effect on the proof stresses corresponding to the lower values of set. Annealing at higher temperature produces relief of lattice expansion, and consequently a lowering of all proof stresses.

8. The tensile or shear modulus of elasticity may be derived from tensile or shear stress-strain lines, corrected for permanent set. Since the elastic moduli of many metals vary with stress, it is convenient to derive the linear stress coefficient C_0, of the modulus at zero stress, and moduli at various values of stress. In order to determine the modulus of elasticity more accurately, the corrected values of strain may be plotted as deviations from a fixed modulus upon an open scale. From the five proof stresses corresponding to permanent sets of 0.001, 0.003, 0.01, 0.03, and 0.1 percent, from the modulus at zero stress and at one or more elevated stresses, and from the linear stress coefficient, C_0, it is possible to obtain a fairly good picture of the elastic properties of a metal in either tension or shear.

9. With increase of extension of an annealed metal, the variation of the tensile or shear modulus is determined by the relative influences of three factors; namely, internal stress, lattice expansion, and crystal reorientation. With variation of the temperature of annealing a cold-worked metal, the modulus is likewise dependent upon the relative influence of these three fundamental factors. Such influence will differ for the several metals tested.

The various metals differ somewhat in the form of the curves obtained showing the variation of the modulus with extension, cold reduction and annealing temperature. Such tension and torsion modulus curves for a single metal are likewise not similar in form.

10. With extension of annealed nickel rod or tubing or copper rod, the tension modulus, E_0, initially decreases sharply to a minimum, rising at greater extensions at a gradually decreasing rate. After appreciable deformation, as obtained with cold reduction of nickel tubing, a more pronounced rise of the tensile modulus occurs.

With tensile extension of annealed monel rod or tubing, or with cold reduction of monel tubing, the tension modulus E_0 shows little variation. Likewise, little variation of E_0 is obtained with extension of annealed Inconel tubing. With initial extension of aluminum-monel tubing, E_0 is found to rise sharply, with no appreciable variations occurring at greater extensions. With extension of annealed Inconel rod, E_0 rises sharply and then decreases more gradually, rising again slightly only at large extensions.

At large cold reductions of both aluminum-monel and Inconel tubing, a sharp rise of the modulus, E_0, is obtained.

11. With extension of annealed 13:2 chromium-nickel steel rod, the tension modulus E_0 decreases gradually, reaching a minimum at beginning local contraction.

With extension of annealed 18:8 chromium-nickel steel rod, E_0, initially rises slightly to a maximum, and then decreases at a fairly constant rate over the remaining range of uniform extension.

12. With extension of annealed nickel and aluminum-monel tubing, the shear modulus, G_0, shows little variation. With extension of annealed monel, Inconel, and 18:8 Cr-Ni steel tubing, G_0 decreases steadily.

With increasing cold reduction of monel and nickel tubing, G_0 rises to a maximum at intermediate reductions and then decreases at greater reductions. With increasing cold reduction of aluminum-monel and Inconel tubing, a steady decrease of G_0 is evident.

13. With increase of the temperature of annealing cold-worked nickel or monel rod or tubing, over the stress-relief annealing range, there is obtained little variation of the tension modulus E_0. Over a similar temperature range, the tension modulus E_0, for cold-reduced Inconel rod and tubing, and aluminum-monel tubing rises. Within the recrystallization range, however, E_0 decreases somewhat for all the above metals except monel tubing. Higher values of E_0 are obtained with factory-annealed than laboratory-annealed tubing.

Air-hardened 13:2 Cr-Ni steel exhibits little variation of the tension modulus, E_0, with tempering temperature. These values are somewhat less than obtained with the factory-annealed metal. With increase of the temperature of annealing cold-drawn 18:8 Cr-Ni steel, the tension modulus increases at a steady rate.

14. Little variation of the shear modulus G_0 is obtained with increase of the temperature of annealing cold-reduced nickel and monel tubing. A steady rise of G_0 is obtained, however, with increase of the temperature of annealing cold-reduced aluminum-monel, Inconel, and 18:8 Cr-Ni steel tubing.

15. The linear stress coefficient of the tension modulus, C_0, for annealed nickel, aluminum-monel, and Inconel rod and tubing and for annealed monel and 18:8 Cr-Ni steel rod rises to maximum, and then

decreases, during extension. With extension of monel tubing and 13:2 Cr-Ni steel rod, no significant variation of C_0 occurs. With extension of annealed copper rod, C_0 drops rapidly to a small value. With cold reduction of monel and nickel tubing, C_0 rises to a maximum at intermediate reductions, and then decreases.

16. The linear stress coefficient of the shear modulus, C_0, rises to maximum values with extension of annealed nickel, monel, aluminum-monel, and Inconel tubing. No significant variation of C_0 is obtained with cold reduction of these metals.

17. With increase of the temperature of annealing nickel and monel rod and monel and aluminum-monel tubing, there is obtained a decrease of the linear stress coefficient of the tension modulus. This decrease obviously corresponds to a decrease in variation of the tension modulus with stress.

With increase of the temperature of annealing monel and aluminum-monel tubing, the linear stress coefficient of the shear modulus likewise decreases. The diagrams for the remaining metals show no significant variation of these coefficients with annealing temperature.

18. An increase of internal stress tends to produce a rise of the tension and shear moduli at zero stress for metals. It evidently is dominant during initial extension of annealed aluminum-monel tubing and annealed Inconel rod, in causing a rise of E_0. It probably also is dominant in producing the rise of E_0 and G_0 with intermediate cold reduction of nickel and monel tubing. It likewise is dominant in affecting a rise of the linear stress coefficients of tensile and shear moduli during initial extension of a number of the metals tested. The wide variation of the tension and shear moduli with stress, and the associated large values of C_0 obtained upon some unannealed cold-worked metals may be associated with the presence of internal stress. The high values of E_0 obtained upon factory-annealed aluminum-monel and Inconel tubing, and 13:2 Cr-Ni steel rod, probably can be attributed to the internal stress produced during finishing.

19. The work-hardening or lattice expansion of metals, as differentiated from changes of crystal orientation, tends to cause a decrease of both tensile and shear moduli. The decrease of the tension modulus with initial extension of nickel, copper, and 13:2 Cr-Ni steel probably can be attributed to the dominant effect of lattice expansion. The drop of E_0 at greater extensions for annealed Inconel and 18:8 Cr-Ni steel rod, as well as the continuous drop of the shear modulus G_0 with

extension of annealed 18:8 Cr-Ni steel tubing may be attributed to this factor.

The rise within the stress relief annealing range of the tension and shear moduli of aluminum-monel, Inconel, and 18:8 Cr-Ni steel probably is due to the removal of the lattice expansion of these metals.

20. A change of crystal orientation of many metal crystals, between states of preferred and random distribution, will tend to change the values of tensile and shear moduli. Such variation of the modulus is dependent not only upon the percentage of the crystals affected, but also upon the directional variation of the modulus of a crystal of the metal concerned.

With cold deformation of some face-centered cubic metals, there is produced a preferred octahedral [111] orientation, which tends to increase the tensile modulus and to decrease the shear modulus. Such a change is dominant in the rise with extension and cold reduction of nickel, with extension of copper, and with large cold reductions of aluminum-monel and Inconel tubing. The rapid drop at large deformations of the shear modulus of nickel, aluminum-monel, and Inconel tubing may be attributed in part to dominance of this factor.

The rapid decrease of the tension modulus E_0 at large extensions of annealed 18:8 Cr-Ni steel, however, may possibly be attributed in part to the dominant effect of production of preferred cubic [100] orientation.

Deformation of annealed 13:2 Cr-Ni steel, is believed to produce a preferred dodecahedral [110] orientation of this metal. Any such change evidently does not have a dominant effect upon the variation of the modulus of this metal.

With soft annealing, the lowering of the tensile moduli of nickel, aluminum-monel, and Inconel may be attributed to the dominant effect of removal of preferred octahedral [111] orientation. Soft annealing of cold-drawn 18:8 Cr-Ni steel, however, tends to raise the tensile modulus, possibly because of the removal of preferred cubic [100] orientation.

The fact that variations of the tensile and shear moduli are less for monel than for nickel or copper suggests that the directional variation of these moduli are less in a crystal of monel than in either nickel or copper. Possibly a similar relationship may be found between other alloys and their constituent metals.

21. Poisson's ratio, μ, as calculated from tensile or shear moduli, will be affected only by those factors which produce anisotropy within a metal.

With extension of monel, aluminum-monel, Inconel, and 18:8 Cr-Ni steel, Poisson's ratio μ_o rises. During prior extension, the direction of the principal shear stresses will be the same as during subsequent tension testing, but not during subsequent torsion testing. The internal stresses produced during prior extension therefore tend to raise the tension modulus to a greater extent than the torsion modulus is raised; it is anisotropic in its effect. The large variation of μ with stress, during extension of these metals, probably likewise is due to this effect.

However, the internal stress produced during small cold reductions evidently tends to be isotropic in its effect upon subsequently measured properties.

22. With large cold reductions, as obtained with nickel, aluminum-monel, and Inconel tubing, there is obtained a marked rise of Poisson's ratio μ; monel tubing likewise shows a small rise of μ with cold reduction. This rise is due to the production of preferred octahedral [111] orientation in these metals, which affects tensile and shear moduli in an opposite manner. The crystal orientation factor therefore, likewise is anisotropic in its effect. On the other hand, Poisson's ratio, μ for cold-drawn 18:8 Cr-Ni steel is very low owing to the production of preferred cubic [100] orientation.

23. With soft annealing of nickel, aluminum-monel, and Inconel tubing, there is obtained a decrease of μ, owing to the removal of preferred orientation; whereas soft annealing of 18:8 Cr-Ni steel causes a rise of μ. Cold-reduced monel shows no appreciable variation of μ with annealing temperature, due in part probably to its lesser degree of cold work of this metal, and in part to the small directional variation of the modulus for a crystal of this alloy.

An appreciable variation of Poisson's ratio from its value in the annealed state gives evidence of anisotropy produced within a metal. Because Poisson's ratio is very sensitive to small changes of either the tensile or shear moduli, only large variations of μ calculated by the method used in this investigation can be considered significant.

24. With lowering of test temperature to -110° F for 18:8 Cr-Ni steel, a general increase of both tensile proof stress and modulus of elasticity is obtained. Such elevation occurs throughout the annealing temperature range investigated.

25. There have been evaluated, for the various metals tested, the tensile-shear proof stress ratios for 0.1-percent set and the work-hardening rates in tension and in shear. The tensile-shear proof stress value for cold-drawn metals is found to be less than for annealed metals or for metals severely work-hardened by the tube-reducer method. The

rate of work hardening of a metal determines the rate of rise at the 0.1-percent proof stress. This rate is greatest for annealed copper and nickel and least for annealed monel and aluminum-monel.

National Bureau of Standards,
Washington, D. C., April 1945.

REFERENCES

1. McAdam, D. J., Jr., and Mebs, R. W.: Tensile Elastic Properties of 18:8 Chromium-Nickel Steel as Affected by Plastic Deformation. NACA Rep. No. 670, 1939.

2. McAdam, D. J., Jr., and Mebs, R. W.: Tensile Elastic Properties of Typical Stainless Steels and Nonferrous Metals as Affected by Plastic Deformation and by Heat Treatment. NACA Rep. No. 696, 1940.

3. Mebs, R. W., and McAdam, D. J., Jr.: The Tensile Elastic Properties at Low Temperatures of 18:8 Cr-Ni Steel as Affected by Heat Treatment and Slight-Plastic Deformation. NACA TN No. 818, 1941.

4. Mebs, R. W., and McAdam, D. J., Jr.: Torsional Elastic Properties of 18:8 Chromium-Nickel Steel as Affected by Plastic Deformation and by Heat Treatment. NACA TN No. 886, 1943.

5. Mebs, R. W., and McAdam, D. J., Jr.: The Influence of Plastic Deformation and of Heat Treatment on Poisson's Ratio for 18:8 Chromium-Nickel Steel. NACA TN No. 928, 1944.

6. Mebs, R. W., and McAdam, D. J., Jr.: Shear Elastic Properties of Some High Strength Nonferrous Metals as Affected by Plastic Deformation and by Heat Treatment. NACA TN No. 967, 1945.

7. McAdam, Dunlap J., Jr., and Mebs, Russell W.: Tensile Elastic Properties of Nickel, Copper, Open-Hearth Iron, and Typical Steels. Res. Paper 1459, Nat. Bur. of Standards Jour. Res., vol. 28, no. 3, March 1942, pp. 311-378.

8. Rosenberg, Samuel J.: Effect of Low Temperatures on the Properties of Aircraft Metals. Res. Paper 1347, Nat. Bur. of Standards Jour. Res., vol. 25, 1940, pp. 673-701.

9. Sayre, M. F.: Plastic Behavior in the Light of Creep and Elastic Recovery Phenomena. Trans. A.S.M.E., RP-56-8, vol. 56, no. 7, July 1934, pp. 559-561.

10. Haigh, B. P.: Hysteresis in Relation to Cohesion and Fatigue. Trans. Faraday Soc., vol. 24, Feb. 1928, pp. 125-137.

11. Heyn, E., and Bauer, O.: Über Spannungen in kaltgereckten Metallen. Int. Zeitschr. f. Metallographie, Bd. 1, 1911, pp. 16-50.

12. Masing, G.: Zur Heyn'schen Theorie der Verfestigung der Metalle durch verborgene elastische Spannungen. Wiss. Veröff a.d. Siemens-Konzern, Bd. 3, Heft 1, May 15, 1923, pp. 231-239.

13. Masing, G.: Rekristallisation und Erholung (Kristallvergütung) bei Metallen. Wiss. Veröff. a.d. Siemens-Konzern, Bd. 4, Heft 2, Oct. 15, 1925, pp. 230-243.

14. Bauschinger, J.: Mitteilungen aus den mechanischen Laboratorium der technischen Hochschule in München. Heft XIII, 1886.

15. Smith, S. L., and Wood, W. A.: A Stress-Strain Curve for the Atomic Lattice of Iron. Proc. Roy. Soc. London, ser. A, vol. 178, no. A 972, May 9, 1941, pp. 93-106.

16. Templin, R. L., and Sturm, R. G.: Some Stress-Strain Studies of Metals. Jour. Aero. Sci. vol. 7, no. 5, March 1940, pp. 189-198.

17. Stang, Ambrose H., Ramberg, Walter, and Back, Göldie: Torsion Tests of Tubes. NACA Rep. No. 601, 1937.

18. Schmid, Erich, and Boas, W.: Kristallplastizität. Julius Springer (Berlin), 1935.

19. Ettisch, M., Polanyi, M., and Weissenberg, K.: Über Faserstruktur bei Metallen. Zeitschr. f. Phys., Bd. 7, Nr. 3, Nov. 3, 1921, pp. 181-184.

20. Ettisch, M., Polanyi, M., and Weissenberg, K.: Faserstruktur hartgezogener Metalldrahte. Zeitschr. Phys. Chem., Bd. 99, Nr. 5, Dec. 9, 1921, pp. 332-337.

21. Sachs, G., and Schiebold, E.: Rekristallisation und Entfestigung im Röntgenbild. Zeitschr. f. Metallkunde, Bd. 17, Nr. 12, Dec. 1925, pp. 400-402.

22. Schmid, E., and Wassermann, G.: Über die Textur hartgezogener Drähte. Zeitschr. f. Phys., Bd. 42, Nr. 11-12, May 16, 1927, pp. 779-794.

23. Greenwood, G.: Fibre Texture in Nickel Wires. Zeitschr. f. Krist., Bd. 72, Nr. 3, 1929, pp. 309-317.

24. Fraser, O. B. J.: Private communication from O. B. J. Fraser, Director of Technical Service of Mill Products, International Nickel Co., Aug. 2, 1939.

25. Genserer, M., and Vukmanic, P. A.: Preferred Orientations in Hot-Rolled Low-Carbon Steel. Trans. Am. Inst. Min. and Met. Eng., vol. 125, 1937, pp. 507-511.

26. Barrett, C. S., and Levenson, L. H.: Structure of Iron after Drawing, Swaging, and Elongating in Tension. Tech. Pub. No. 1038, Metals Technology, vol. 6, no. 2, Feb. 1939.

27. Kawai, T.: The Effect of Cold-Working on Young's Modulus of Elasticity. Sci. Rep., Tohoku Imperial Univ., vol. 19, no. 2, May 1930, pp. 209-234.

28. Nádai, A.: Plasticity. McGraw-Hill Book Co. Inc.(New York and London), 1931.

29. Southwell, R. V.: Theory of Elasticity. Clarendon Press (Oxford), 1936.

30. Grüneisen, E.: Die elastischen Konstanten der Metalle bei kleiner Deformation. II. Ann. d. Phys., IV. Folge, Band 25, Heft 5, April 28, 1908, pp. 825-851.

Table 1.- Chemical Compositions.

Metal	Designation	Diameter or Dimensions as received (in.)	Gage Diameter (in.)	Chemical Composition (percent)									
				C	Fe	Ni	Cu	Cr	Mn	Al	P	S	Si
Nickel rod	R	0.625	0.417	0.07	0.08	99.49	0.03	—	0.24	—	-	0.005	0.08
Nickel tubing	TR	1 x 0.085	—	.04	.05	99.53	.04	—	.28	—	-	.005	.03
Monel rod	G	0.875	.500	.18	1.24	Diff.	24.86	—	.94	—	-	.007	.10
Monel tubing	TG	1 x 0.085	—	.13	1.49	67.64	29.70	—	.96	—	-	.005	.05
Aluminum-monel tubing	TH	1 x 0.085	—	.16	0.33	66.42	29.68	—	.25	2.80	-	.005	.33
Inconel rod	L	0.5	.333	.23	5.3	Diff.	—	13.2	—	—	-	—	—
Inconel tubing	TL	1 x 0.085	—	.08	6.40	79.33	0.15	13.64	.20	—	-	.011	.17
Copper rod	N	0.875	.500	—	—	—	99.97	—	—	—	-	—	—
13:2 Cr-Ni steel rod	E	.875	.500	.09	Diff.	2.08	—	13.3	.48	—	-	—	.26
Annealed 18:8 Cr-Ni steel rod	DA	.625	.417	.07	Diff.	8.63	—	18.22	.44	—	0.012	.018	.50
Cold-drawn 18:8 Cr-Ni steel rod	DM	.625	.417	.10	Diff.	9.38	—	18.82	.47	—	.015	—	.35
18:8 Cr-Ni steel tubing	TC	1 x 0.1	—	.07	Diff.	10.4	—	18.5	—	—	-	—	—

Table 2.- Thermal Treatments of Rod Materials.

Material	Treatment As Received	Specimen Designation	Temperature (°F)	Time Held (hrs)	Cooled In	Temperature (°F)	Time Held (hrs)	Cooled In
Nickel	Cold drawn 60 percent	R	—	—	As received			
		R-2	200	2	Furnace			
		R-3	300	2	Air			
		R-5	500	2	Furnace			
		R-7	700	2	"			
		R-9	900	2	"			
		R-11	1100	2	"			
		R-12	1200	2	"			
		R-14	1400	2	"			
Monel	Cold drawn 40 percent	G	—	—	As received			
		G-3	300	2	Air			
		G-4.5	450	3	Air			
		G-6.5	650	2	Air			
		G-8	800	5	Furnace			
		G-9	900	2	Air			
		G-9.75	975	2	Air			
		G-11	1100	1	Air			
		G-12	1200	2	Furnace			
		G-14	1400	1	Furnace			
Inconel	Cold drawn	L			As received			
		L			As received, 40 months later			
		L-2	200	6	Air			
		L-3	300	2	Air			
		L-4.5	450	3	Air			
		L-6.5	650	2	Air			
		L-7.5	750	6	Air			
		L-8.5	850	2	Furnace			
		L-9.75	975	2	Air			
		L-11	1100	2	Furnace			
		L-14.5	1450	1	Furnace			
		L-17.5	1750	2	Furnace			
Copper	Cold rolled 75 percent	N			As received			
		N-6	600	22	Air			
13:2 Cr-Ni Steel	Annealed	E	1240(a)		Furnace(a)	As received		
		E-A	1750	1	Air	As air cooled		
		E-A-6			"	600	2	Furnace
		E-A-7.5			"	750	3	
		E-A-8.5			"	850	2	
		E-A-9.5			"	950	2	
		E-A-11			"	1100	1	
		E-A-12			"	1200	2	
		E-A-14.5			"	1450	1	
		E-F			Furnace	As furnace cooled		

Table 2.- Continued.

Material	Treatment As Received	Specimen Designation	Temperature (°F)	Time Held (hrs)	Cooled In	Temperature (°F)	Time Held (hrs.)	Cooled In
18:8 Cr-Ni Steel	Annealed	DA			As received			
		DM			As received	Tested at room and low temperatures		
		DM-4.8	480	44	Air	Tested at room temperature		
		DM-5	500	½	"	Tested at room and low temperatures		
	Cold drawn	DM-7	700	½	"	" " " " " "		
		DM-9	900	½	"	" " " " " "		
		DM-10.25	1025	½	"	Tested at room temperature		
		DM-18.3	1830	½	Water	Tested at room and low temperatures		

(a) By manufacturer.

Table 5.- Work-Hardening Rates[a] for Annealed Metals and Alloys.

Method of Measuring and Form	Material						
	Nickel	Monel	Aluminum-Monel	Inconel	Copper	13:2 Cr-Ni Steel	18:8 Cr-Ni Steel
Tension, rod	1.87	1.30	—	1.45	2.15	1.43	1.67
Tension, tubing	1.94	1.32	1.28	1.36	—	—	—
Shear, tubing	2.33	1.33	1.15	1.21	--	—	1.70

(a) Ratio of 0.1-percent proof stress for metal extended to 3 percent equivalent reduction to that for unextended metal.

Table 3.- Details of Thermal and Mechanical Treatments of Tubing

Metal	Treatments Received	Specimen Designation	No. of Specimens	Annealing Temperature (deg. F)	Time Held (hours)	Cooled In	Mechanical Treatment (a)	Remarks
Nickel TR	Cold drawn 10 percent	TRA	2	—	As received			
	Cold drawn 20 percent	TRB	2	—	As received			
	Cold drawn 30 percent	TRC	2	—	As received			
	Cold drawn 40 percent	TRD	2	—	As received			
	Tube reducer 75 to 80 percent	TRE	2	—	As received			
		TRE-3	2	300	1	Air	Tested as annealed	
		TRE-5	2	500				
		TRE-7	2	700				
		TRE-9	2	900				
		TRE-10	2	1000				
		TRE-11	2	1100				
		TRE-12	2	1200				
	Tube reducer 75 to 80 percent normalized at 500°F	TRF-14.5	2	1450			Tested as annealed	
		TRF-14.5R-0.5	2				Extended 0.5 percent	
		TRF-14.5R-1.0	2				" 1.0 "	
		TRF-14.5R-2.0	2				" 2.0 "	
		TRF-14.5R-3.0	2				" 3.0 "	
		TRF-14.5R-5.0	2				" 5.0 "	
		TRF-14.5R-10.0	2				" 10.0 "	
Monel TG	Cold drawn 10 percent	TGA	2	—	As received			
	Cold drawn 20 percent	TGB	2	—	As received			
	Cold drawn 30 percent	TGC	2	—	As received			
	Cold drawn 40 percent	TGD	2	—	As received			
		TGD-3	2	300	1	Air	Tested as annealed	
		TGD-5	2	500				
		TGD-7	2	700				
		TGD-9	2	900				
		TGD-10	2	1000				
		TGD-11	2	1100				
		TGD-12	2	1200				

Table 3a.- Continued.

Metal	Treatments Received	Specimen Designation	No. of Specimens	Annealing Temperature (deg. F)	Time Held (hours)	Cooled In	Mechanical Treatment (a)	Remarks
Monel TG	Tube reducer 75 to 80 percent, normalized at 500°F	TGE-14	2				Tested as annealed	
		TGE-14R-0.5	2				Extended 0.5 percent	
		TGE-14R-1.0	2				" 1.0 "	
		TGE-14R-2.0	2	1400	1	Air	" 2.0 "	
		TGE-14R-3.0	2				" 3.0 "	
		TGE-14R-5.0	2				" 5.0 "	
		TGE-14R-10.0	2				" 10.0 "	
Aluminum-Monel TH	Annealed	THA	2		As received			
	Cold drawn 40 percent	THB	2		As received			
	Tube reducer 60 percent	THC	2		As received			
		THC-3	2	300				
		THC-5	2	500				
		THC-7	2	700	1	Air	Tested as annealed	
		THC-9	2	900				
		THC-10	2	1000				
		THC-10.75	2	1075	10	Air	Tested as annealed	
		THC-12.00	2	1200	1	Oil	Tested as annealed	
	Tube reducer 60 percent, normalized at 500°F	THD-15.5	2				Tested as annealed	
		THD-15.5R-0.5	2				Extended 0.5 percent	
		THD-15.5R-1.0	1				" 1.0 "	Tested in tension only.
		THD-15.5R-2.0	2	1550	1	Oil	" 2.0 "	
		THD-15.5R-3.0	2				" 3.0 "	
		THD-15.5R-5.0	2				" 5.0 "	
		THD-15.5R-10.0	2				" 10.0 "	
Inconel TL	Annealed	TLA	2	—	As received			
	Cold drawn 50 percent	TLB	2	—	As received			
	Tube reducer 75 - 80 percent	TLC	2	—	As received			
		TLC-3	2	300				
		TLC-5	2	500				
		TLC-7	2	700				
		TLC-9	2	900	1	Air	Tested as annealed	
		TLC-11	2	1100				
		TLC-13	2	1300				
		TLC-15	2	1500				

Table 3b.- Continued.

Metal	Treatments Received	Specimen Designation	No. of Specimens	Annealing Temperature (deg. F)	Time Held (hours)	Cooled In	Mechanical Treatment (a)	Remarks
Inconel TL	Tube reducer 75 - 80 percent, normalized at 5000°F	TLD-17.5	2	1750	1	Air	Tested as annealed	
		TLD-17.5R-0.5	2				Extended 0.5 percent	
		TLD-17.5R-1.0	2				" 1.0 "	
		TLD-17.5R-2.0	2				" 2.0 "	
		TLD-17.5R-3.0	2				" 3.0 "	
		TLD-17.5R-5.0	2				" 5.0 "	
		TLD-17.5R-10.0	2				" 10.0 "	
		TLD-17.5R-17.0	1				" 17.0 "	Tested in tension only.
		TLD-17.5R-17.25	1				" 17.25 "	Tested in torsion only.
18:8 Cr-Ni Steel TC	Cold-drawn	TC	1		As received			" " " "
		TC-3	1	300				" " " "
		TC-5	1	500				" " " "
		TC-7	1	700	1	Air	Tested as annealed	" " " "
		TC-9	1	900				" " " "
		TC-11	1	1100				" " " "
		TC-13	1	1300			Tested as annealed	" " " "
		TC-19	1				" " "	" " " "
		TC-19R-0.5	1				Extended 0.5 percent	" " " "
		TC-19R-1.0	1				" 1.0 "	" " " "
		TC-19R-2.0	1	1900	1	Water	" 2.0 "	" " " "
		TC-19R-3.0	1				" 3.0 "	" " " "
		TC-19R-5.0	1				" 5.0 "	" " " "
		TC-19R-10.0	1				" 10.0 "	" " " "
		TC-19R-20.0	1				" 20.0 "	" " " "

(a) Only nominal extensions indicated; for actual values, see diagrams.

Table 4.- Hysteresis

Specimen No.	Cycle No.	True Stress Range	Total Cycle Time	Time Interval After Preceding Cycle	Strain Range	Loop Width	Permanent Set Due to Cycle, %		Total Permanent Set	Negative Creep at Bottom, %			Positive Creep Below Top
							Before Negative Creep	Net		1 min.	2 min.	3 min.	
		(lb per in.^{2})	(min.)	(hr:min)	(%)	(%)			(%)				(%)
DA-5	1	1.4-75.5x10^3	——	——	15.3	—	—	15.00	15.00	—	—	—	—
	2	1.7-75.5	13.0	0:0	0.424	0.145	0.094	0.086	15.086	0.006	—	0.008	—
	3	1.7-75.5	14.0	0:0	.366	.092	.038	.034	15.120	.003	—	.004	—
	4	1.7-75.5	10.5	0:0	.349	.076	.022	.018	15.138	.002	—	.004	—
	5	1.7-75.5	11.0	0:0	.346	.074	.023	.015	15.153	.004	—	.008	0.008
	6	1.7-75.5	10.5	0:0	.345	.069	.018	.015	15.168	.001	—	.003	.005
	8	1.7-75.5	8.0	0:0	.337	.065	.013	.009	15.187	.003	—	.004	.005
	35	1.7-75.5	9.0	0:0	.329	.055	.010	.005	15.249	.003	—	.005	.003
	39	1.7-75.5	11.0	0:0	.329	.057	.008	.005	15.266	.002	—	.003	.005
	140	1.7-75.5	12.0	0:0	.324	.049	.006	.003	15.344	.002	—	.003	.003
	155	1.7-75.5	10.0	24:0	.353	.067	.032	.027	15.387	.004	—	.005	.005
	156	1.7-75.5	9.0	0:0	.331	.054	.008	.004	15.391	.002	—	.004	.005
	157	1.7-75.5	10.0	0:0	.333	.054	.009	.005	15.396	.003	—	.004	.003
	159	1.7-75.5	57.5	0:0	.335	.055	.010	.006	15.404	.002	—	.004	.003
	161	1.7-75.5	10.0	0:0	.328	.050	.005	.001	15.409	.003	—	.004	.004
DA-3	1	1.4-45.5x10^3	29.0	——	3.36	3.20	—	3.185	3.185	—	—	—	—
	2	1.5-45.5	16.5	0:0	0.329	0.187	0.166	0.156	3.341	—	0.010	—	—
	3	1.5-45.5	8.5	0:0	.232	.092	.061	.060	3.401	—	.001	—	—
	4	1.5-45.5	8.5	0:0	.230	.083	.054	.051	3.452	—	.003	—	—
	5	1.5-45.5	9.0	0:0	.221	.084	.036	.034	3.486	—	.002	—	0.030
DA-4	1-30	1.5-45.5x10^3	1.0 (Avg.)-		—	—	—	3.50	3.50	—	—	—	—
	31	1.5-45.5	10.0	0:0	0.224	0.076	0.055	0.052	3.552	—	0.003	—	0.015
	83	1.5-45.5	13.5	0:02	.178	.026	.0088	.0064	3.791	0.0024	—	—	.0038
	116	1.5-45.5	10.0	72:0	.187	.031	.0175	.0137	3.867	.0038	—	—	.0016
	118	1.5-45.5	12.5	0:02	.175	.022	.0055	.0034	3.873	.0021	—	—	.0037
	376	1.5-45.5	17.0	0:02	.176	.024	.0053	.0030	3.955	.0023	—	—	.0052
	377	1.5-45.5	13.5	0:02	.178	.025	.0077	.0057	3.963	.0020	—	—	.0026
	388	1.5-45.5	71.0	0:02	.185	.032	.0120	.0112	3.981	.0008	—	—	.0024

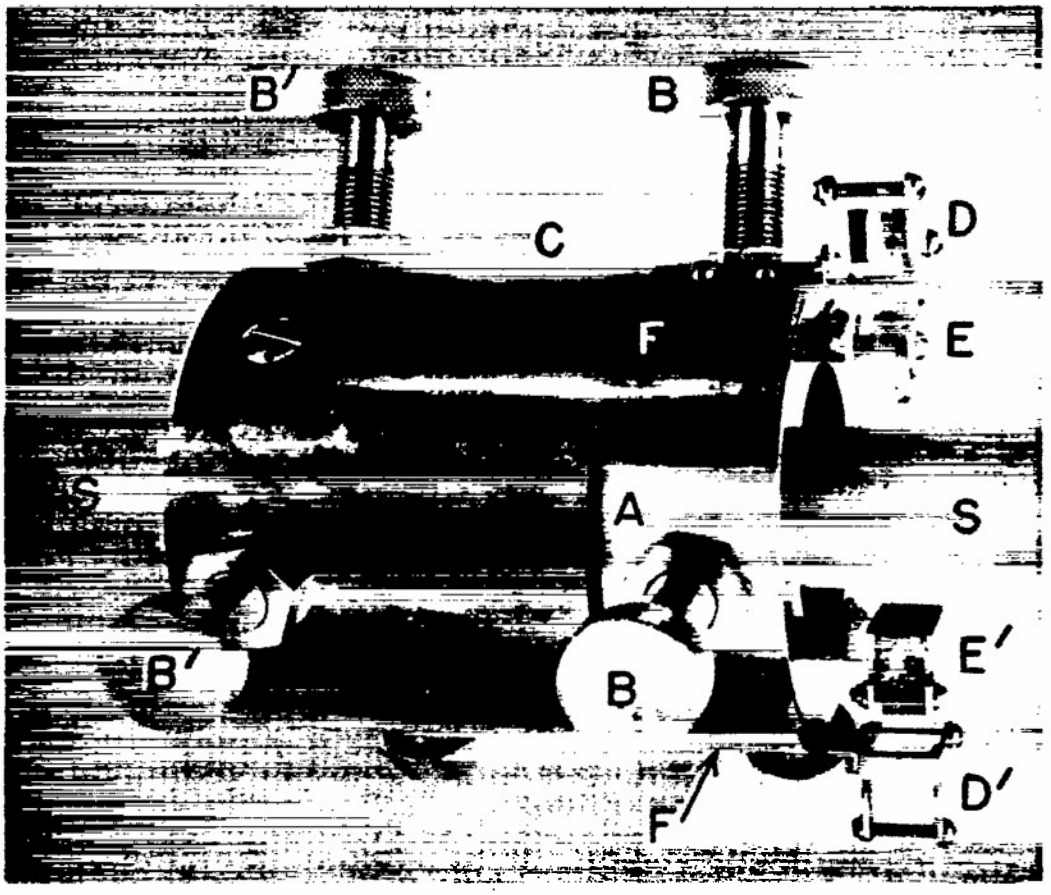

S	Specimen
A, A'	Gage rings
B, B'	Set screws
C	Cylinder
D, D'	Standard prisms
E, E'	Roof prisms
F	Placement screw positions

Figure 1.- Optical torsion meter.

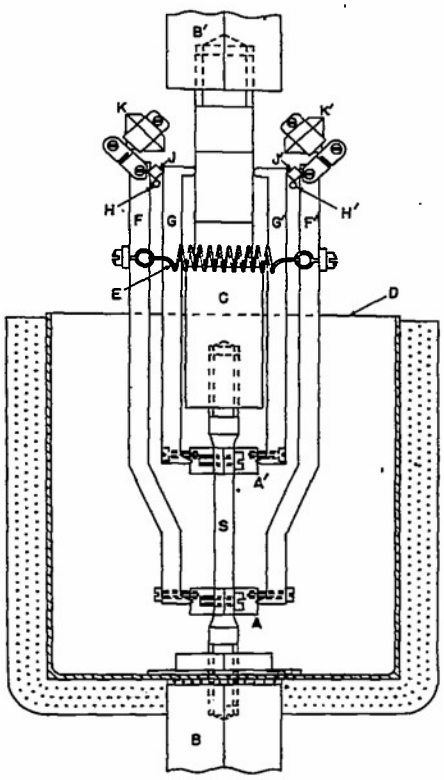

S	Test specimen
A, A'	Specimen clamps
B, B'	Amsler testing machine adapters
C	Special adapter
D	Insulated cooling system
E	Helical spring
F, F'	Outer extension arms
G, G'	Inner extension arms
H, H'	Heating coils
J, J'	Stellite prismatic lozenges
K, K'	Roof prisms

Figure 2.- Assembly of low temperature, tension testing apparatus.

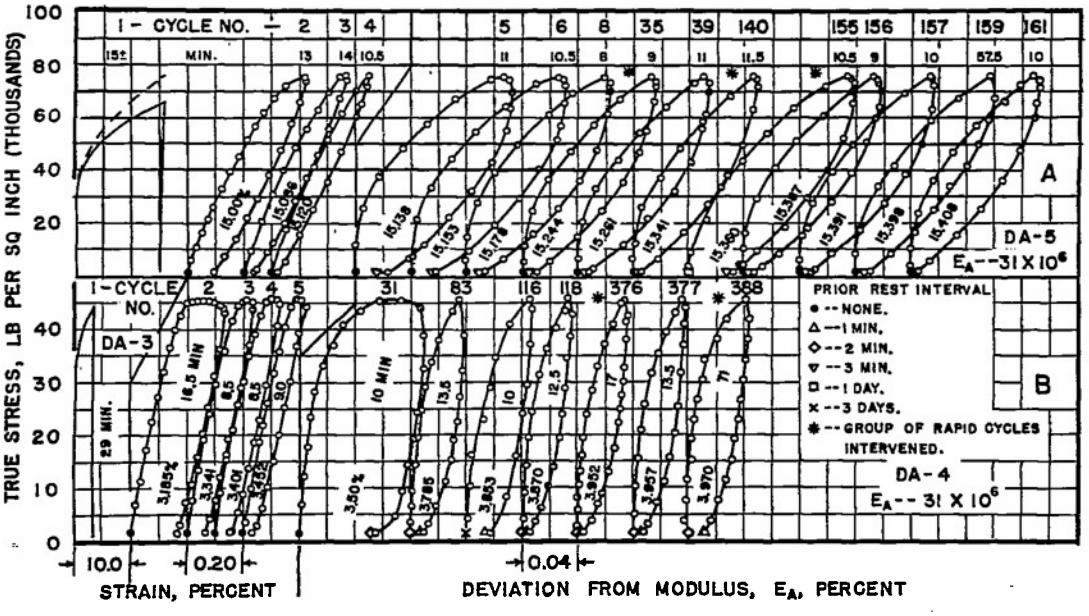

Figure 3.- Variation of form of hysteresis loops with cyclic repetition.

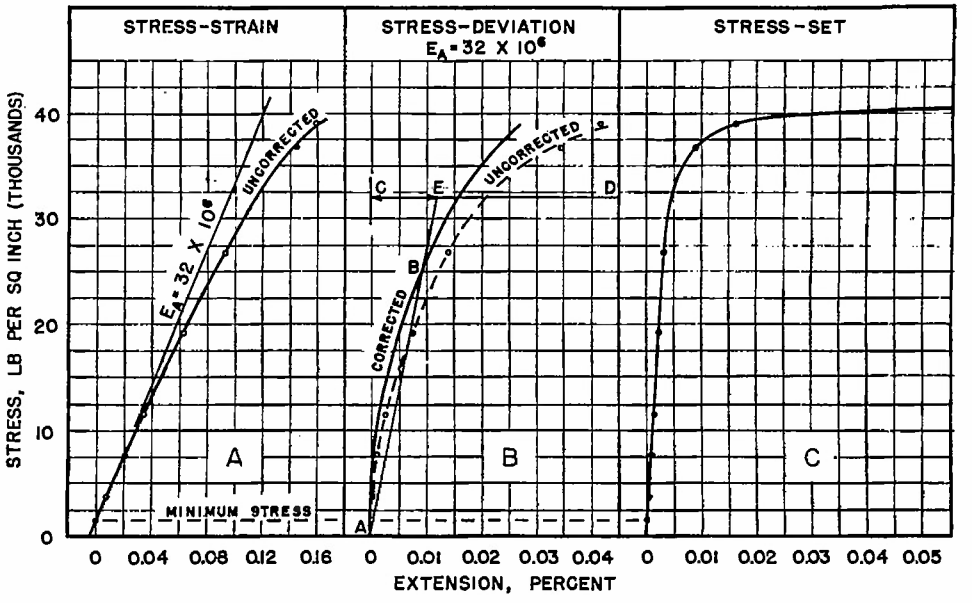

Figure 4.- Typical correlated stress-strain, stress-deviation and stress-set curves, annealed and extended nickel R-14.

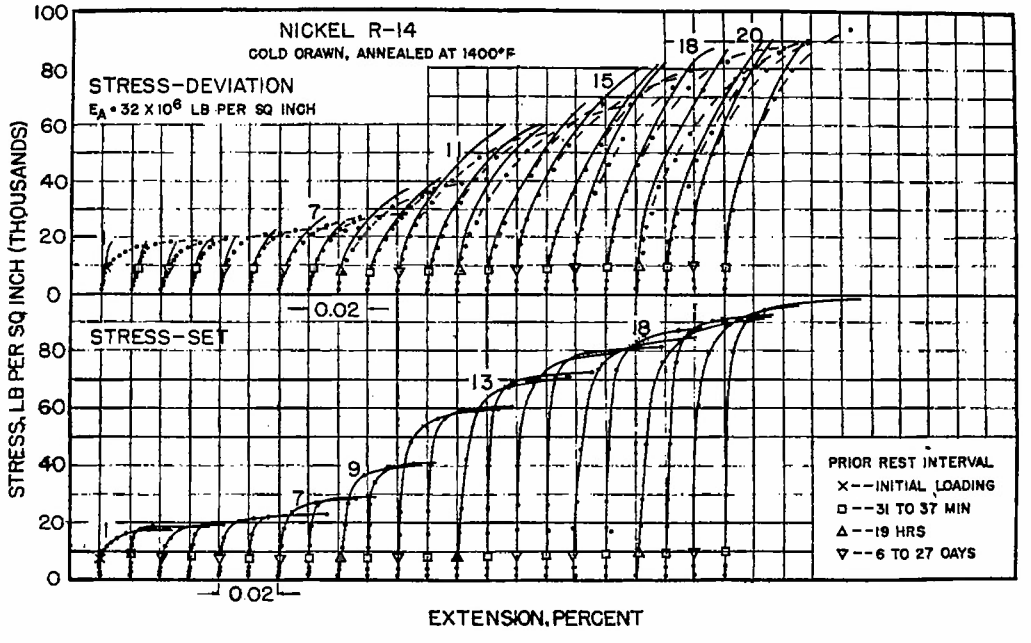

Figure 5.- Tension stress-deviation and stress-set curves for annealed nickel rod R-14 as influenced by prior extension.

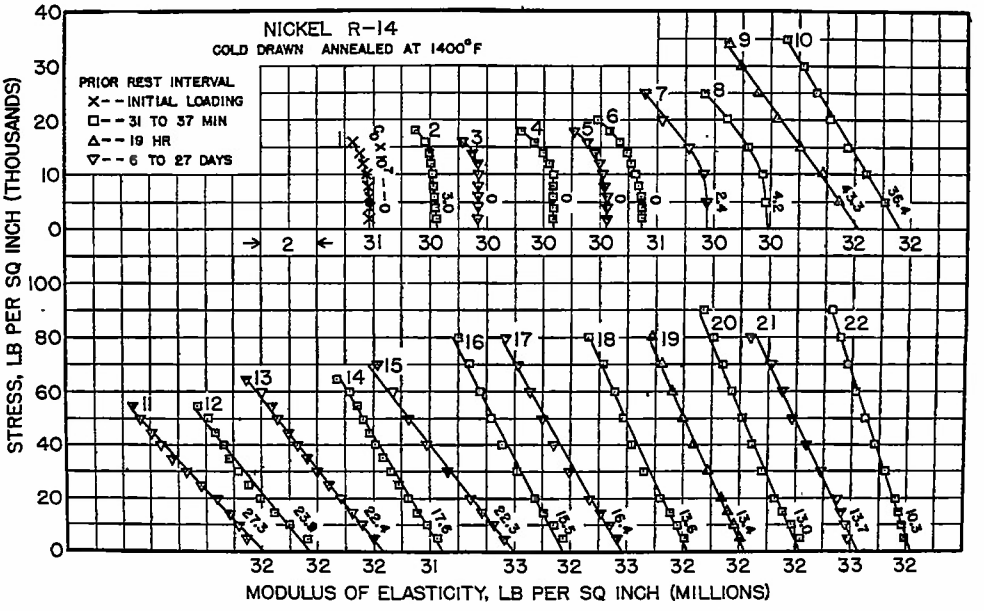

Figure 6.- Tension stress-modulus lines for annealed nickel rod R-14 as influenced by prior extension.

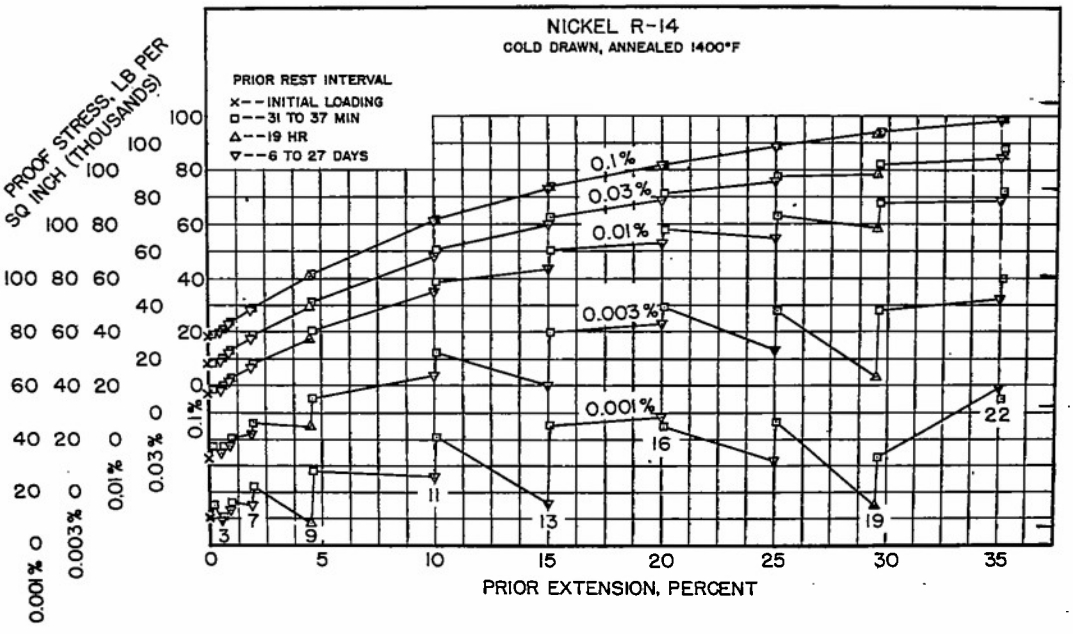

Figure 7.- Variation of tensile proof stresses with prior extension for annealed nickel rod R-14.

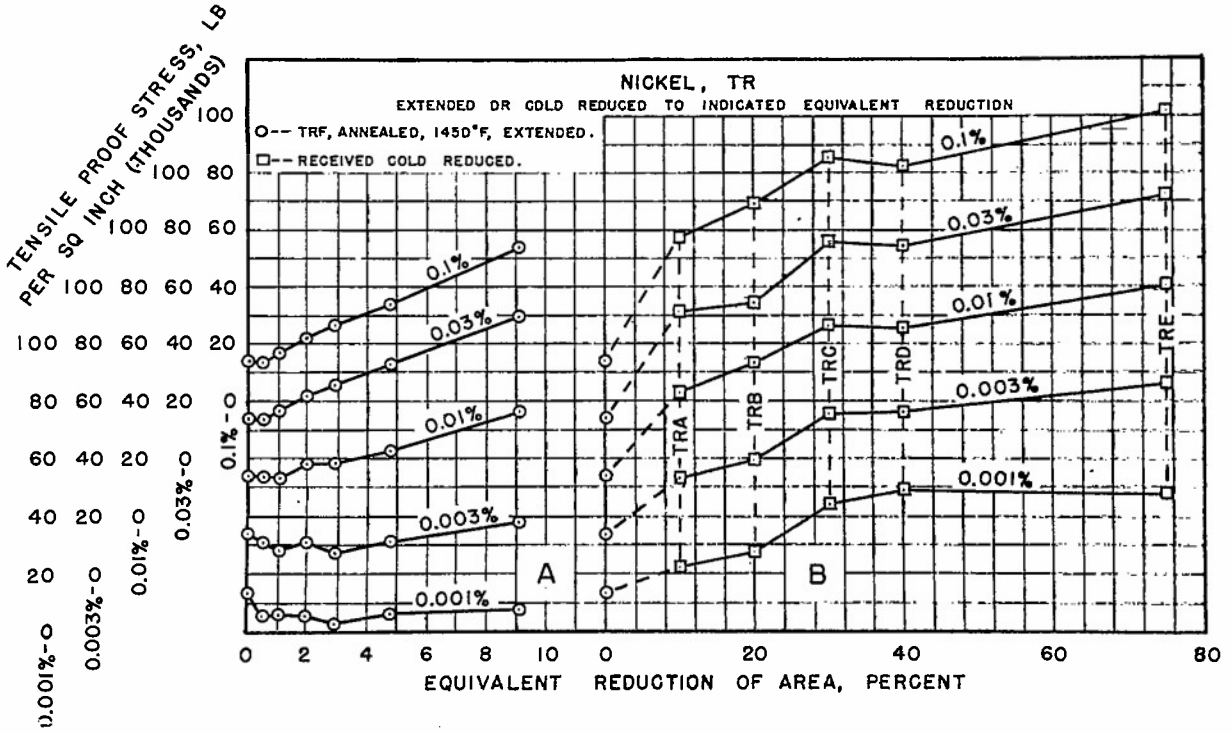

Figure 8.- Variation of tensile proof stresses with prior deformation for nickel tubing TR. A-Nickel TRF, annealed and extended. B-Cold-reduced nickel.

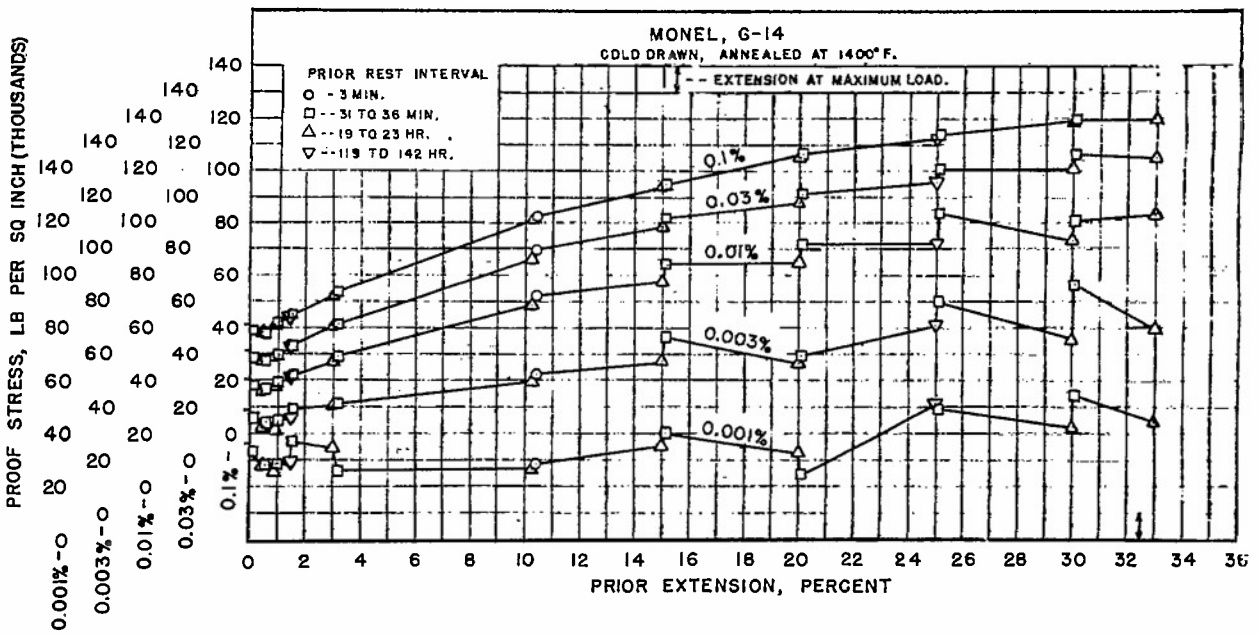

Figure 9.- Variation of tensile proof stresses with prior extension of annealed monel rod G-14.

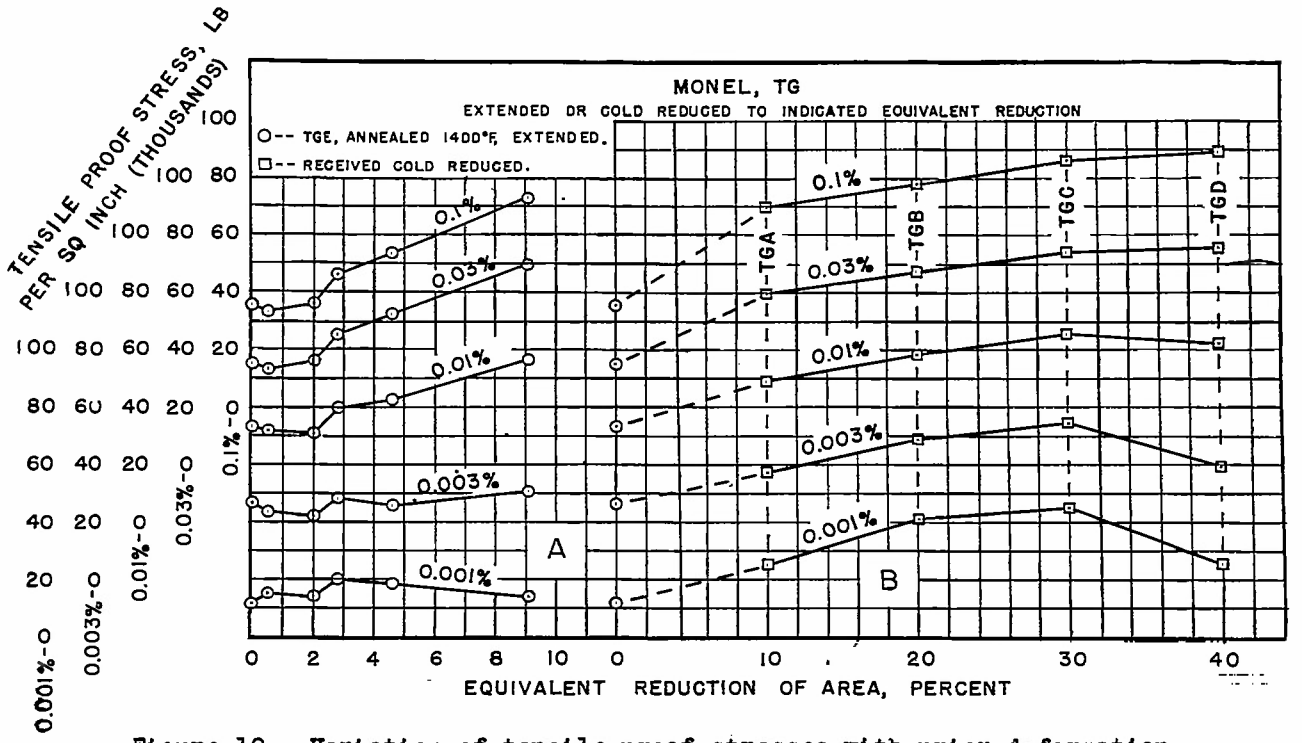

Figure 10.- Variation of tensile proof stresses with prior deformation for monel tubing TG. A-Monel TGE, annealed and extended. B-Cold-reduced monel.

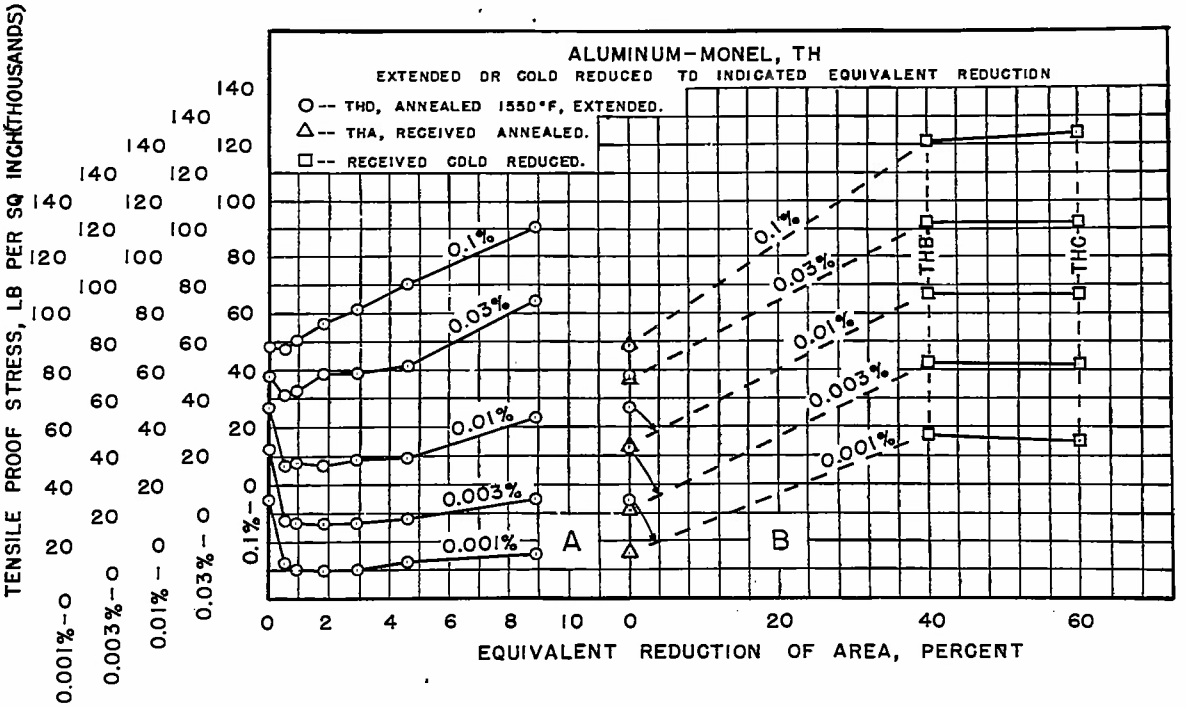

Figure 11.- Variation of tensile proof stress with plastic deformation for aluminum-monel tubing TH. A-Aluminum-monel THD, annealed and extended. B-Cold-reduced aluminum-monel.

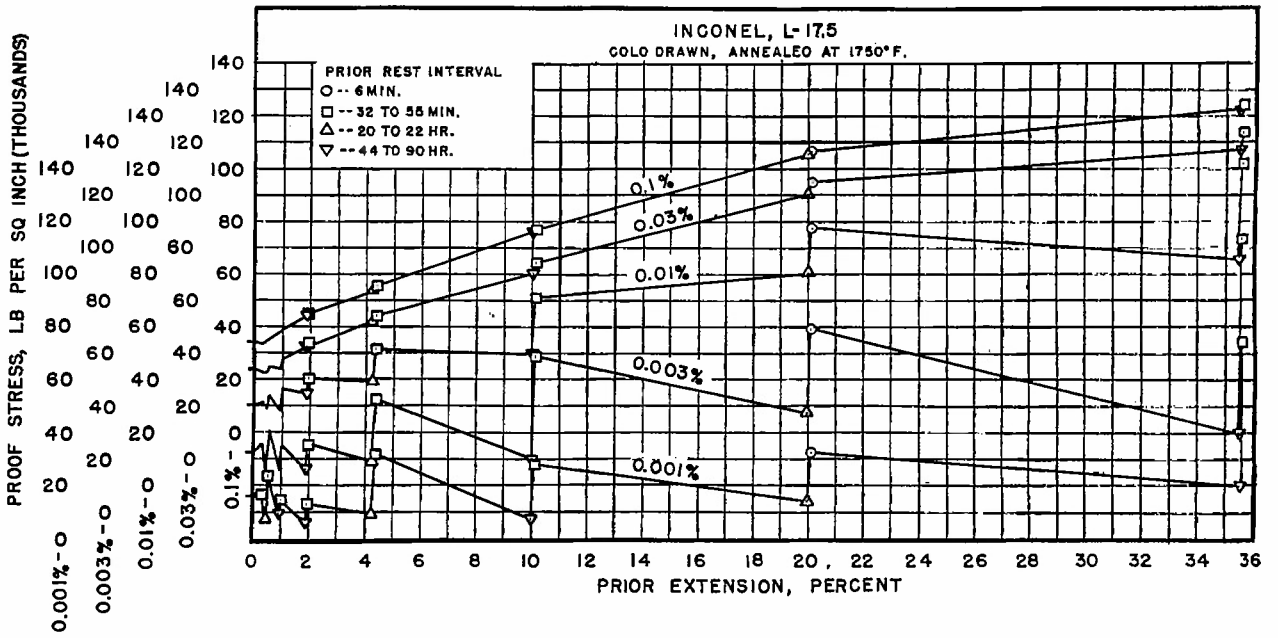

Figure 12.- Variation of tensile proof stresses with prior extension for annealed Inconel rod L-17.5.

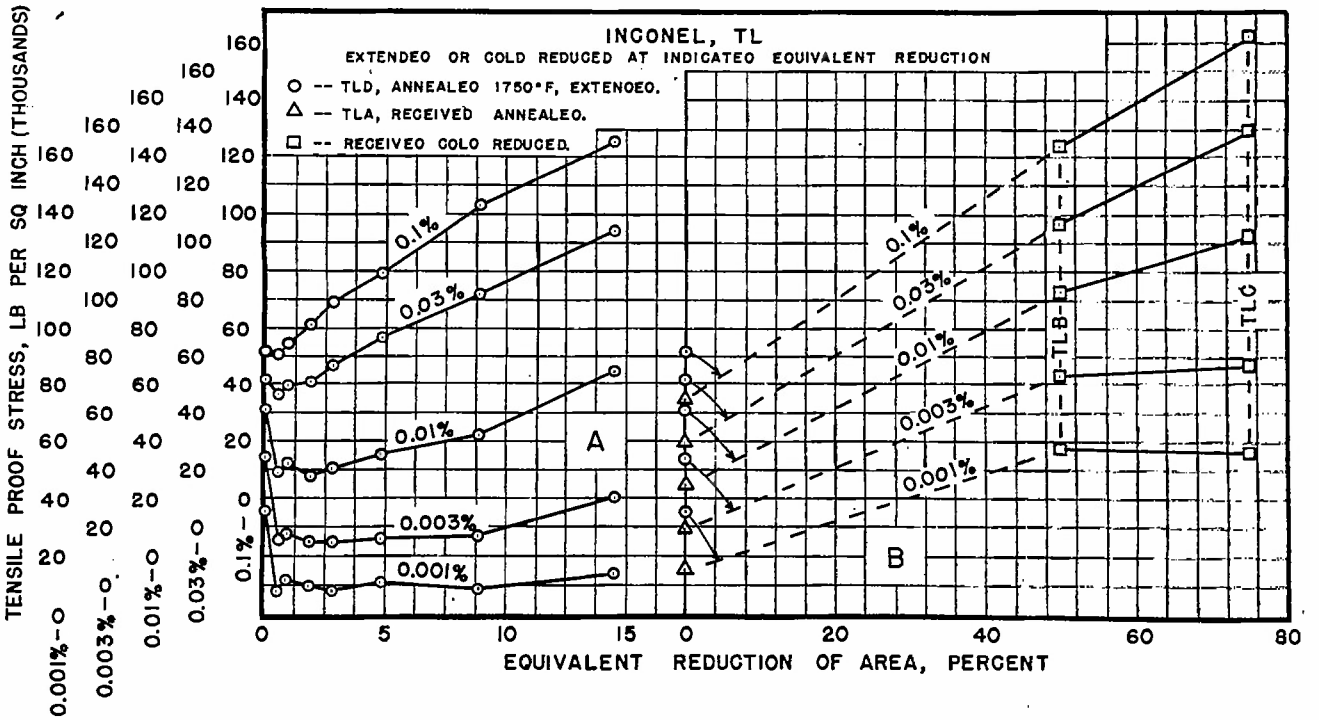

Figure 13.- Variation of tensile proof stresses with plastic deformation for Inconel tubing TL. A-Inconel TLD, annealed and extended. B-Cold-reduced Inconel.

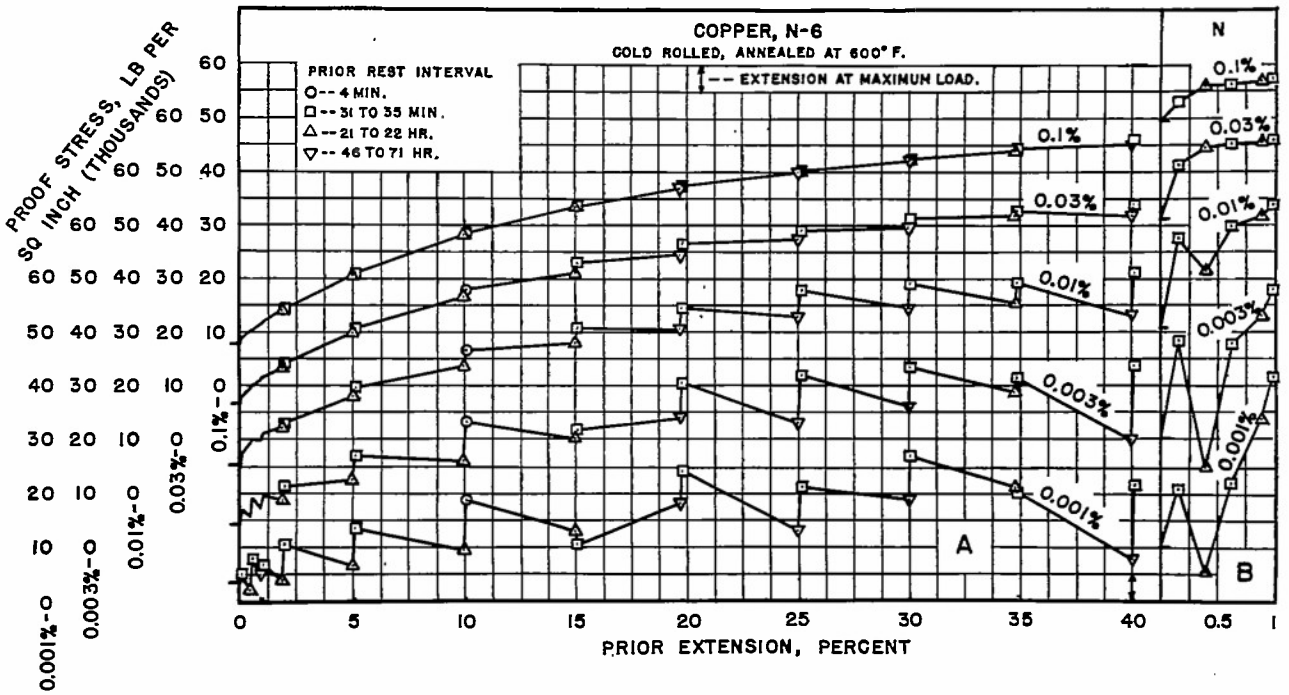

Figure 14.- Variation of tensile proof stresses with prior extension for copper rod. A-Annealed copper N-6. B-Cold rolled copper N.

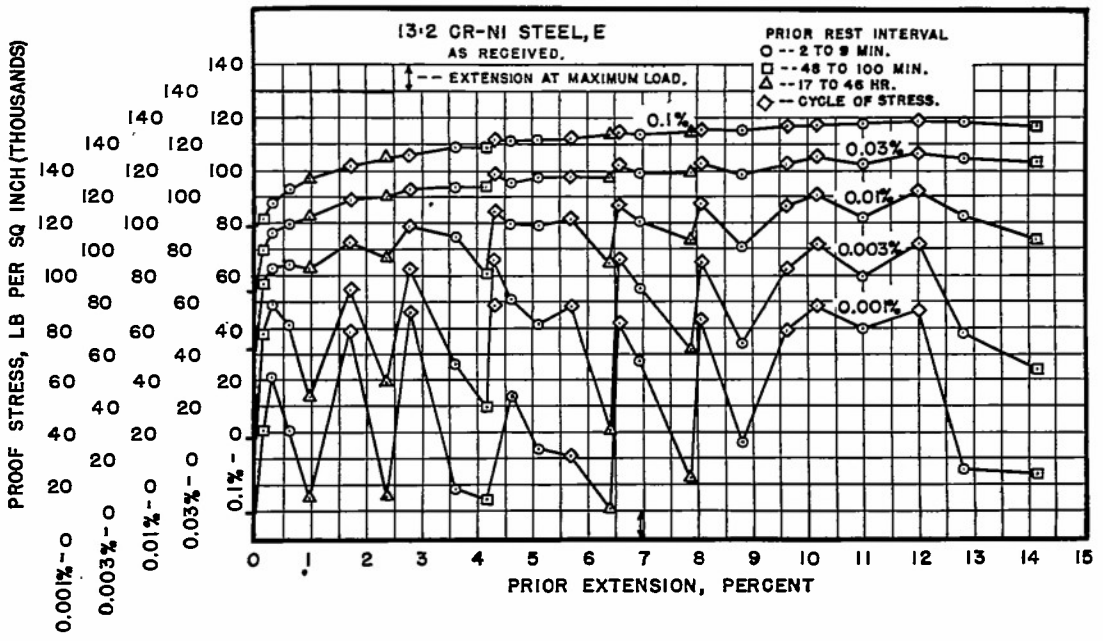

Figure 15.- Variation of tensile proof stresses with prior extension for 13:2 chromium-nickel steel E; as received.

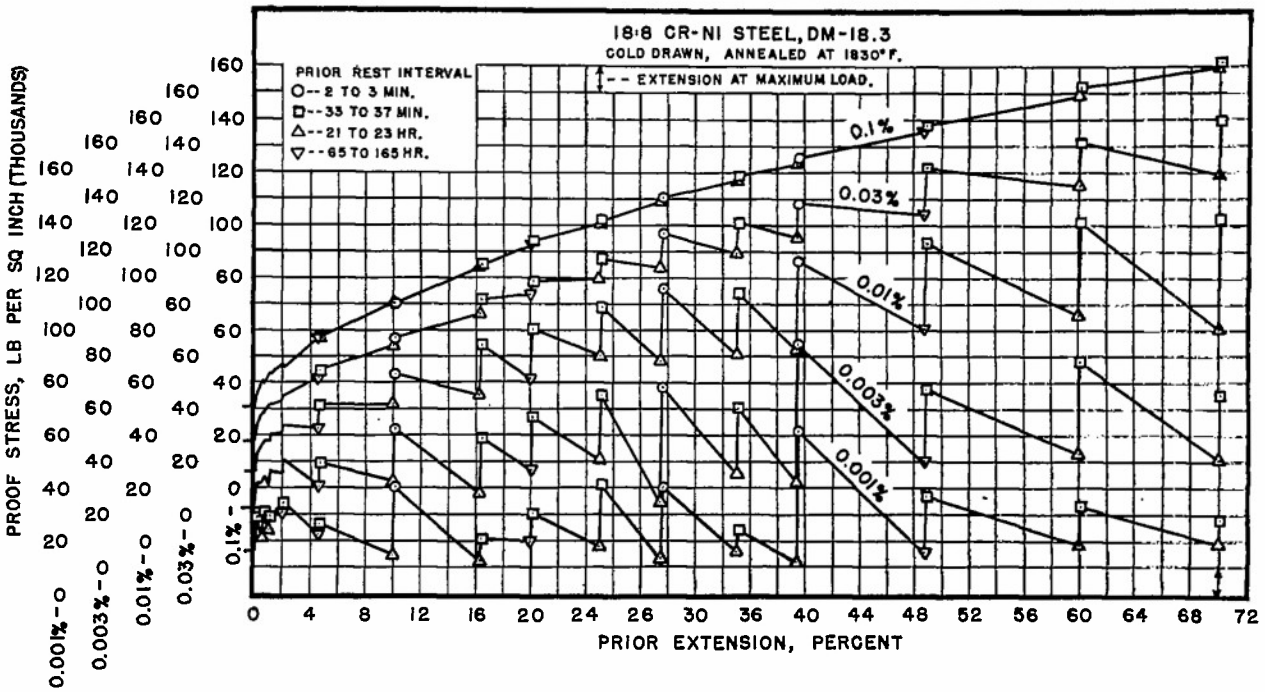

Figure 16.- Variation of tensile proof stresses with prior extension for annealed 18:8 chromium-nickel steel DM-18.3.

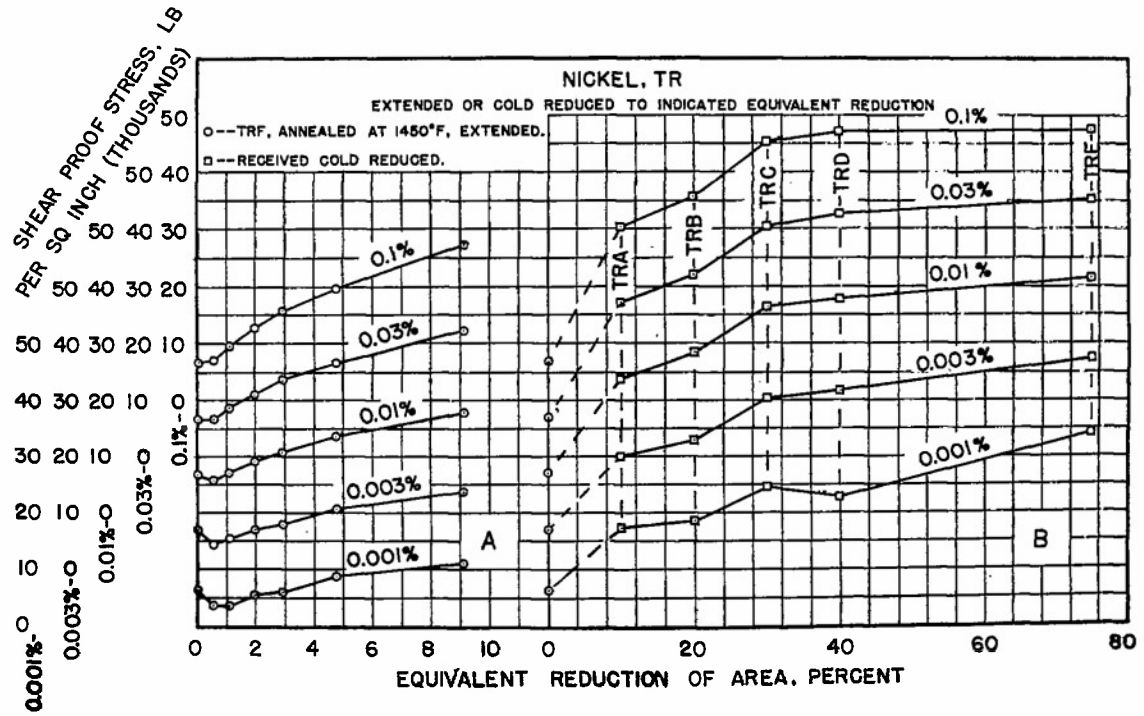

Figure 17.- Variation of shear proof stress with prior deformation for nickel tubing TR. A-Nickel TRF, annealed and extended. B-Cold-reduced nickel.

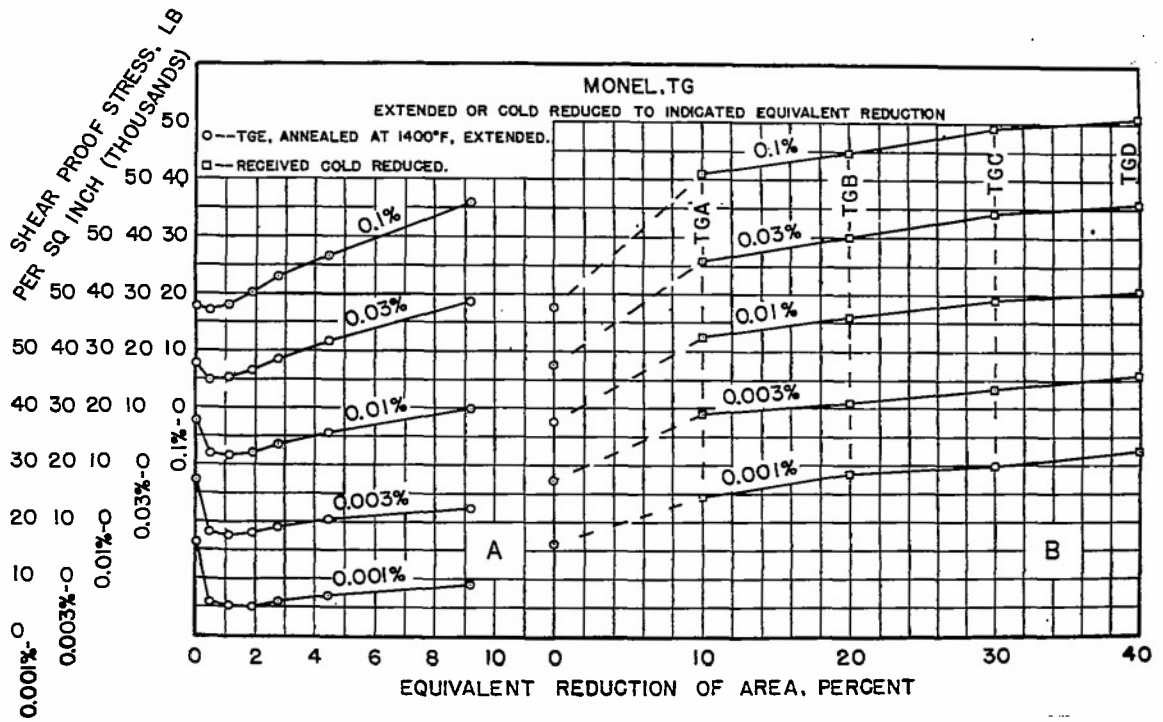

Figure 18.- Variation of shear proof stresses with prior deformation for monel tubing TG. A-Monel TGE, annealed and extended. B-Cold-reduced monel.

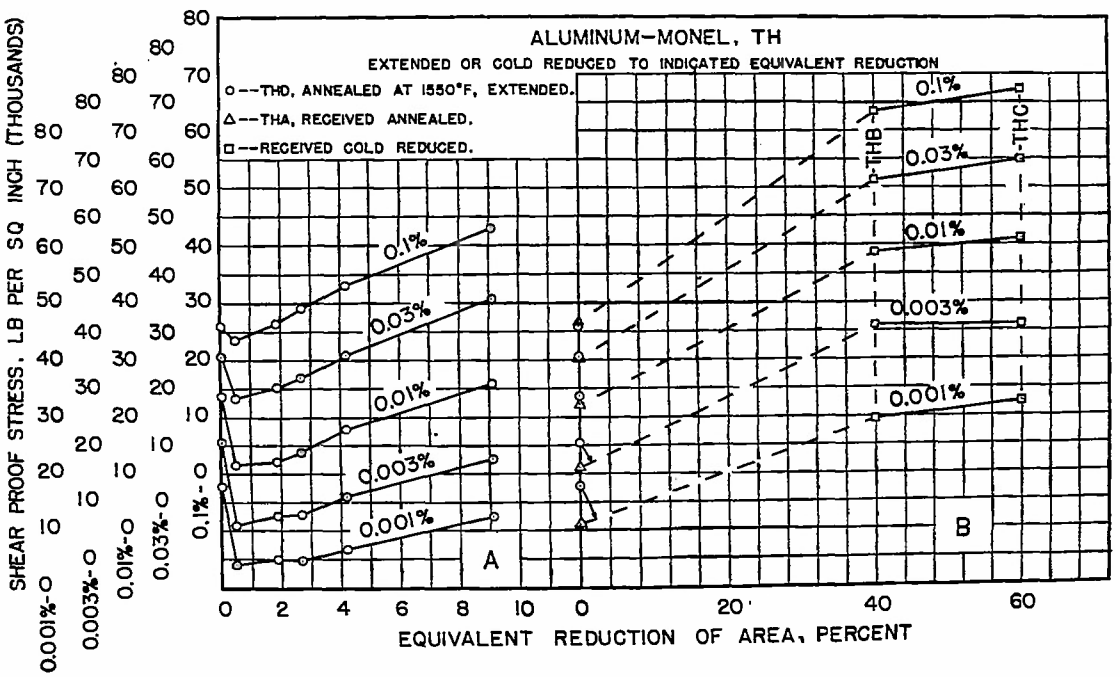

Figure 19.- Variation of shear proof stresses with prior deformation for aluminum-monel tubing TH. A-Aluminum-monel THD, annealed and extended. B-Cold-reduced aluminum-monel.

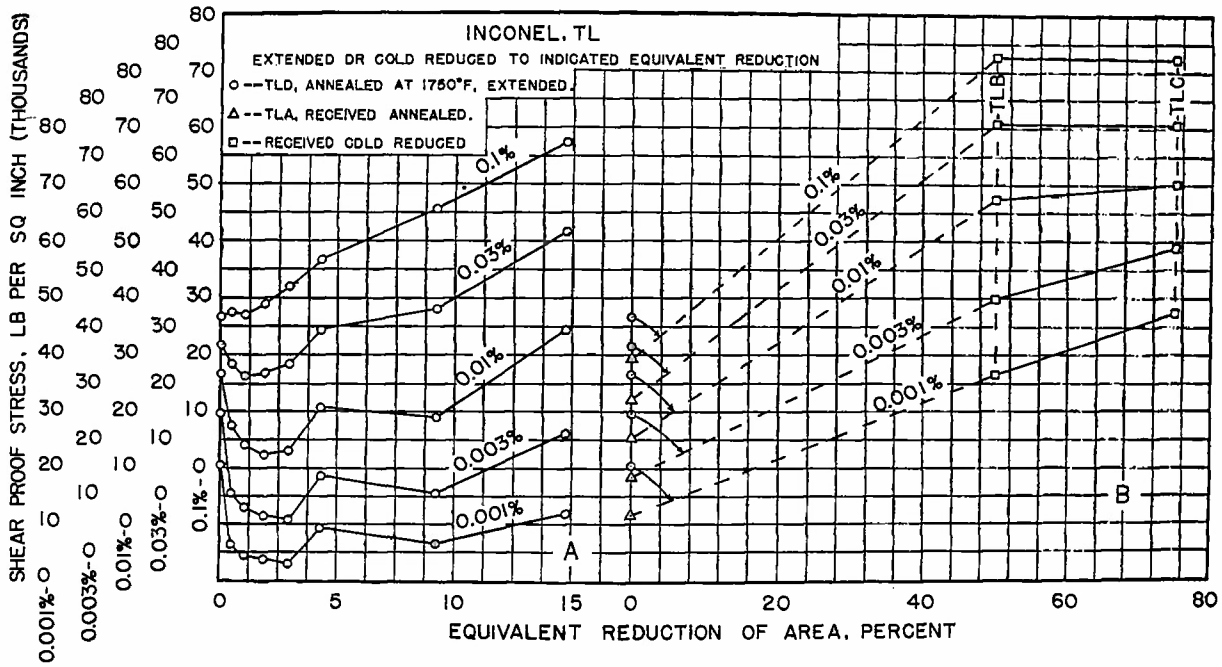

Figure 20.- Variation of shear proof stresses with prior deformation for Inoonel tubing TL. A-Inconel TLD, annealed and extended. B-Cold-reduced Inconel.

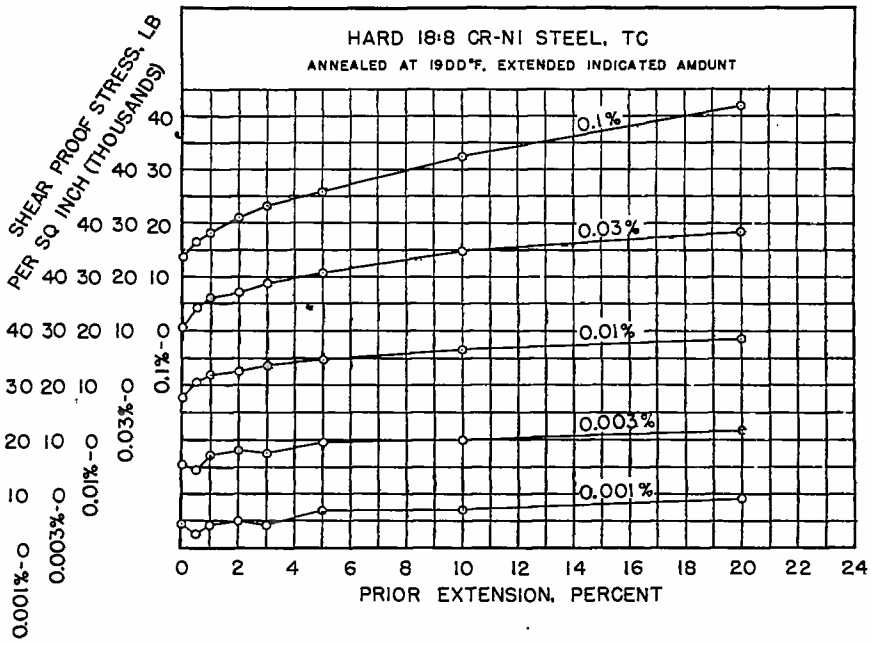

Figure 21.- Variation of shear proof stresses with prior extension for annealed 18:8 chromium-nickel steel tubing TC-19.

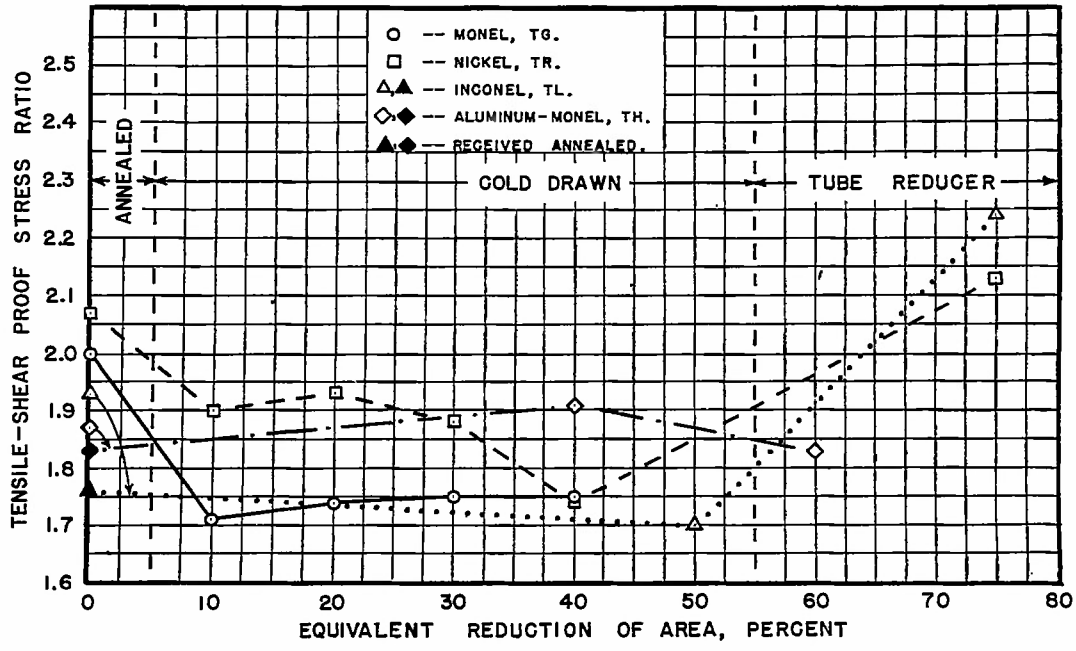

Figure 22.- Influence of cold-reduction on the ratio of 0.1-percent proof stress in tension and in shear for nonferrous metal tubing.

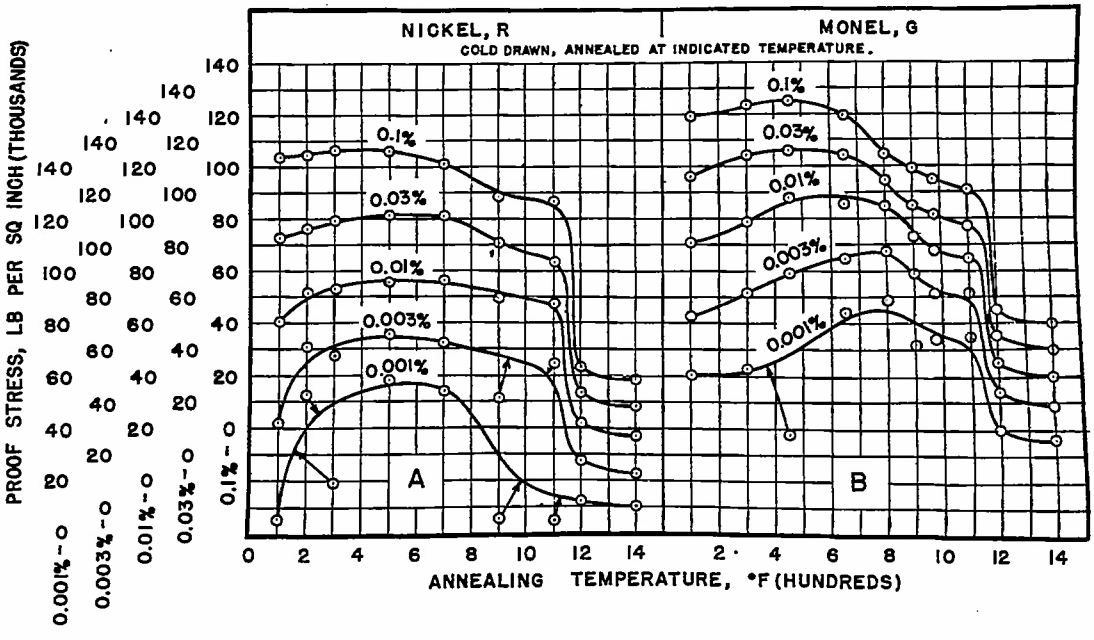

Figure 23.- Variation of tensile proof stresses with annealing temperature. A-Cold-drawn nickel rod R. B-Cold-drawn monel rod G.

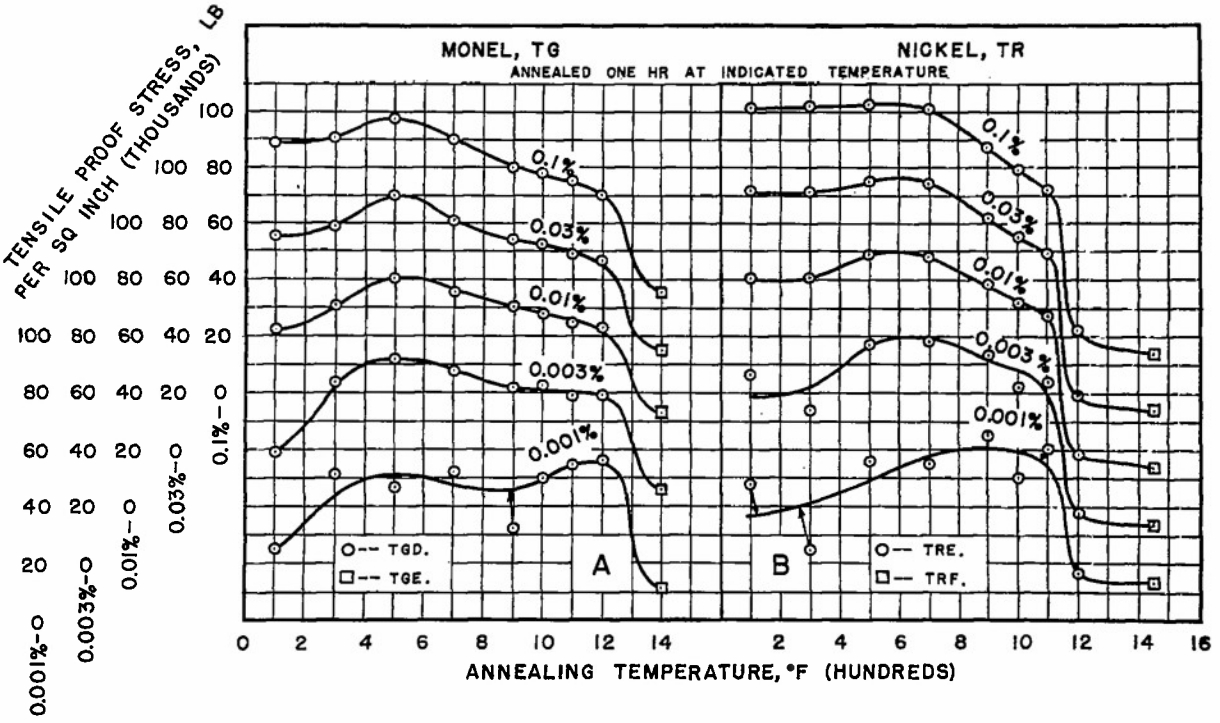

Figure 24.- Variation of tensile proof stresses with annealing temperature. A-Cold-reduced monel tubing TG. B-Cold-reduced nickel tubing TR.

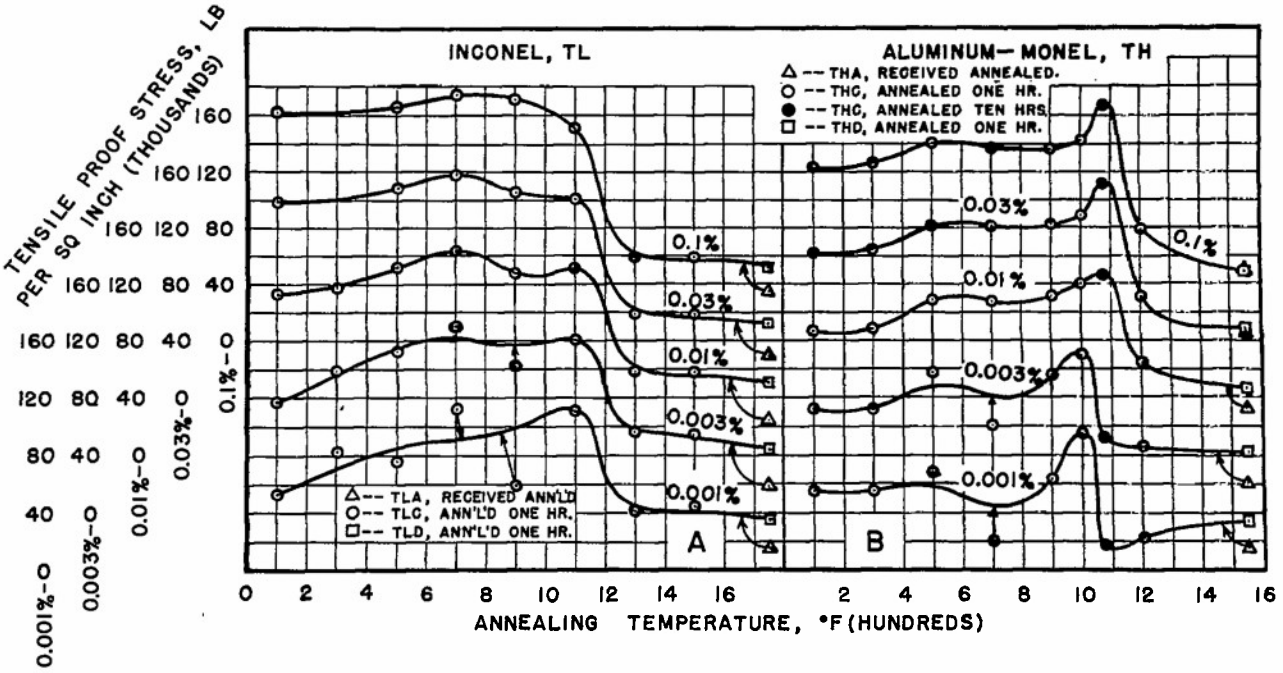

Figure 25.- Variation of tensile proof stresses with annealing temperature. A-Cold-reduced Inconel tubing TL. B-Cold-reduced aluminum-monel tubing TH.

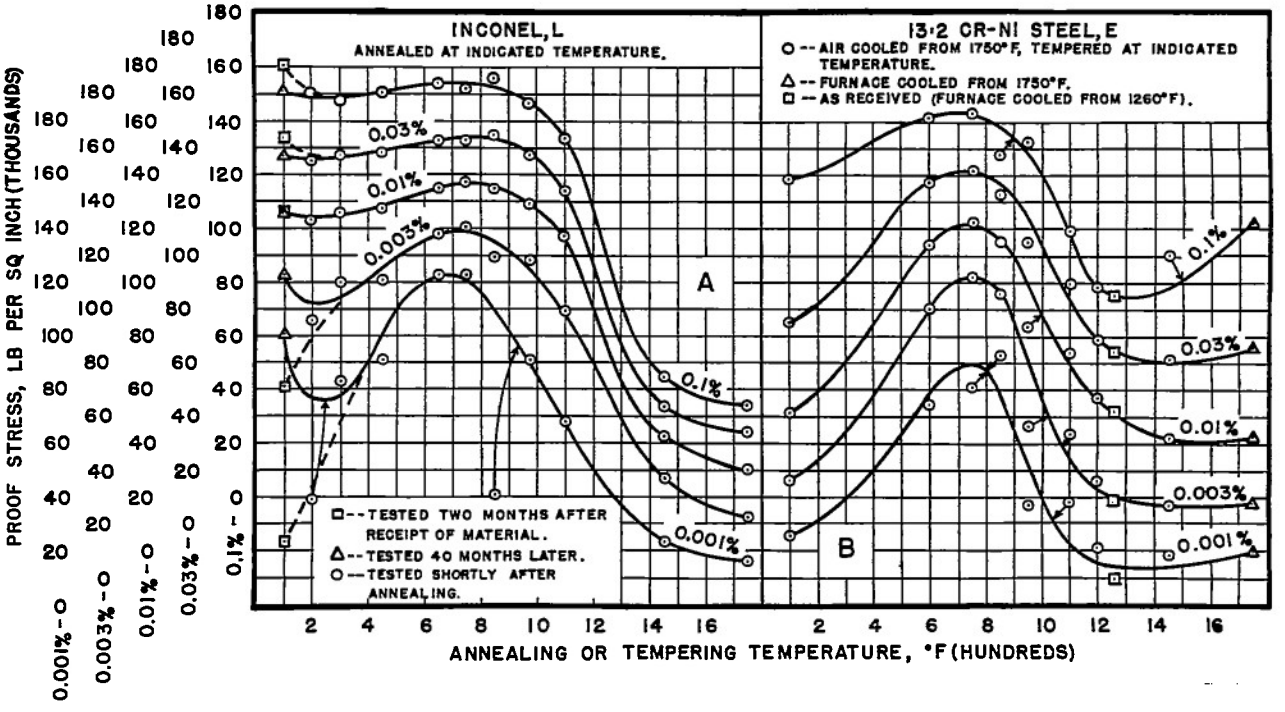

Figure 26.- Variation of tensile proof stresses with annealing or tempering temperature. A-Cold-drawn Inconel rod L. B-Air-cooled 13:2 chromium-nickel steel, E.

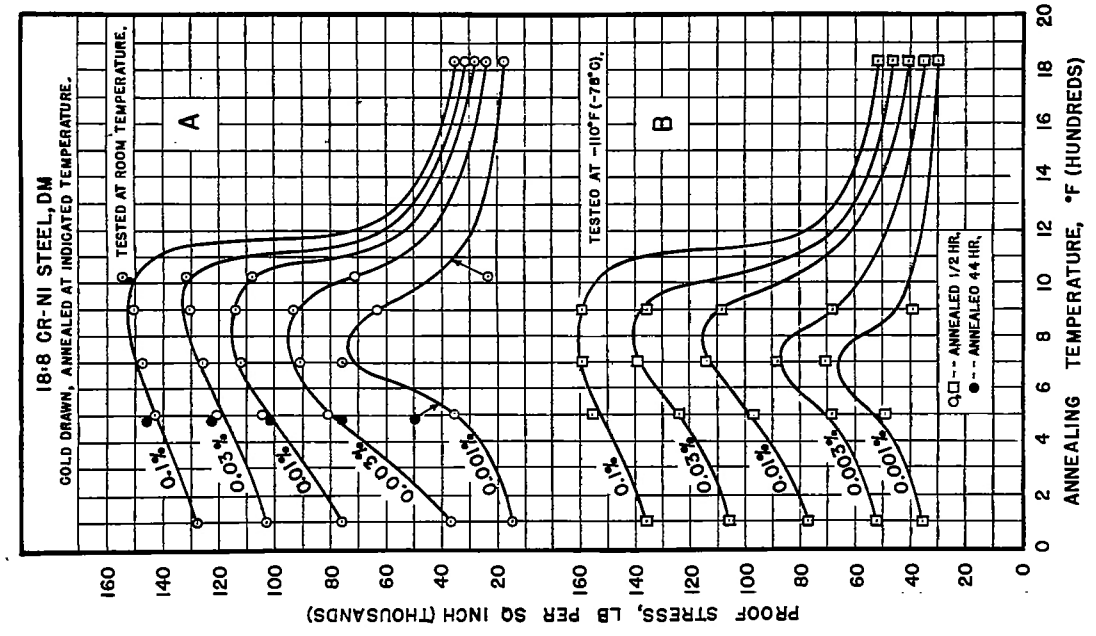

Figure 27.- Variation of tensile proof stresses with annealing temperature for half-hard 18:8 chromium-nickel steel DM. A-Room temperature tests. B-Tested at -110°F.

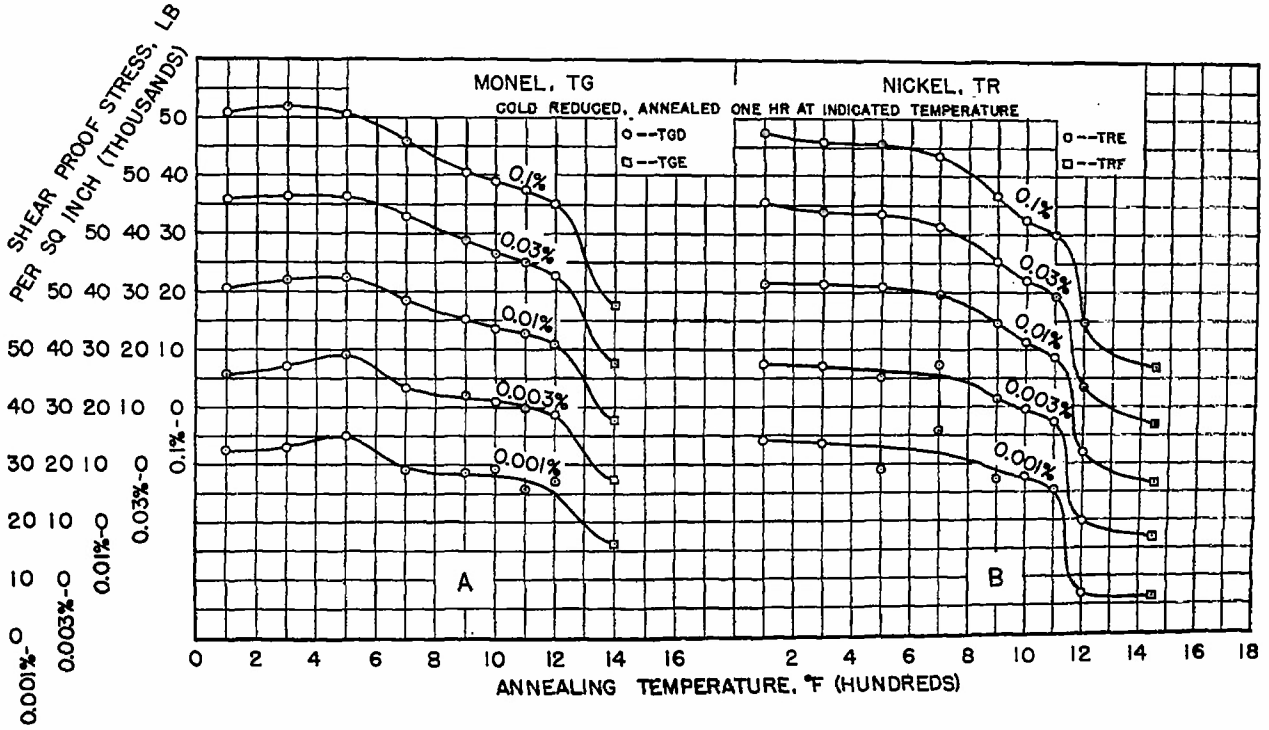

Figure 28.- Variation of shear proof stresses with annealing temperature. A-Cold-reduced monel tubing TG. B-Cold-reduced nickel tubing TR.

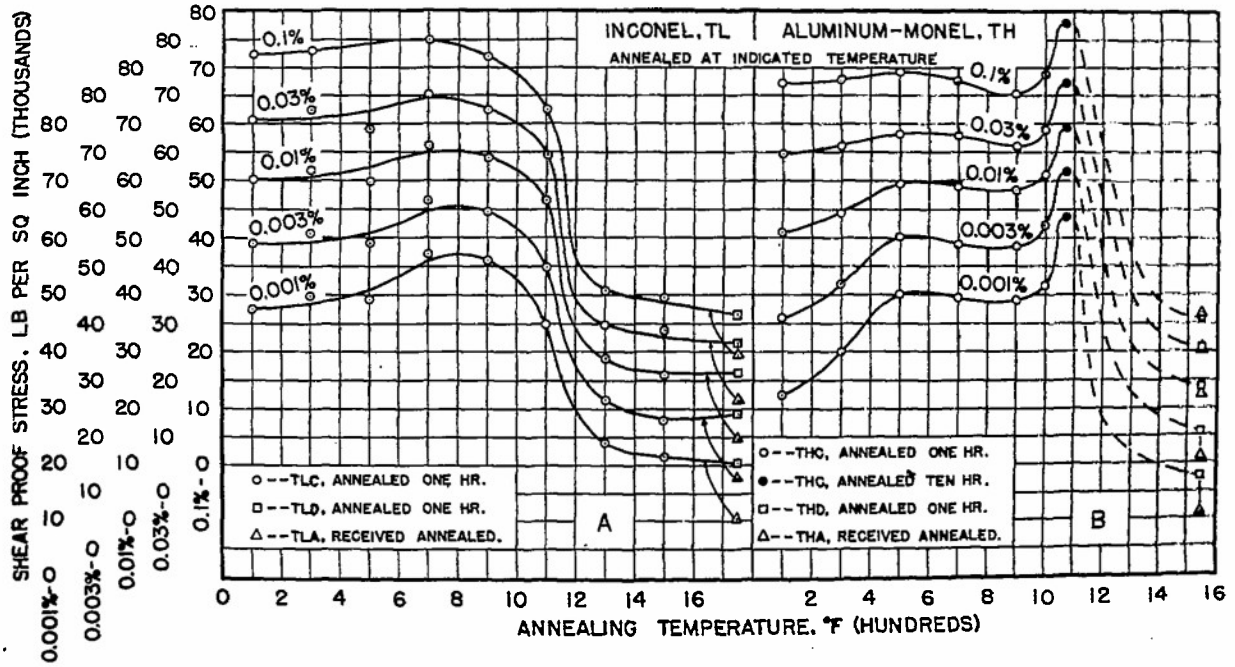

Figure 29.- Variation of shear proof stresses with annealing temperature. A-Cold-reduced Inconel tubing TL. B-Cold-reduced aluminum-monel tubing TH.

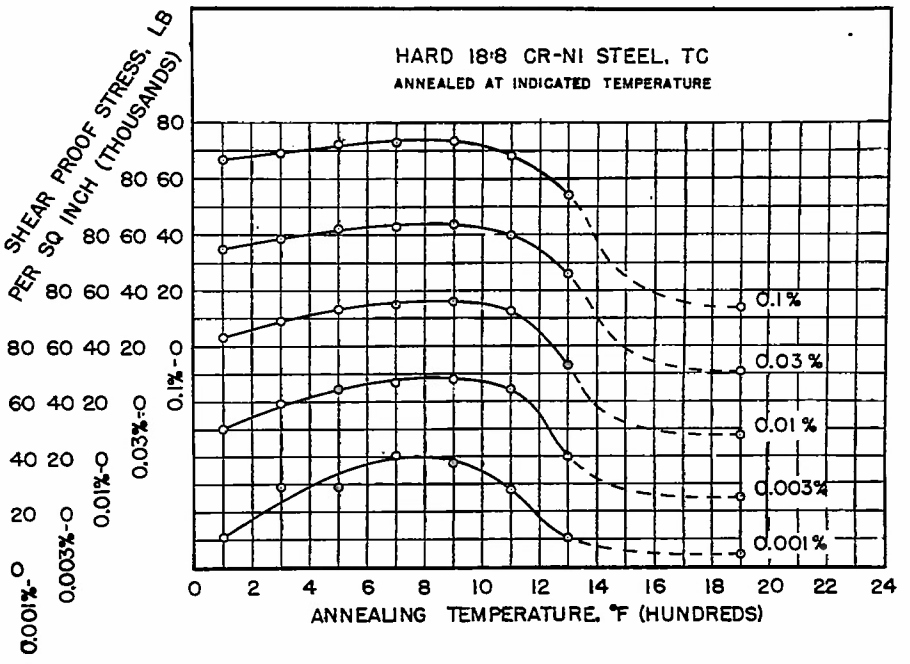

Figure 30.- Variation of shear proof stresses with annealing temperature for cold-drawn 18:8 chromium-nickel steel tubing TC.

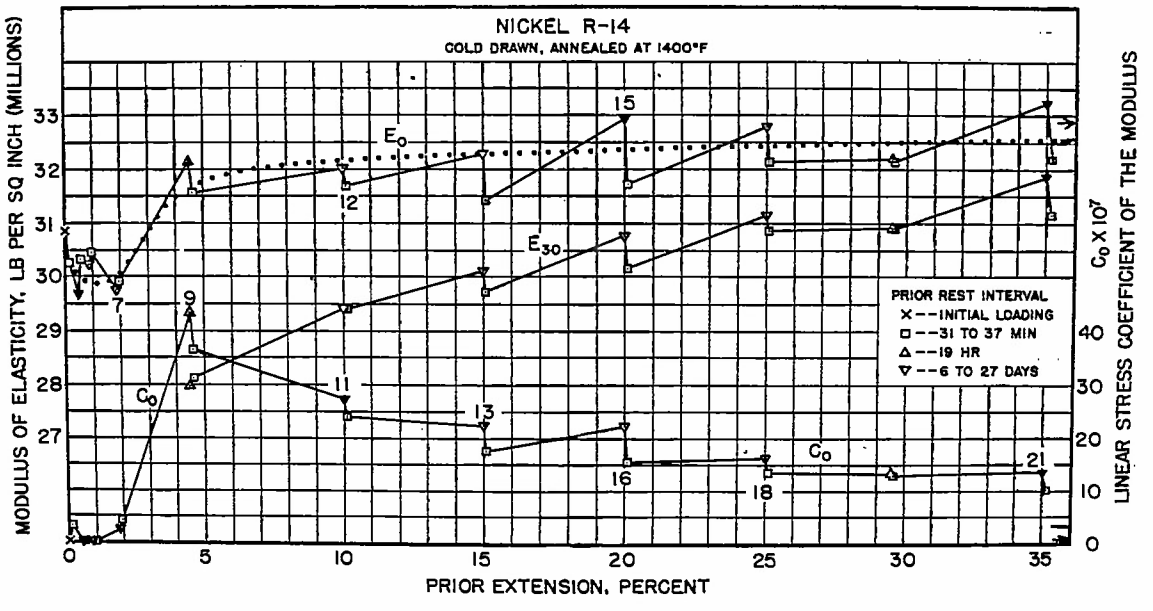

Figure 35.- Variation of tensile modulus of elasticity and its linear stress coefficient with prior extension for annealed nickel rod R-14.

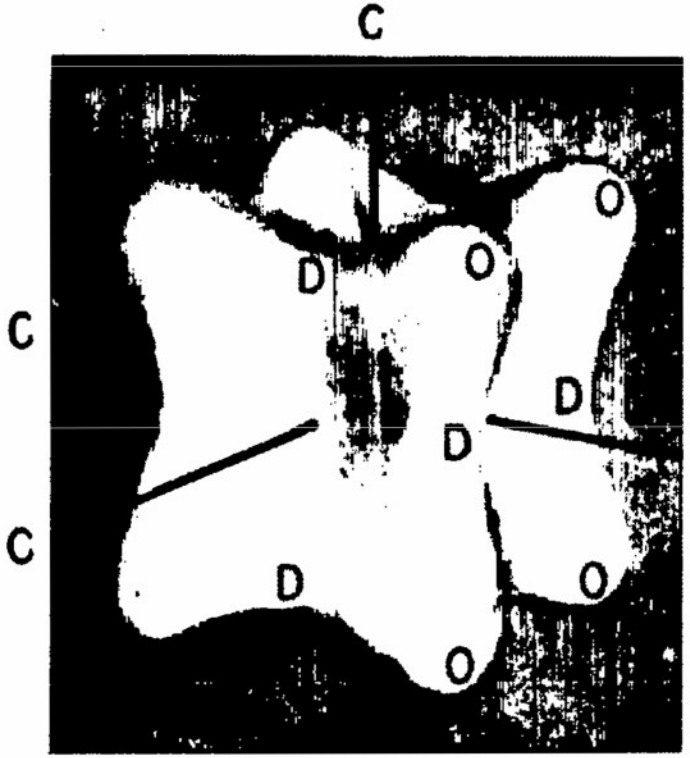

Figure 31.- Directional variation of the tensile modulus at elasticity of a crystal of gold.

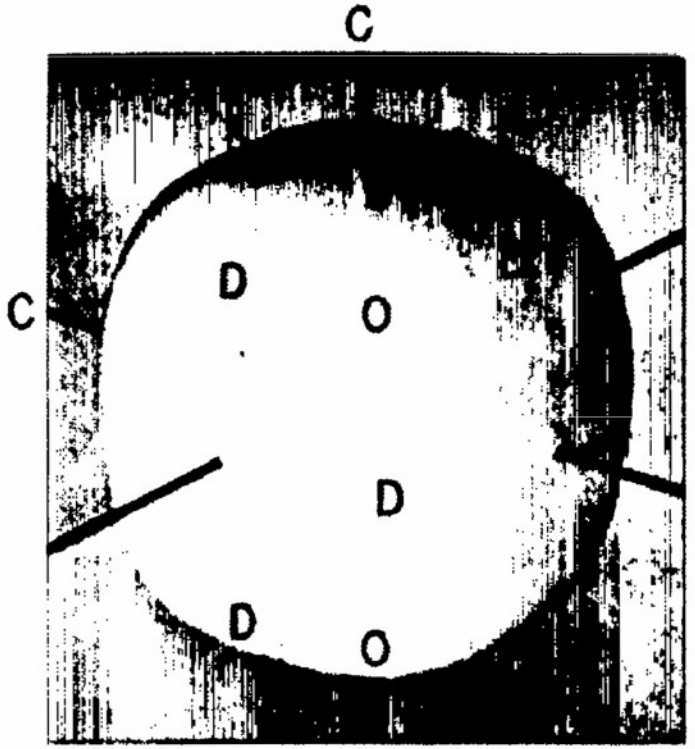

Figure 32.- Directional variation of the tensile modulus at elasticity of a crystal of aluminum.

Key to figures 31 to 34.

Mark	Crystallographic direction name	Symbol
C	Cubic	(100)
O	Octahedral	(111)
D	Dodecahedral	(110)

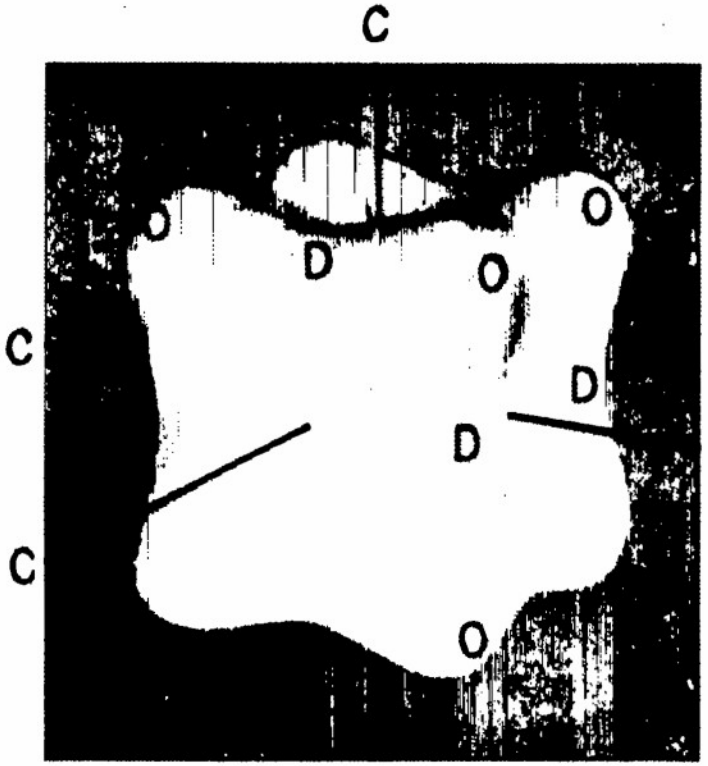

Figure 33.- Directional variation of the tensile modulus of elasticity of a crystal of alpha iron.

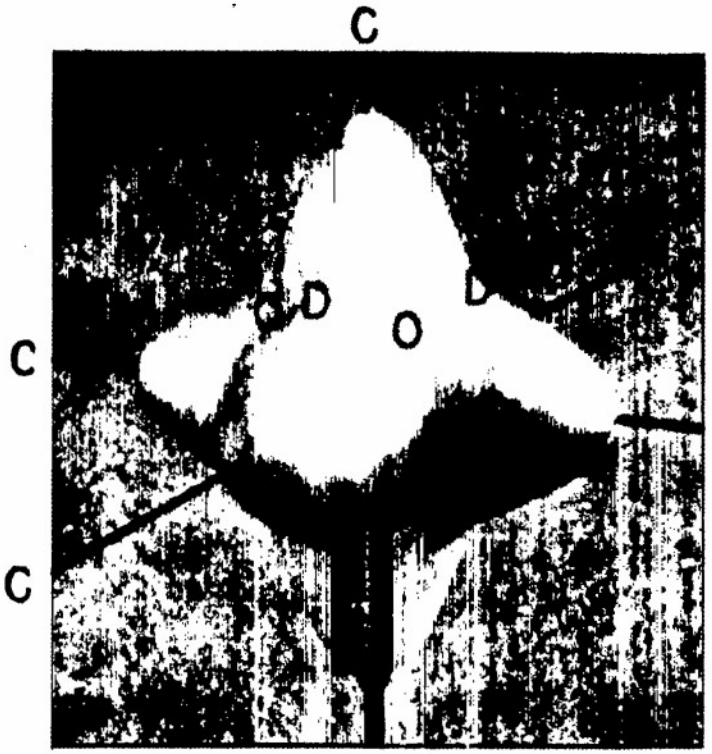

Figure 34.- Directional variation of the shear modulus of elasticity of a crystal of alpha iron.

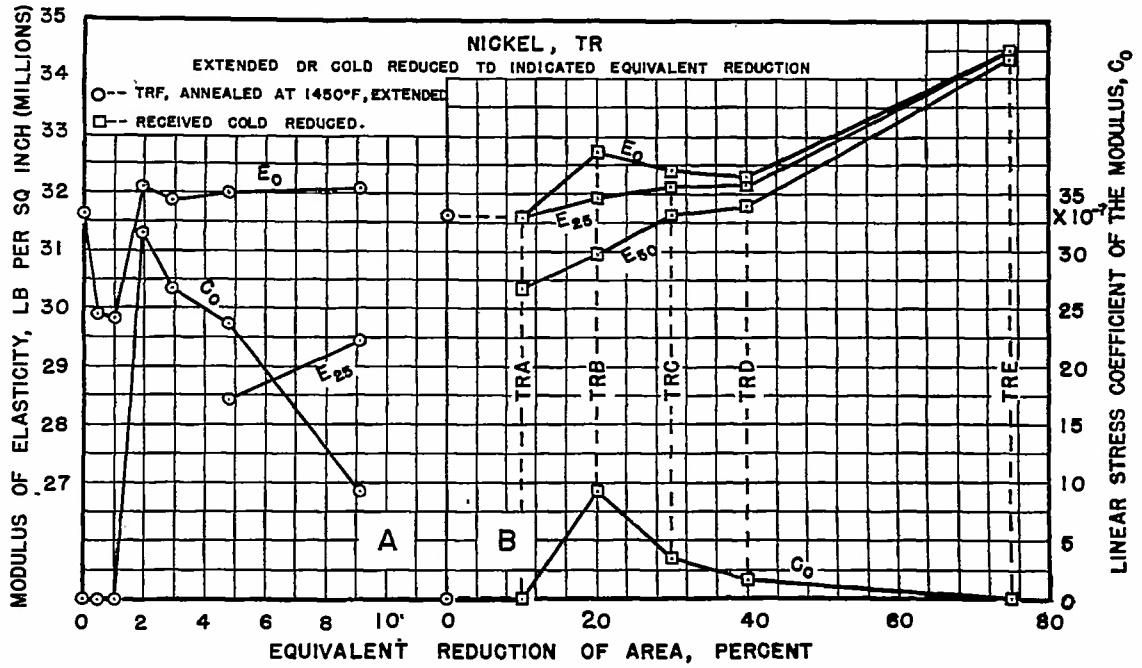

Figure 36.- Variation of tensile modulus of elasticity and of its linear stress coefficient with prior deformation for nickel tubing TR. A-Nickel TRF, annealed and extended. B-Cold-reduced nickel.

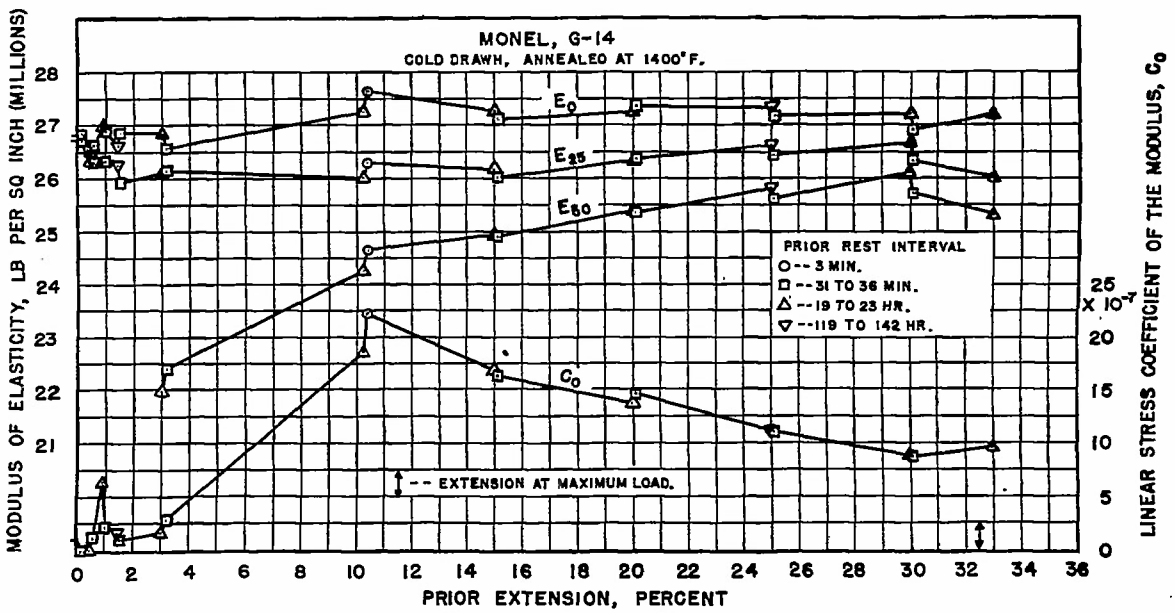

Figure 37.- Variation of tensile modulus of elasticity and its linear stress coefficient with prior extension of annealed monel rod G-14.

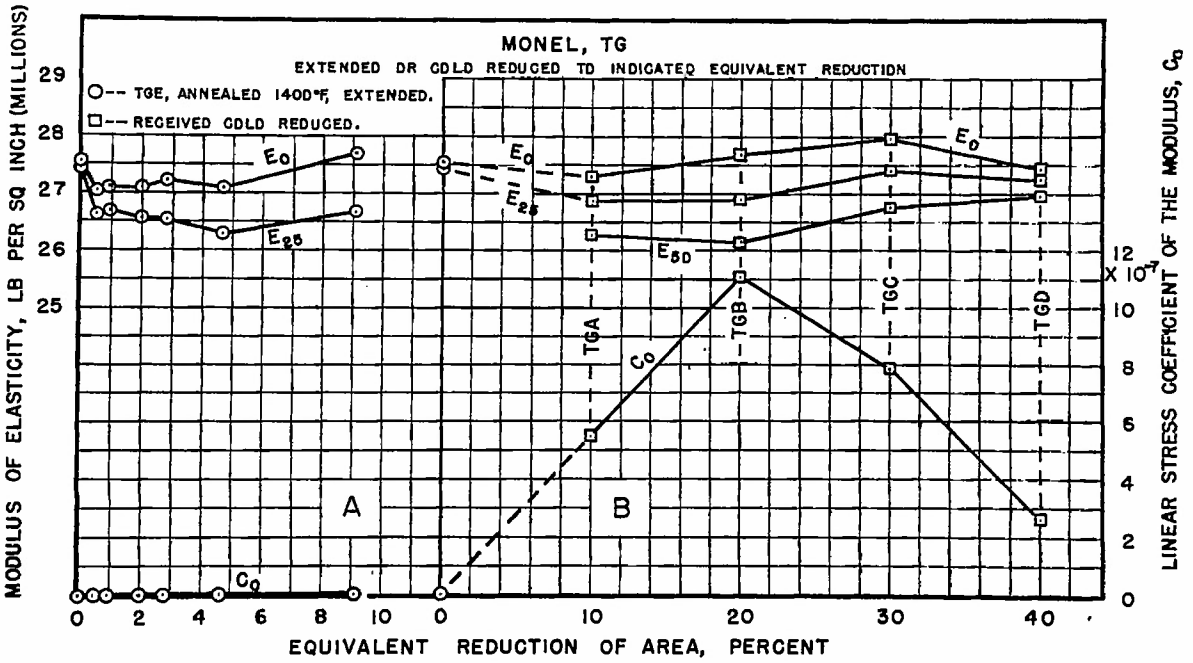

Figure 38.- Variation of tensile modulus of elasticity and its linear stress coefficient with prior deformation for monel tubing TG. A-Monel TGE, annealed and extended. B-Cold-reduced monel.

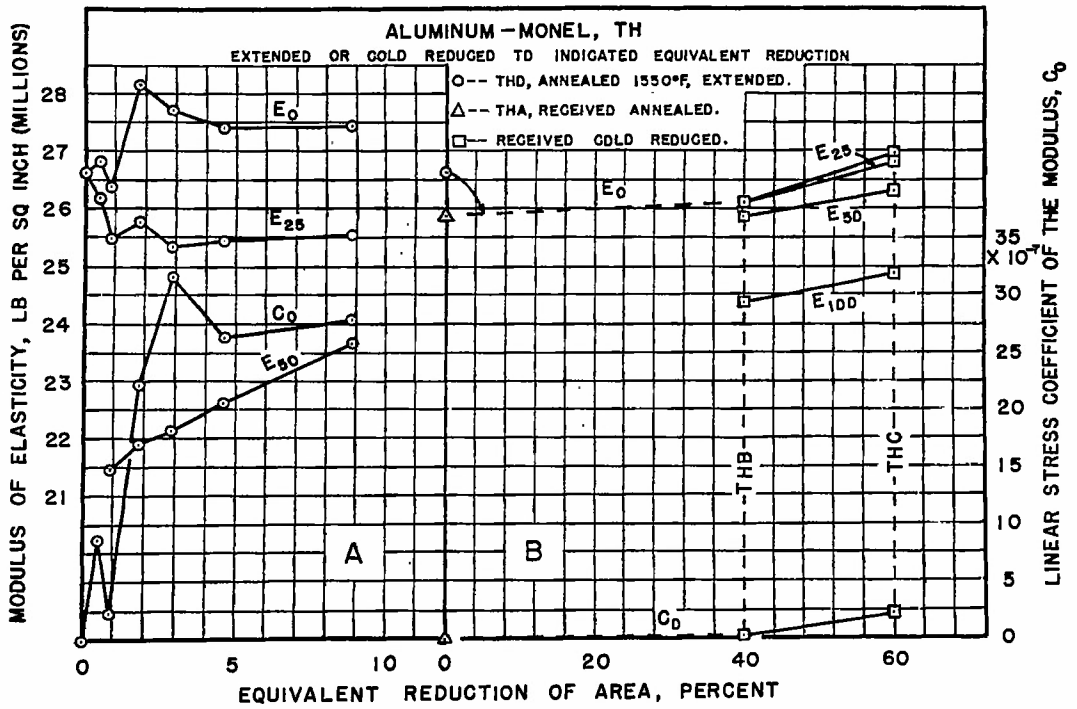

Figure 39.- Variation of tensile modulus of elasticity and its linear coefficient with prior deformation for aluminum-monel tubing TH. A-Aluminum-monel THD, annealed and extended. B-Cold-reduced aluminum-monel.

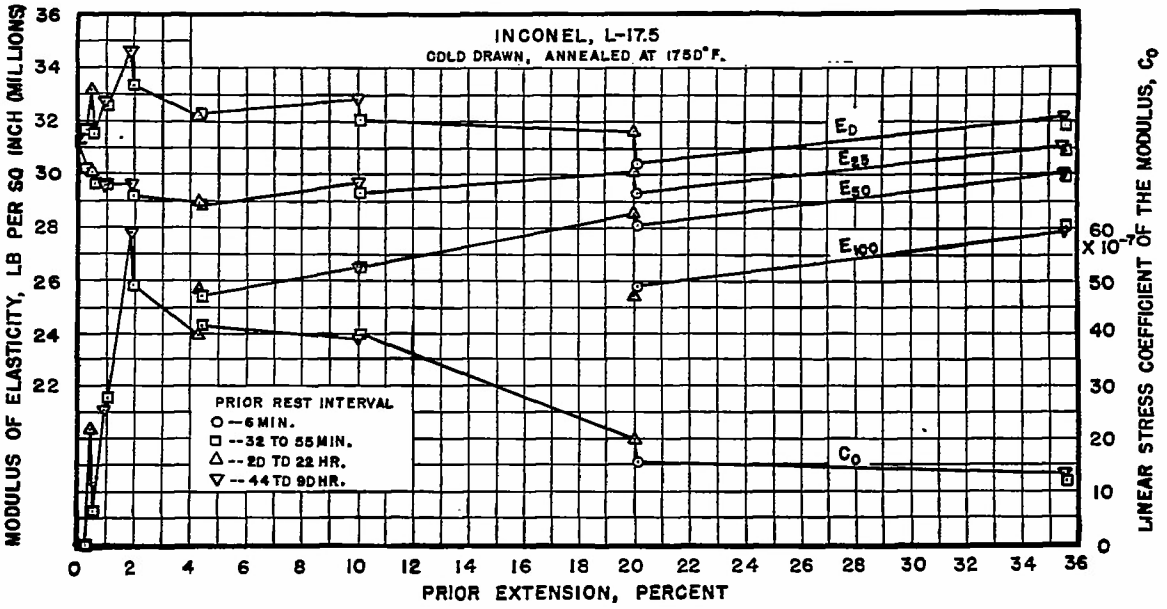

Figure 40.- Variation of tensile modulus of elasticity and its linear stress coefficient with prior extension for annealed Inconel rod L-17.5.

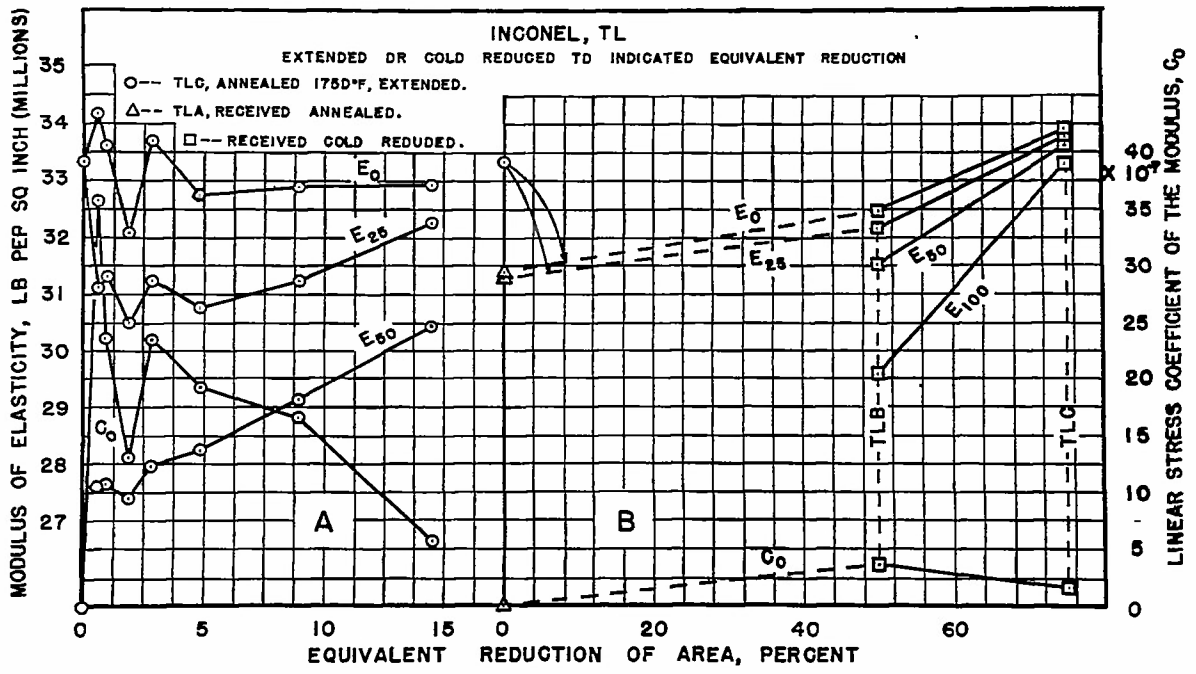

Figure 41.- Variation of tensile modulus of elasticity and its linear stress coefficient with prior deformation for Inconel tubing TL. A-Inconel TLD, annealed and extended. B-Cold-reduced Inconel.

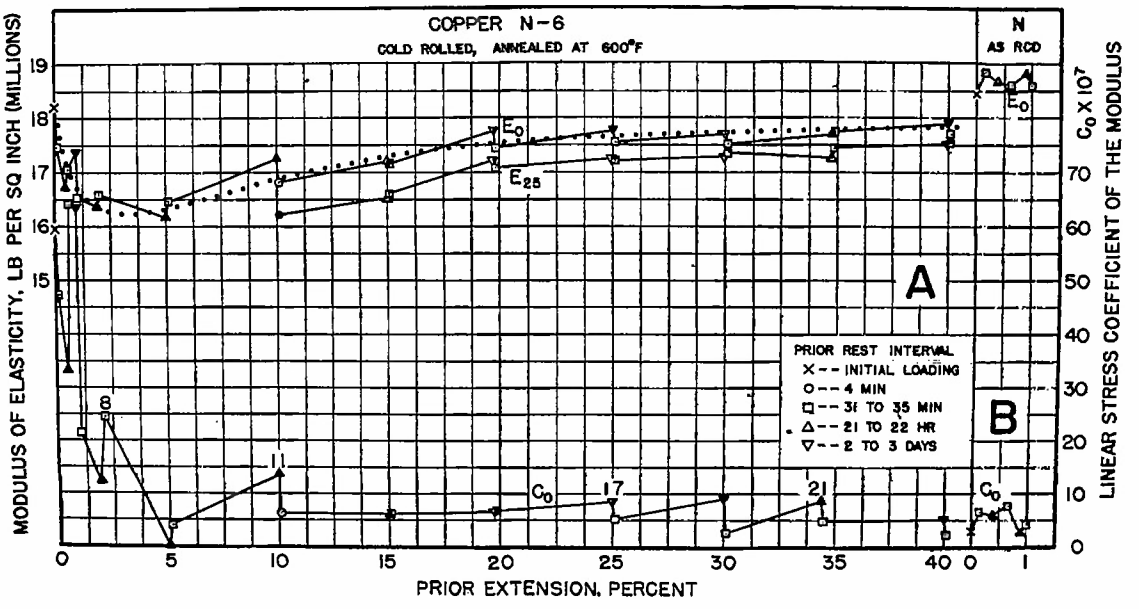

Figure 42.- Variation of tensile modulus of elasticity and its linear stress coefficient with prior extension for copper rod. A-Annealed copper N-6. B-Cold rolled copper N.

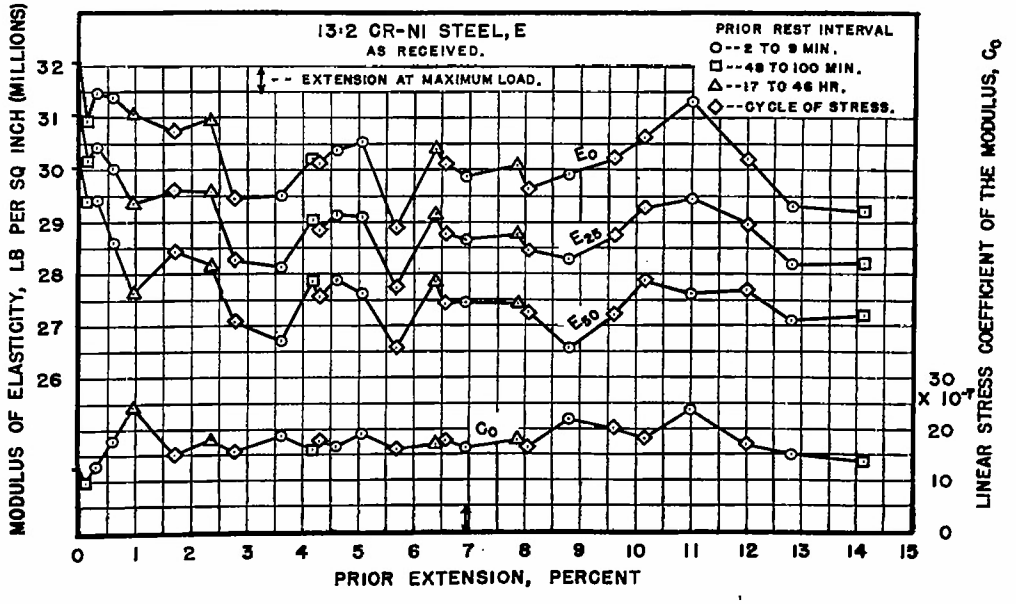

Figure 43.- Variation of tensile modulus of elasticity and its linear stress coefficient with prior extension for 13:2 chromium-nickel steel E; as received.

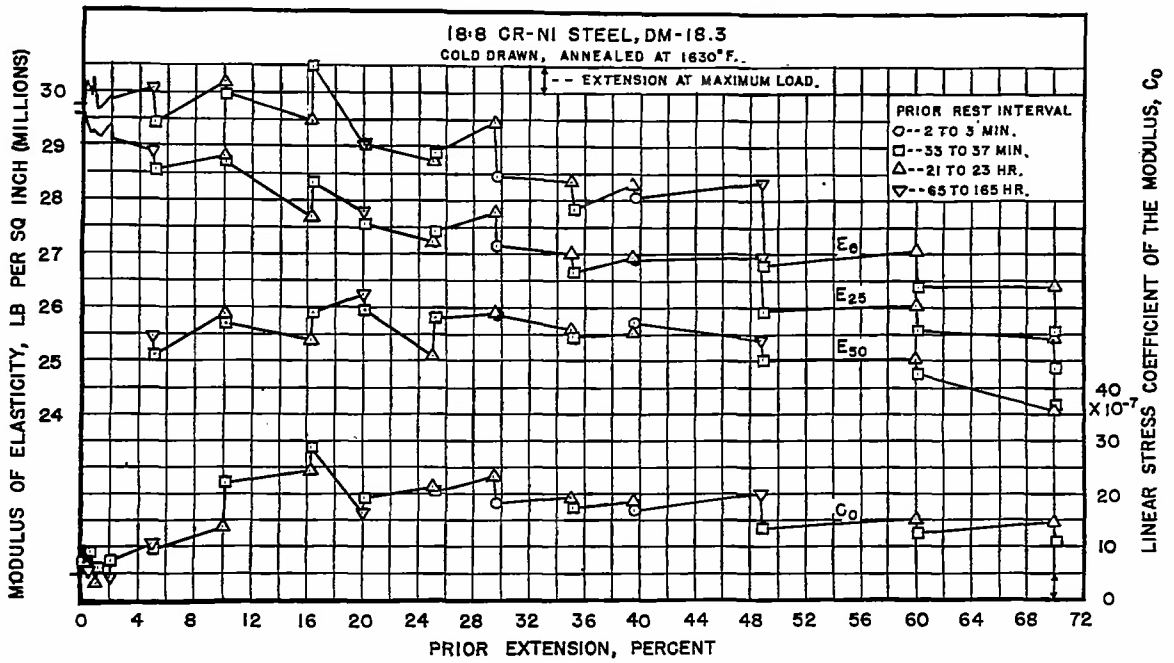

Figure 44.- Variation of tensile modulus of elasticity and its linear stress coefficient with prior extension for annealed 18:8 chromium-nickel steel DM-18.3.

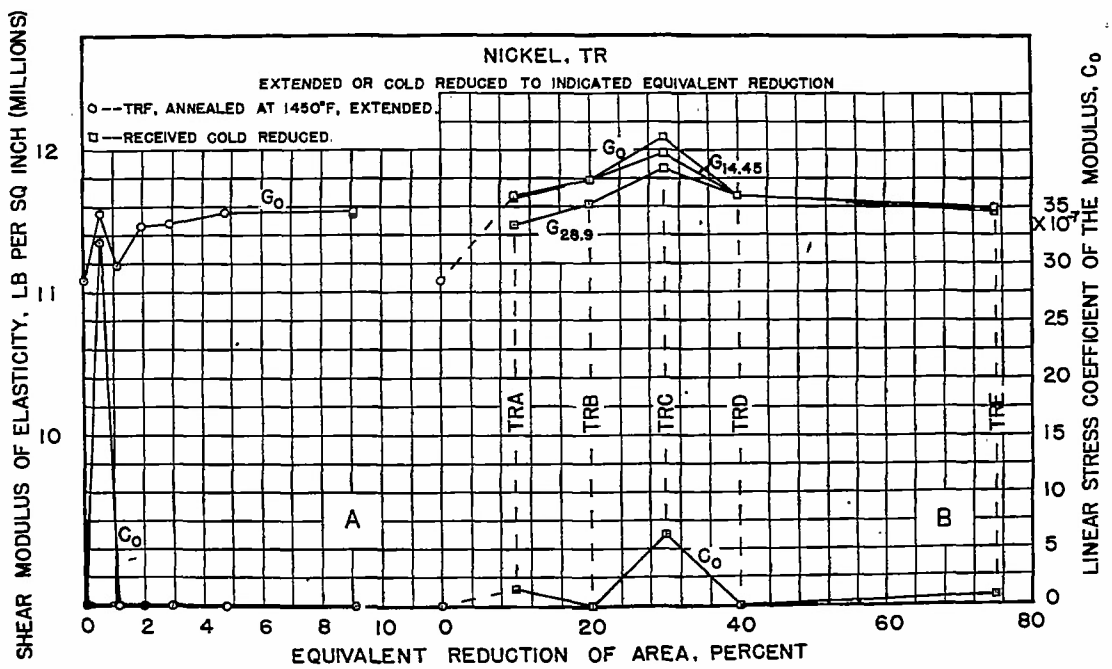

Figure 45.- Variation of shear modulus of elasticity and its linear stress coefficient with prior deformation for nickel tubing TR. A-Nickel TRF, annealed and extended. B-Cold-reduced nickel.

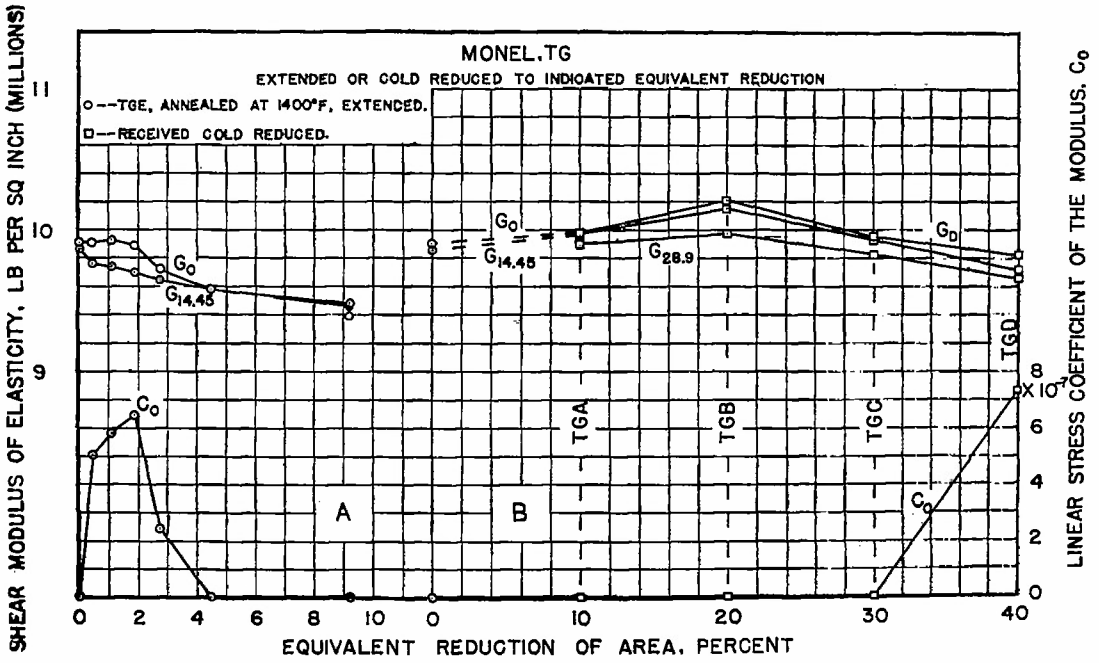

Figure 46.- Variation of shear modulus of elasticity and its linear stress coefficient with prior deformation for monel tubing TG. A-Monel TGE, annealed and extended. B-Cold-reduced monel.

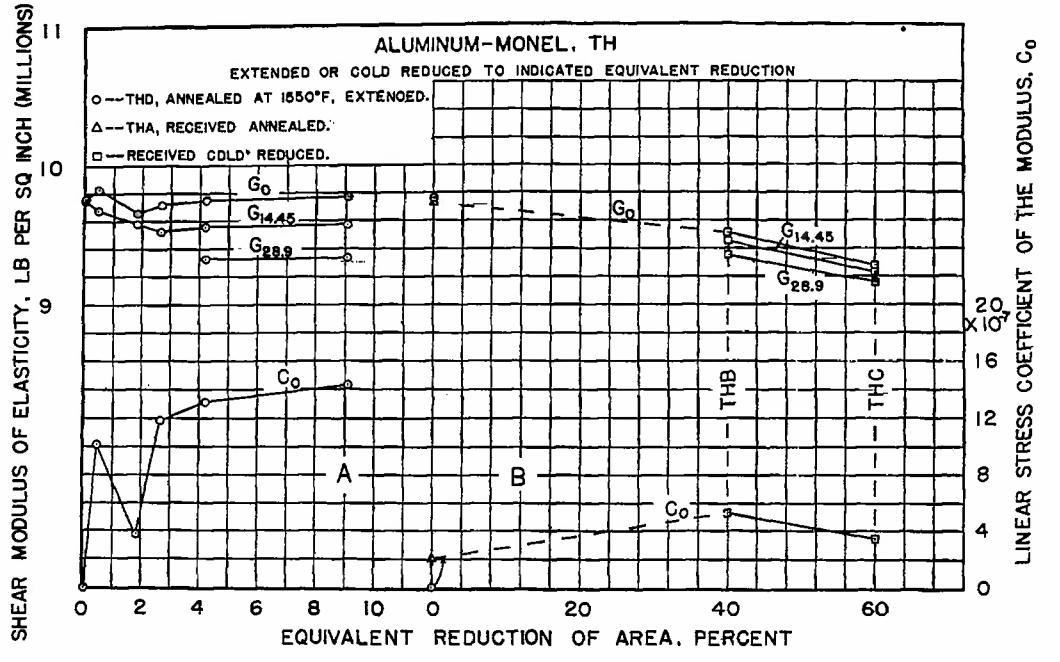

Figure 47.- Variation of shear modulus of elasticity and its linear stress coefficient with prior deformation for aluminum monel tubing TH. A-Aluminum-monel THD, annealed and extended. B-Cold-reduced aluminum-monel.

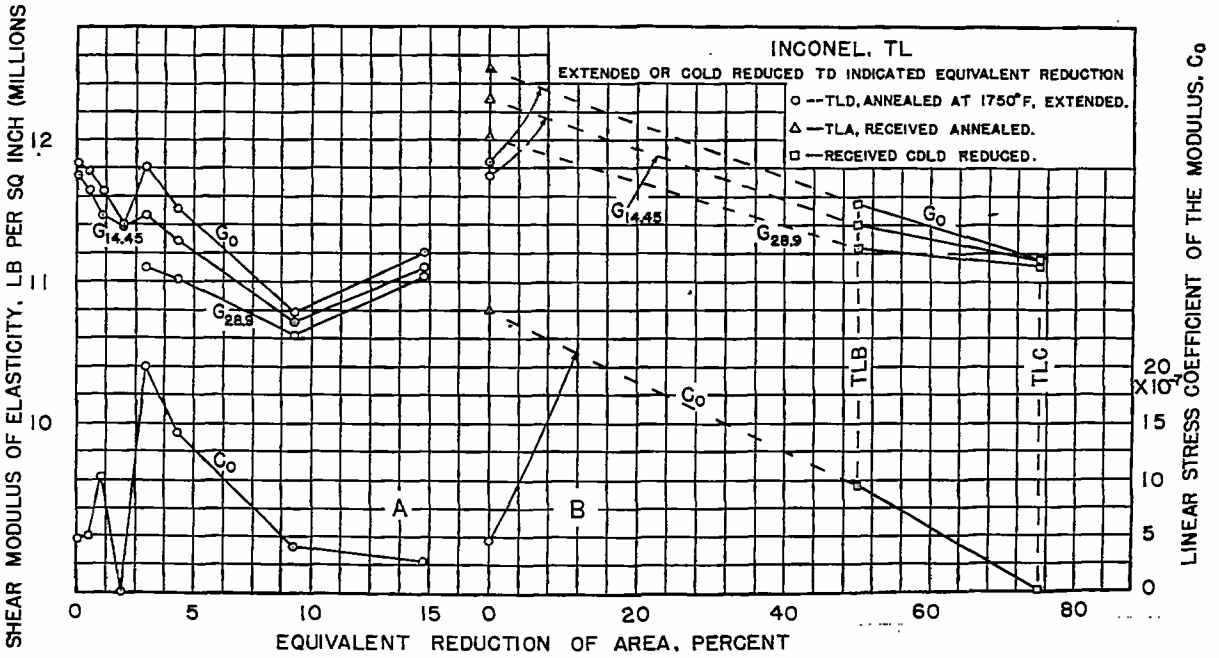

Figure 48.- Variation of shear modulus and its linear stress coeffioient with prior deformation for Inconel tubing TL. A-Inconel TLD, annealed and extended. B-Cold-reduced Inoonel.

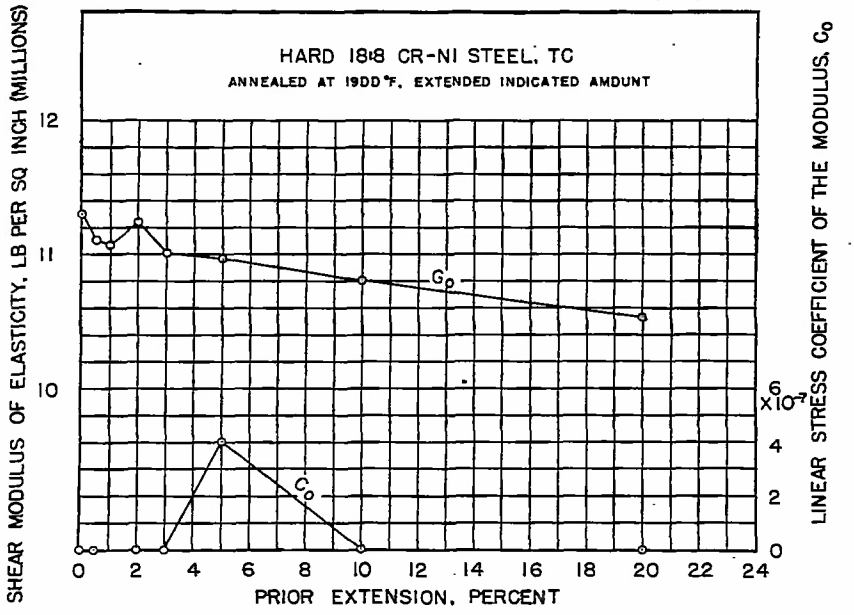

Figure 49.- Variation of shear modulus of elasticity and its linear stress coefficient with prior extension for annealed 18:8 ohromium-nickel steel tubing TC-19.

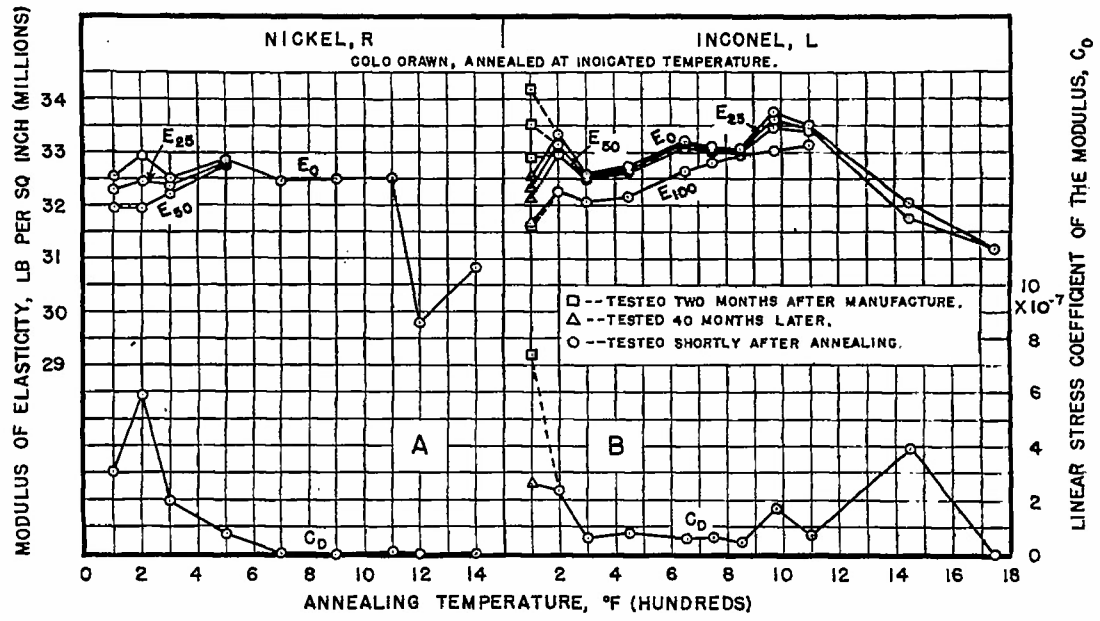

Figure 50.- Variation of tensile modulus of elasticity and of its linear stress coefficient with annealing temperature. A-Cold-drawn nickel rod R. B-Cold-drawn Inconel rod L.

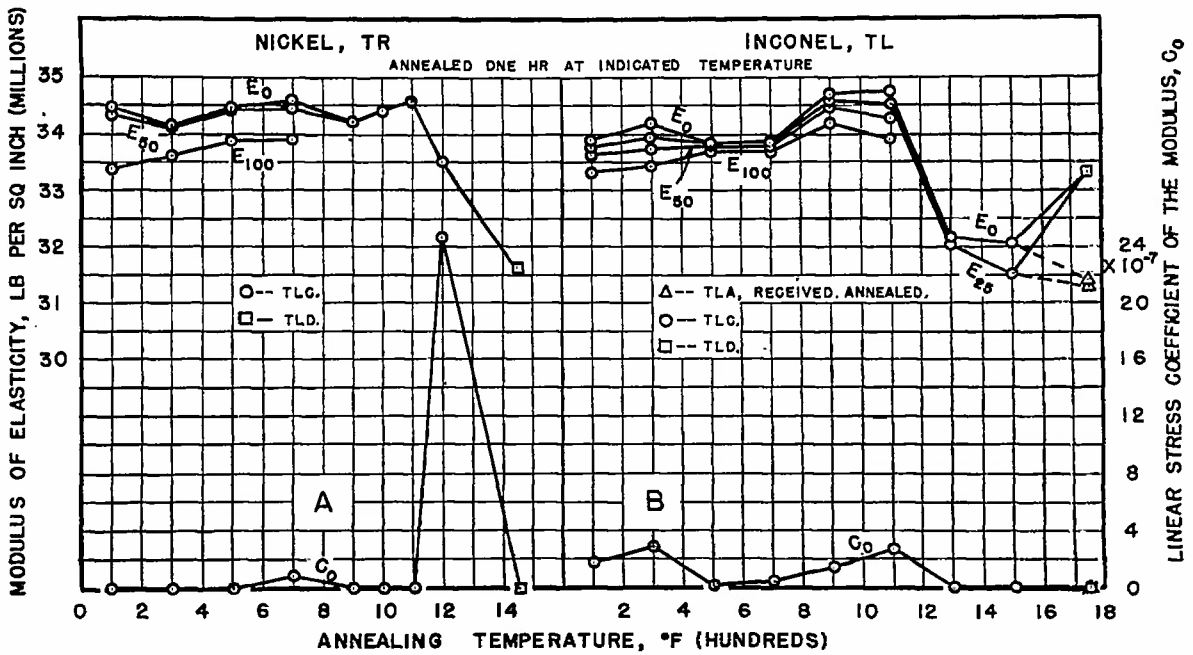

Figure 51.- Variation of tensile modulus of elasticity and its linear stress coefficient with annealing temperature. A-Cold-reduced nickel tubing TR. B-Cold-reduced Inconel tubing TL.

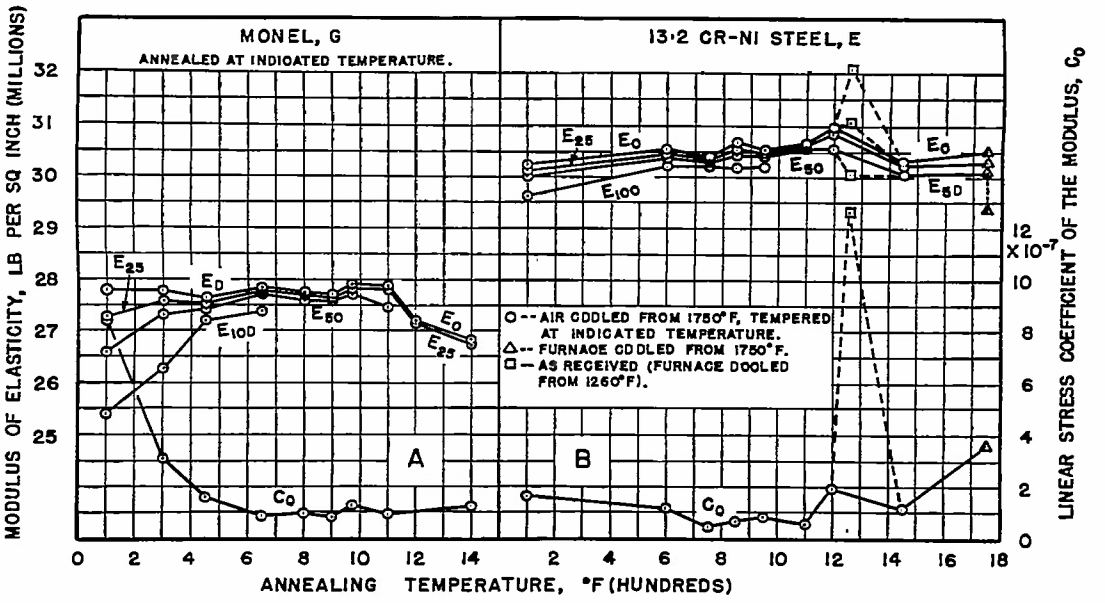

Figure 52.- Variation of tensile modulus of elasticity and its linear stress coefficient with annealing or tempering temperature. A-Cold-drawn monel rod G. B-Air-cooled 13:2 chromium-nickel steel.

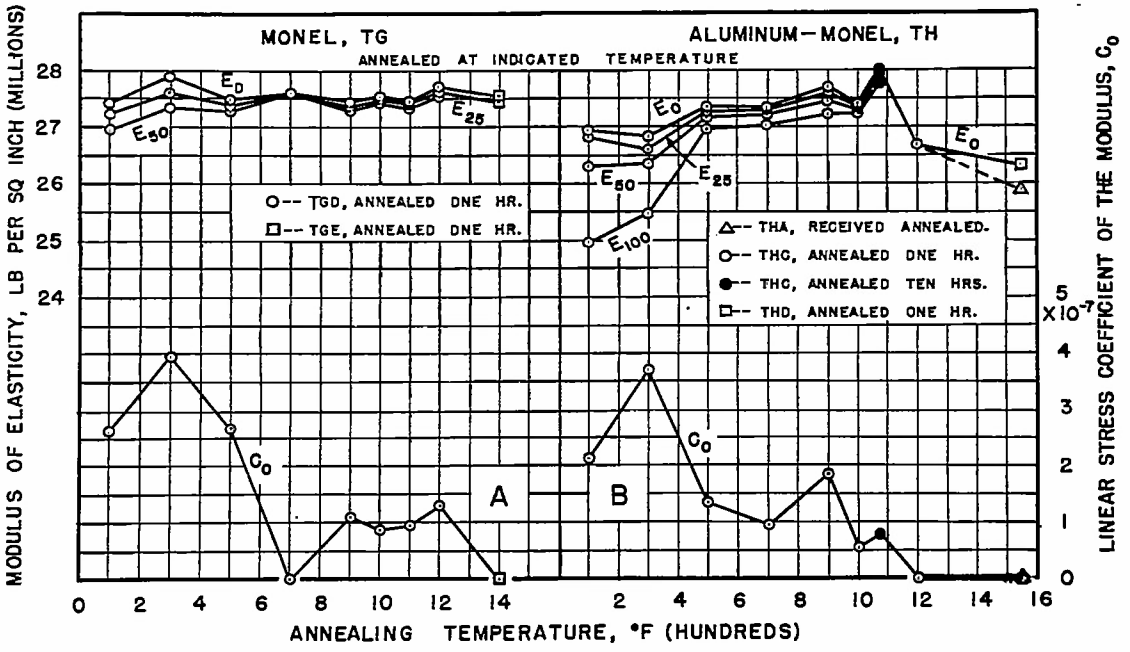

Figure 53.- Variation of tensile modulus of elasticity and its linear stress coefficient with annealing temperature. A-Cold-reduced monel tubing TG. B-Cold-reduced aluminum-monel tubing TH.

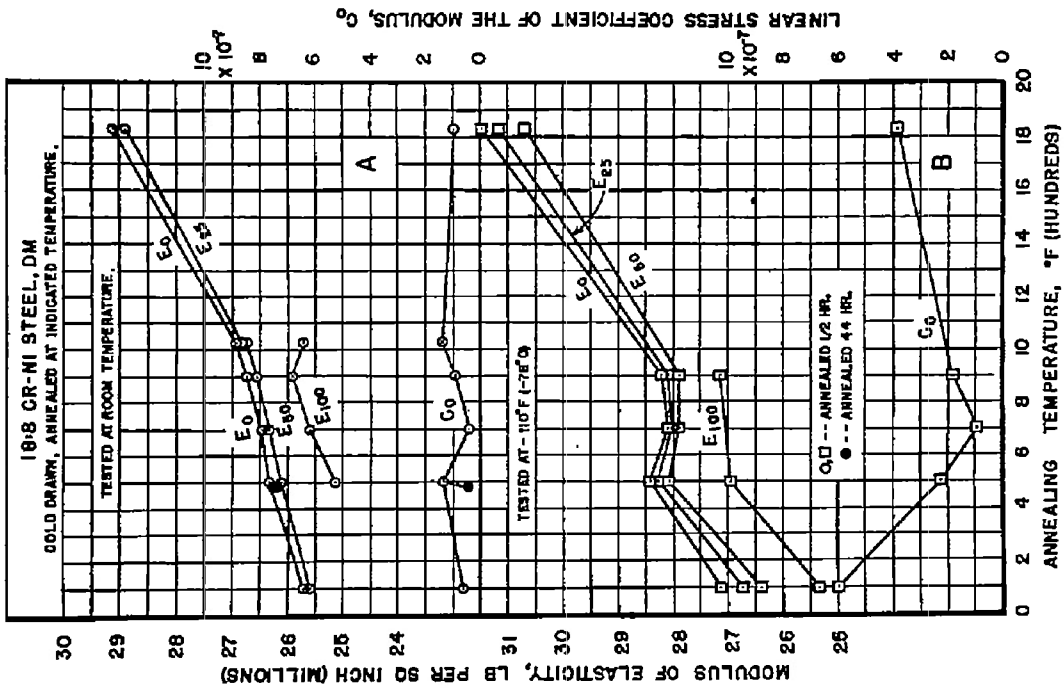

Figure 54.- Variation of tensile modulus of elasticity and its linear stress coefficient with annealing temperature for half-hard 18:8 chromium-nickel steel DM. A-Room temperature tests. B-Tested at -110°F.

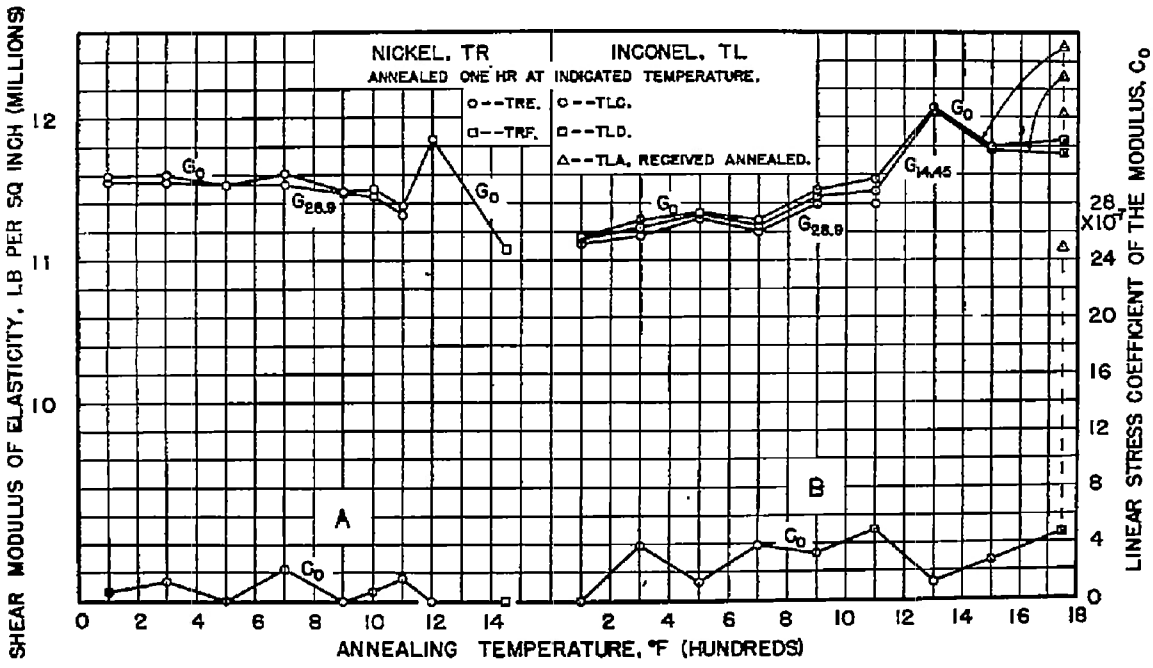

Figure 55.- Variation of shear modulus of elasticity and its linear stress coefficient with annealing temperature. A-Cold-reduced nickel tubing TR. B-Cold-reduced Inconel tubing TL.

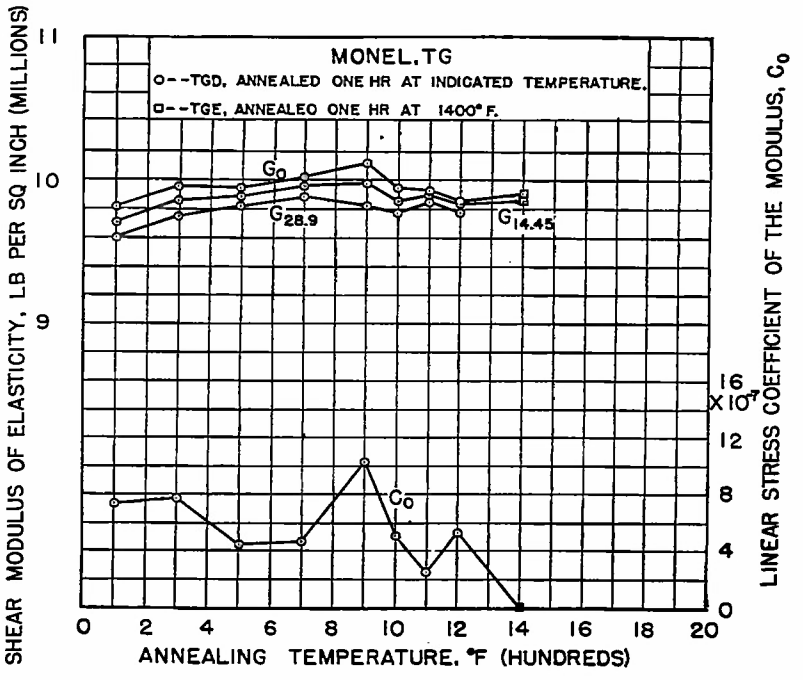

Figure 56.- Variation of shear modulus of elasticity and its linear stress coefficient with annealing temperature for cold-reduced monel tubing TG.

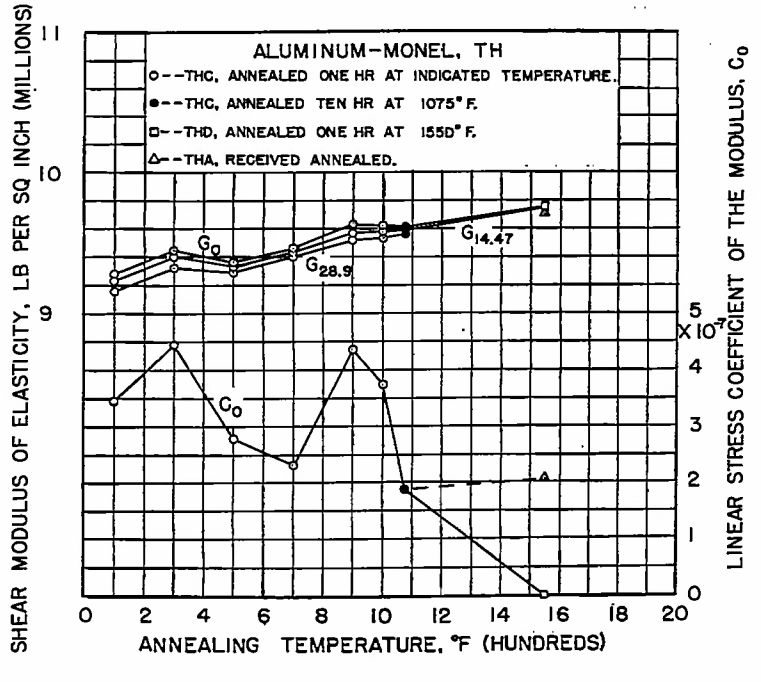

Figure 57.- Variation of shear modulus of elasticity and its linear stress coefficient with annealing temperature for cold-reduced aluminum-monel tubing TH.

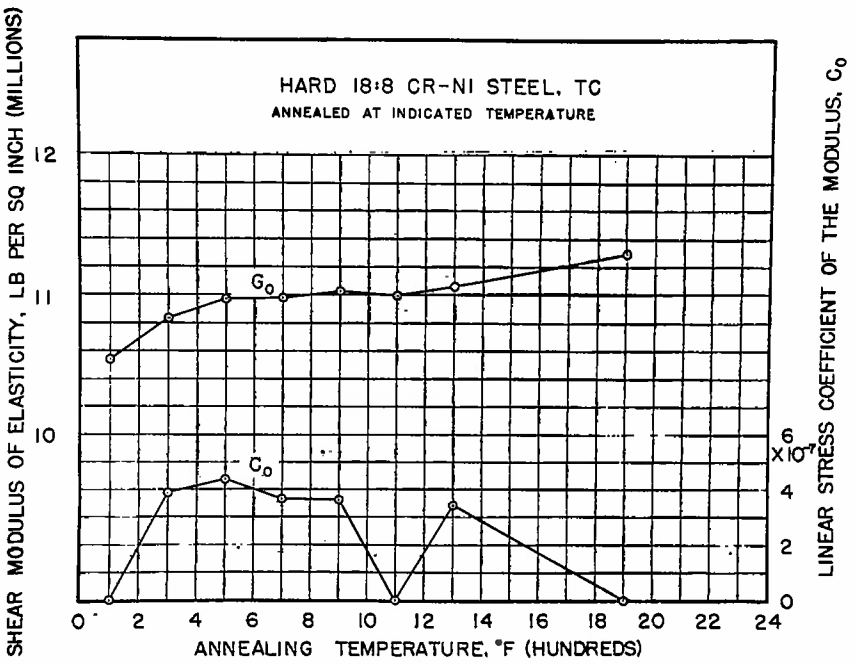

Figure 58.- Variation of shear modulus of elasticity and its linear stress coefficient with annealing temperature for cold-drawn 18:8 chromium-nickel steel tubing TC.

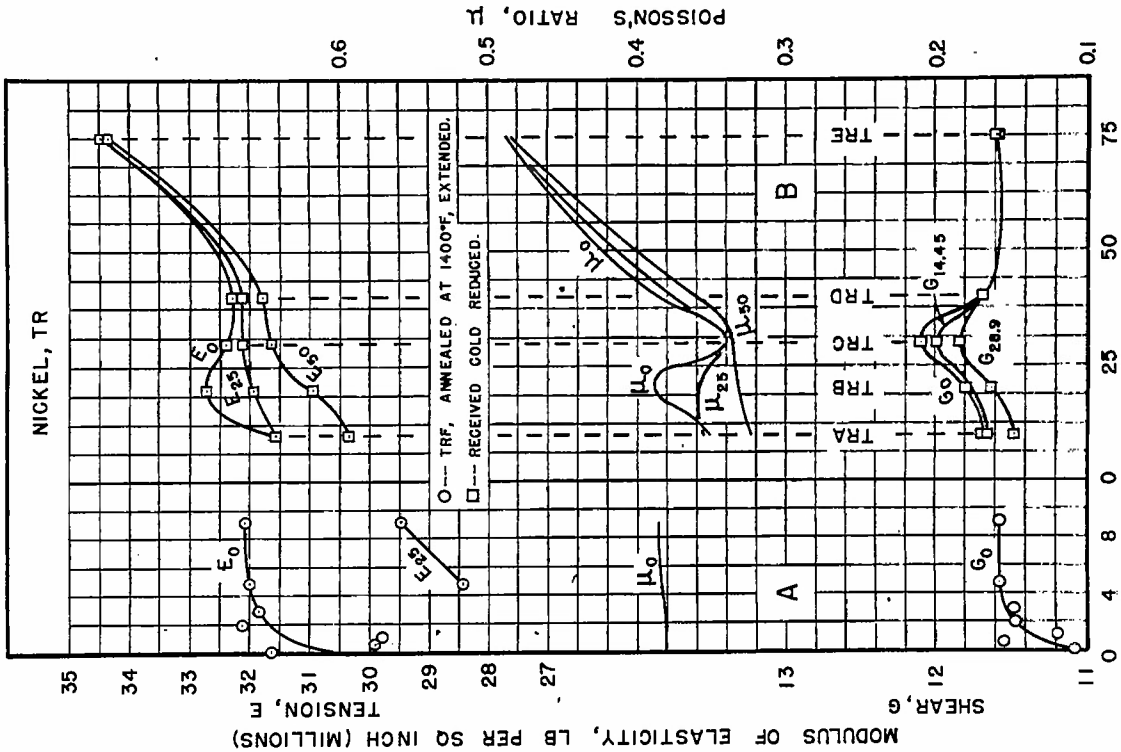

Figure 59.- Variation of Poisson's ratio with prior deformation for nickel tubing. A-Nickel TRF, annealed and extended. B-Cold-reduced nickel tubing.

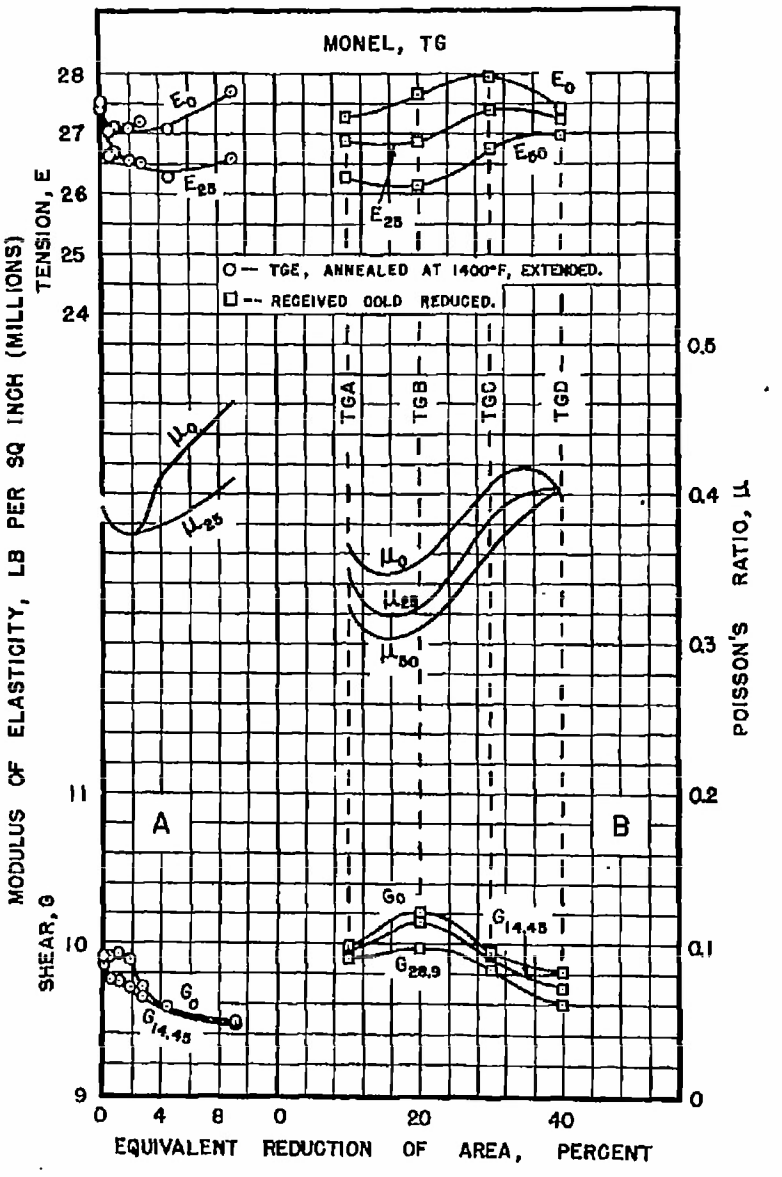

Figure 60.- Variation of Poisson's ratio with prior deformation for monel tubing TG. A-Monel TGE, annealed and extended. B-Cold-reduced monel.

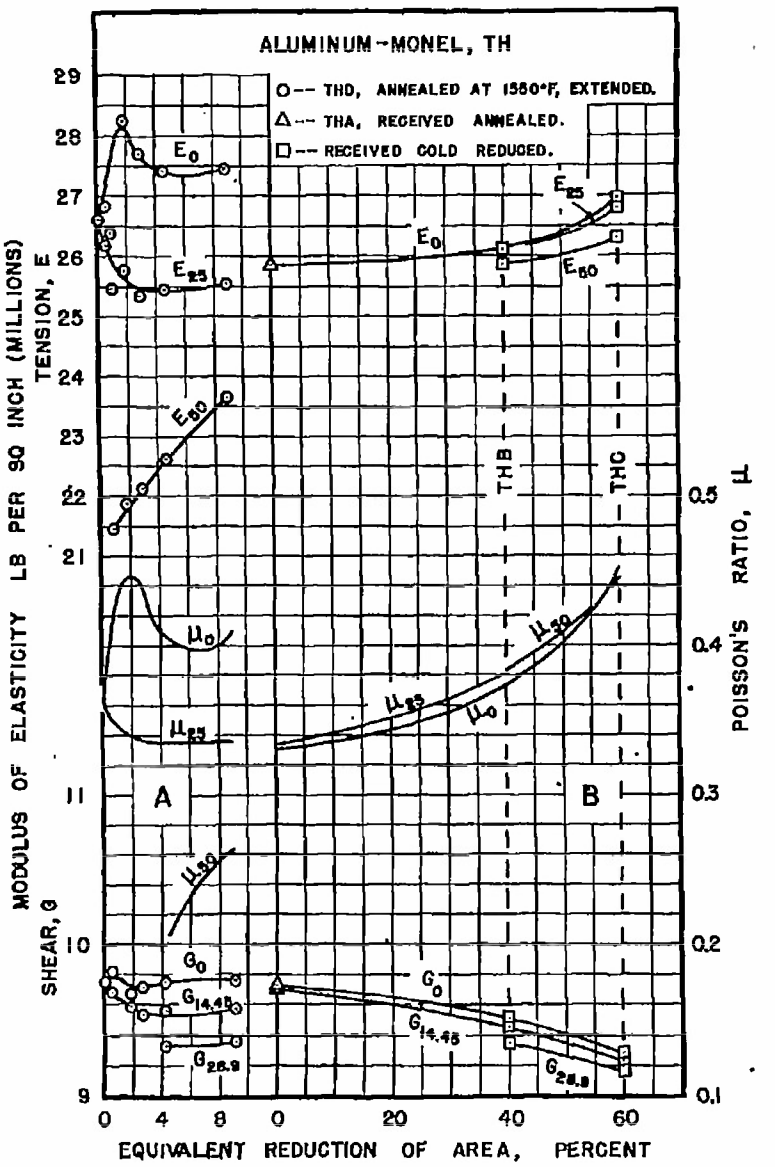

Figure 61.- Variation of Poisson's ratio with prior deformation for aluminum-monel tubing TH. A-Aluminum-monel THD, annealed and extended. B-Cold-reduced aluminum-monel.

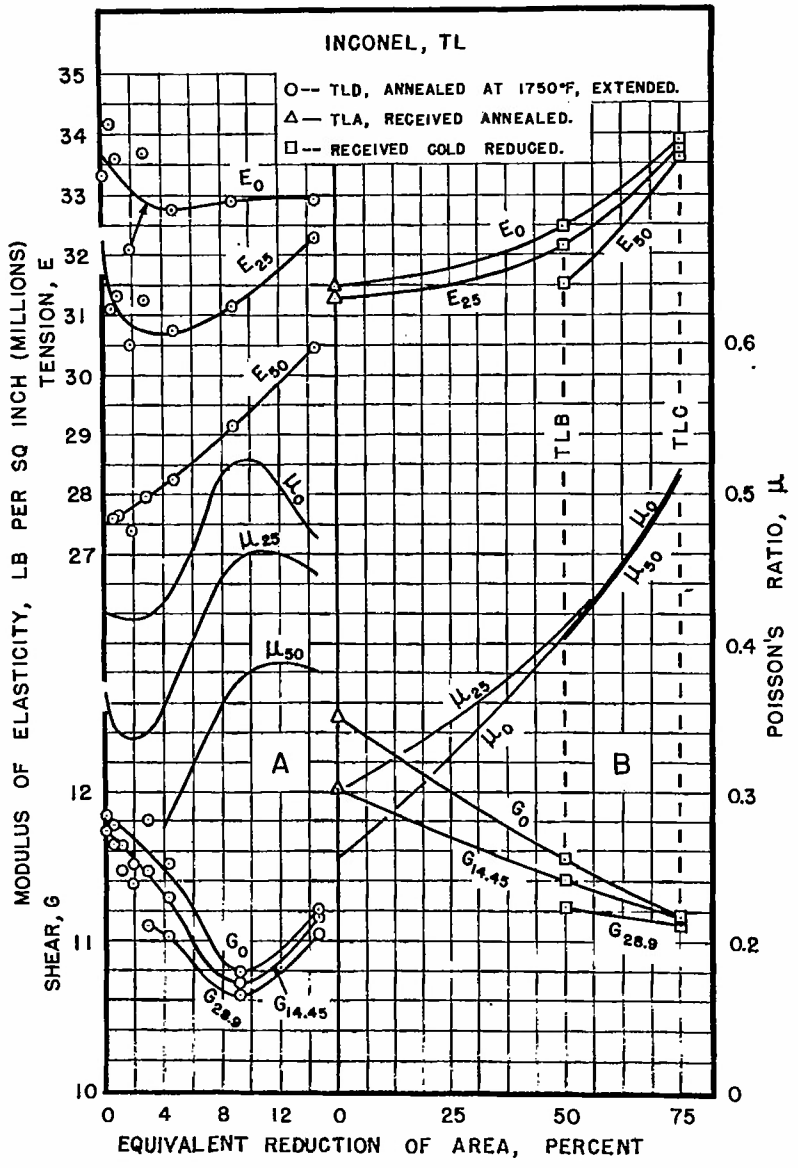

Figure 62.- Variation of Poisson's ratio with prior deformation for Inconel tubing TL. A-Inconel TLD, annealed and extended. B-Cold-reduced Inconel.

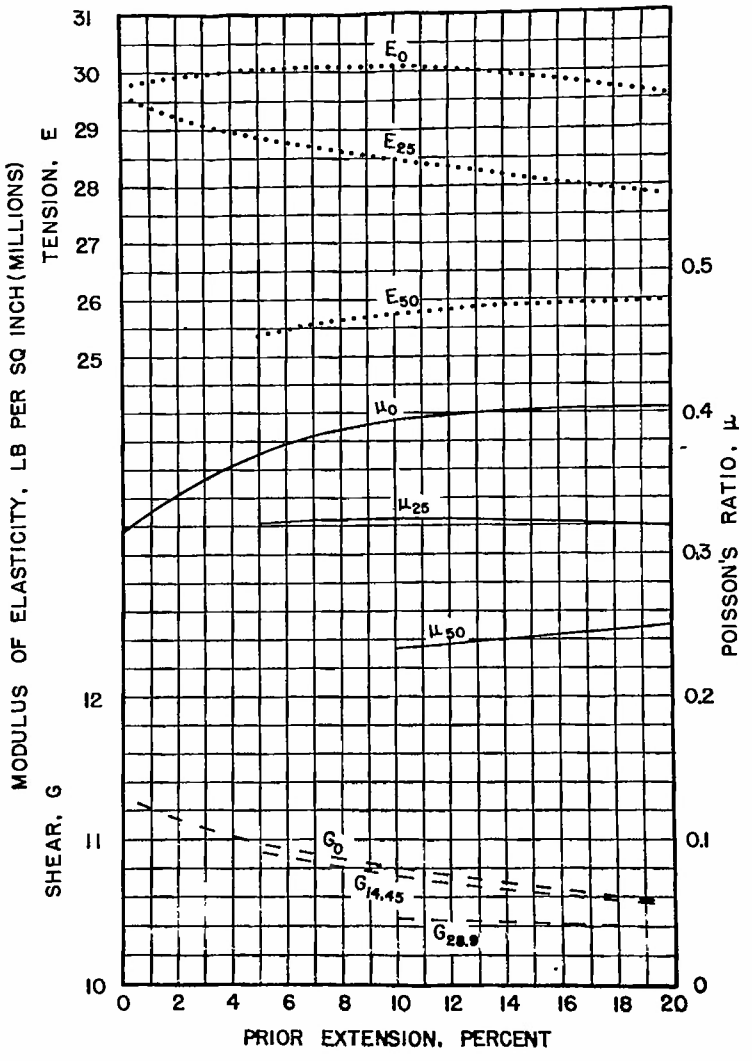

Figure 63.- Variation of Poisson's ratio with extension for annealed 18:8 chromium-nickel steel.

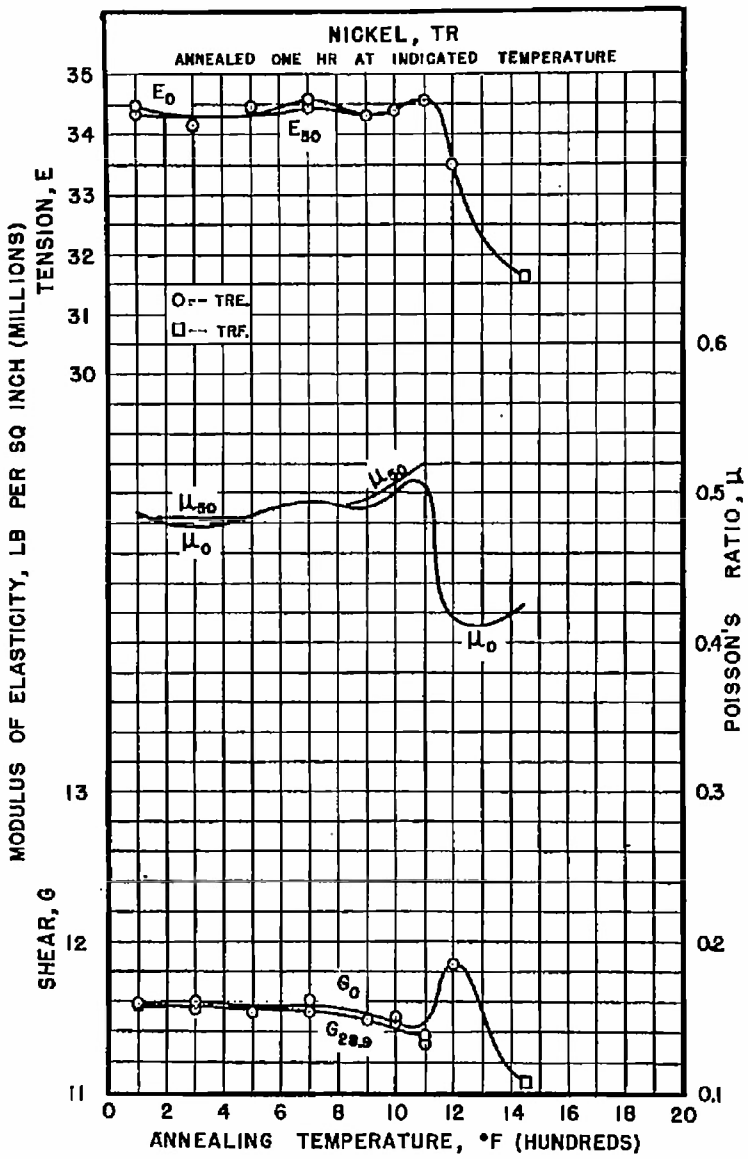

Figure 64.- Variation of Poisson's ratio with annealing temperature, for nickel tubing TR.

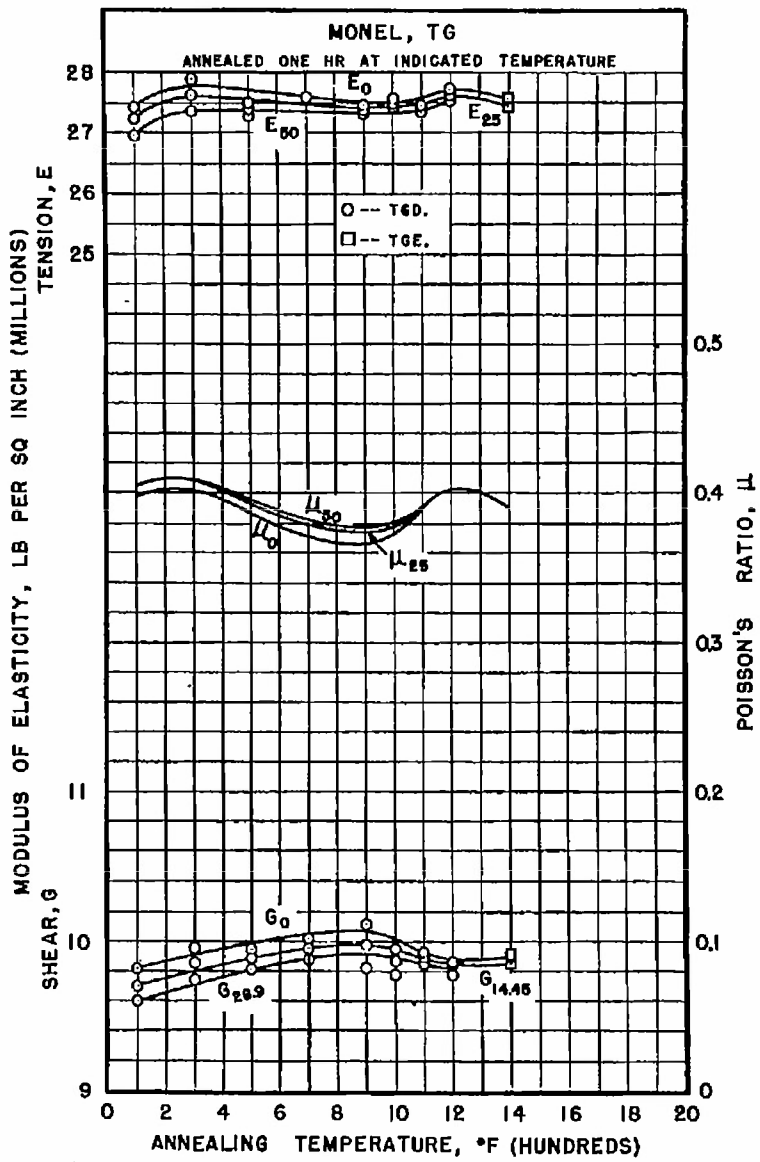

Figure 65.- Variation of Poisson's ratio with annealing temperature for monel tubing TG.

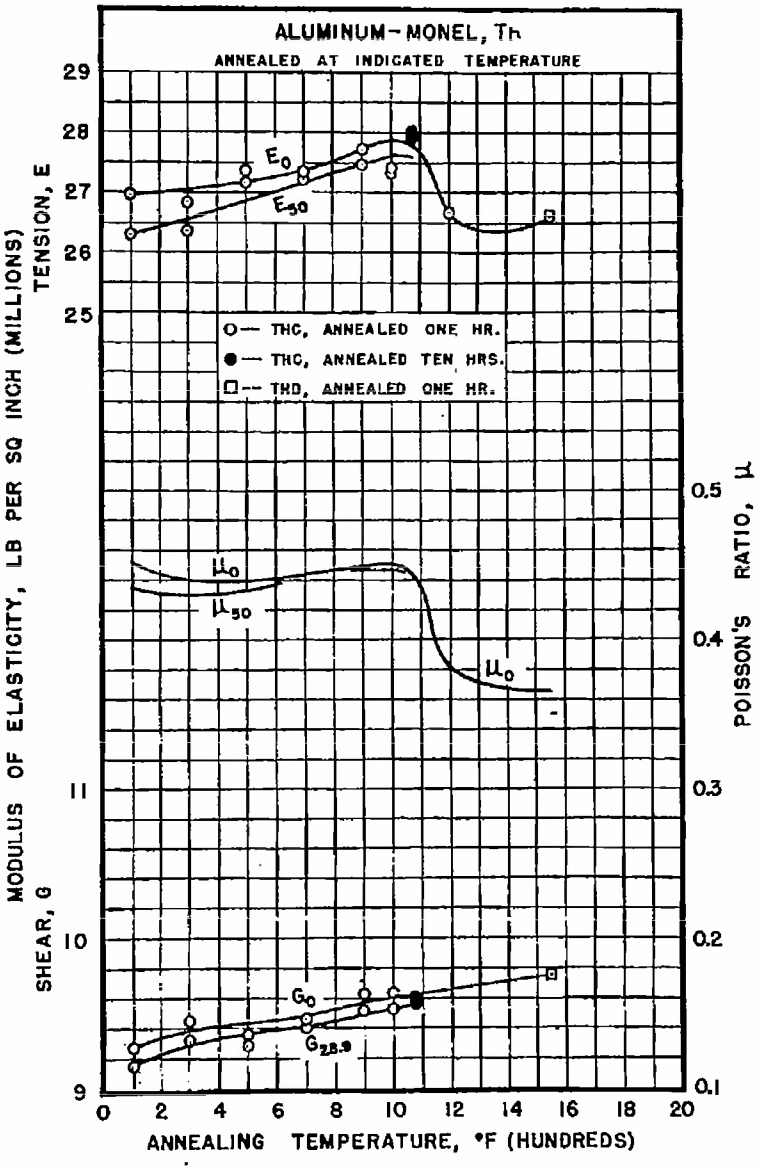

Figure 66.- Variation of Poisson's ratio with annealing temperature for aluminum-monel tubing TH.

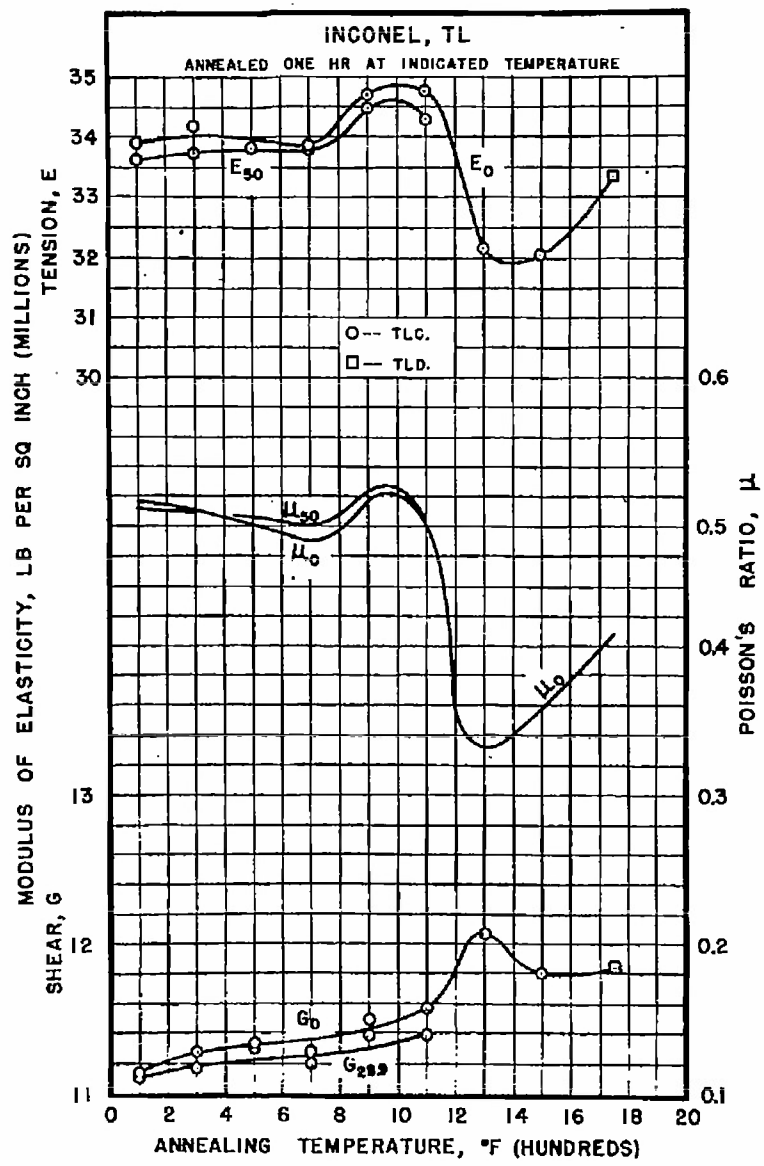

Figure 67.- Variation of Poisson's ratio with annealing temperature for Inconel tubing TL.

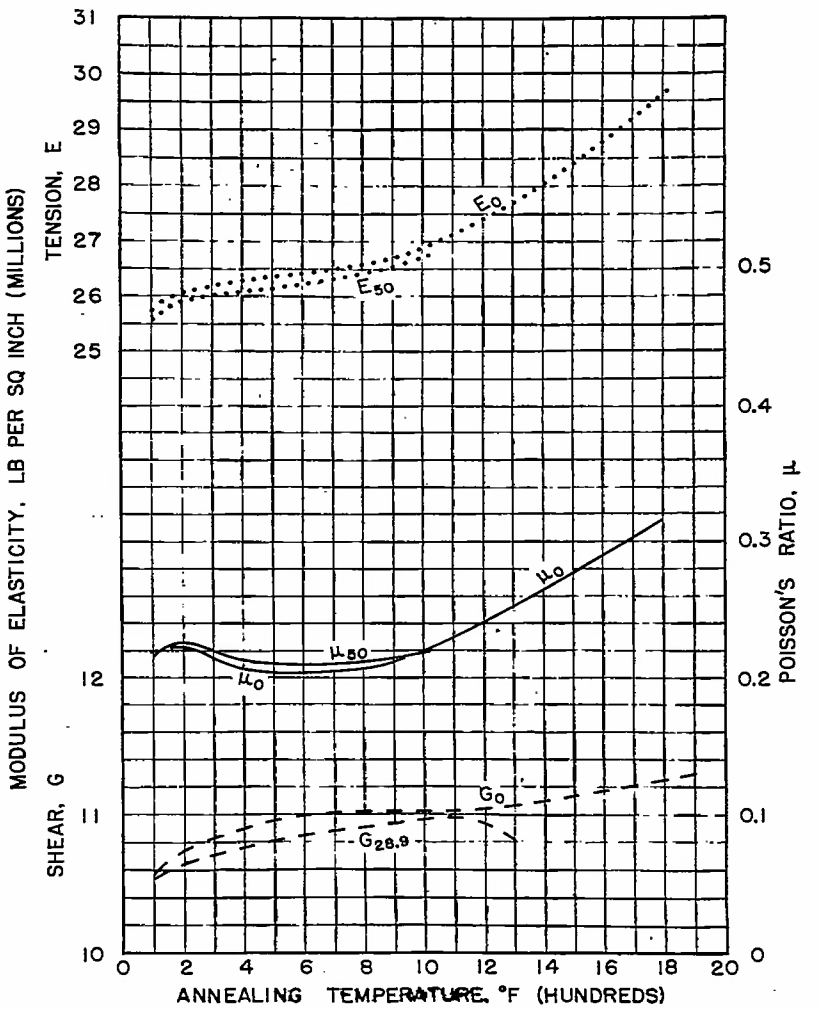

Figure 68.- Variation of Poisson's ratio with annealing temperature for cold-drawn 18:8 chromium-nickel steel.

TSDIN FORM 69 (13 MCR 47)

Mebs, R. W.
McAdam, D. J.

AUTHOR(S)

DIVISION: Materials (8) 56

SECTION: Misc. Non-Ferrous Metals and Alloys (12)

CROSS REFERENCES: Metals - Elasticity (61037)

P-8-12-4

P11/6.1

ATI- 8814

ORIG. AGENCY NUMBER TN-1100

REVISION

AMER. TITLE: Elastic properties in tension and shsar of high strength non-ferrous metals and stainless steel - Effect of previous deformation and heat treatment

FORG'N. TITLE:

ORIGINATING AGENCY: National Advisory Committee for Aeronautics, Washington, D. C.

TRANSLATION:

COUNTRY	LANGUAGE	FORG'N.CLASS	U. S.CLASS.	DATE	PAGES	ILLUS.	FEATURES
U.S.	Eng.		Unclass.	Mar'47	105	76	photos, tables, graphs

ABSTRACT

Elastic properties of nonferrous metals and stainless steels in the form of rods and tubes were tested in tension and shear. Effect of annealing temperature and prior plastic deformation on tensile properties and the elastic modulus are investigated. Study is made of the variation of the several elastic properties in tension and shear with cold de ... Conclusions are bassd on a comparison of the tabulated te...

ust be addressed to: N.A.C.A.,

AL INDEX

WRIGHT FIELD, OHIO, USAAF

P.40400

WF-O-21 MAR 47 20M